Adaptive Transmission Schemes for Spectrum Sharing Systems: Trade-offs and Performance Analysis

Zied Bouida

A Thesis

in

The Department

of

Electrical and Computer Engineering

Presented in Partial Fulfillment of the Requirements
for the Degree of Doctor of Philosophy at
Concordia University
Montréal, Québec, Canada

January, 2015

CONCORDIA UNIVERSITY
SCHOOL OF GRADUATE STUDIES

This is to certify that the thesis prepared

By: Zied Bouida

Entitled: Adaptive Transmission Schemes for Spectrum Sharing Systems: Trade-
                offs and Performance Analysis

and submitted in partial fulfillment of the requirements for the degree of

                Doctor of Philosophy   (Electrical and Computer Engineering)

complies with the regulations of the University and meets the accepted standards with
respect to originality and quality.

Signed by the final examining committee:

_____ Chair
Dr. S. Bergler

_____ External Examiner
Dr. F. Gagnon

_____ External to Program
Dr. X. Zhou

_____ Examiner
Dr. Y.R. Shayan

_____ Examiner
Dr. M.R. Soleymani

_____ Thesis Co-Supervisor
Dr. A. Ghrayeb

_____ Thesis Co-Supervisor
Dr. K. Qarage

Approved by: _____
                        Dr. A.R. Sebak, Graduate Program Director

January 9, 2015   Dr. A. Asif, Dean
                       Faculty of Engineering & Computer Science

Abstract

Adaptive Transmission Schemes for Spectrum Sharing Systems: Trade-offs and Performance Analysis

Zied Bouida, PhD.

Concordia University, 2015

Cognitive radio (CR) represents a key solution to the existing spectrum scarcity problem. Under the scenario of CR, spectrum sharing systems allow the coexistence of primary users (PUs) and secondary users (SUs) in the same spectrum as long as the interference from the secondary to the primary link stays below a given threshold. In this thesis, we propose a number of adaptive transmission schemes aiming at improving the performance of the secondary link in these systems while satisfying the interference constraint set by the primary receiver (PR). In the proposed techniques, the secondary transmitter (ST) adapts its transmission settings based on the availability of the channel state information (CSI) of the secondary and the interference links. In this context, these schemes offer different performance tradeoffs in terms of spectral efficiency, energy efficiency, and overall complexity.

In the first proposed scheme, power adaptation (PA) and adaptive modulation (AM) are jointly used with switched transmit diversity in order to increase the capacity of the secondary link while minimizing the average number of antenna switching. Then, the concept of minimum-selection maximum ratio transmission (MS-MRT) is proposed as an adaptive variation of maximum ratio transmission (MRT) in a spectrum sharing scenario in order to maximize the capacity of the secondary link while minimizing the average number of transmit antennas. In order to achieve this performance, MS-MRT assumes that the secondary's CSI (SCSI) is perfectly known at the ST, which makes this scheme challenging from a practical point of view. To overcome this challenge, another transmission technique based on orthogonal space time bloc codes (OSTBCs) with transmit antenna selection (TAS) is proposed. This scheme uses the full-rate full-diversity Alamouti scheme in an underlay CR scenario in order to maximize the secondary's transmission rate.

While the solutions discussed above offer a considerable improvement in the performance of spectrum sharing systems, they generally experience a high overall system complexity and are not optimized to meet the tradeoff between spectral efficiency and energy efficiency. In order to address this issue, we consider using spatial modulation (SM) in order to come with a spectrum sharing system optimized in terms spectral efficiency and energy efficiency. Indeed, SM can be seen as one of the emerging and promising new technologies optimizing the communication system while reducing the energy consumption thanks to the use of a single radio frequency (RF) chain for transmission. In this context, we propose the adaptive spatial modulation (ASM) scheme using AM in order to improve the spectral efficiency of SM. We also extend ASM to spectrum sharing systems by proposing a number of ASM-CR schemes aiming at improving the performance of these systems in terms of spectral efficiency and energy efficiency.

While the use of a single RF-chain improves the energy efficiency of the above schemes, the RF-chain switching process between different transmissions comes with additional complexity and implementation issues. To resolve these issues, we use the concept of reconfigurable antennas (RAs) in order to improve the performance of space shift keying (SSK). In this context, employing RAs with SSK instead of conventional antennas allows for implementing only one RF chain and selecting different antenna-states for transmission without the need for RF switching. Moreover, the reconfigurable properties of RAs can be used as additional degrees of freedom in order to enhance the performance of SSK in terms of throughput, system complexity, and error performance. These RAs-based schemes are also extended to spectrum sharing systems in order to improve the capacity of the secondary link while reducing the energy consumption and the implementation complexity of the SU.

In summary, we propose in this thesis several adaptive transmission schemes for spectrum sharing systems. The performance of each of these schemes is confirmed via Monte-Carlo simulations and analytical results and is shown to offer different tradeoffs in terms of spectral efficiency, energy efficiency, reliability, and implementation complexity. In this context, these proposed schemes offer different solutions in order to improve the performance of underlay cognitive radio systems.

To my family

Acknowledgments

I would like to acknowledge many people who helped me during the course of this work. First, I would like to express my gratitude to my thesis advisor, Professor Ali Ghrayeb, for giving me the chance to take part of his research group. I am greatly indebted to him for his full support and availability. His broad expertise and valuable discussions have greatly influenced my technical skills and are reflected throughout the presentation of this dissertation.

I am also grateful to my co-advisor, Professor Khalid Qaraqe, for providing guidance and timely help during my visit to Texas A&M University at Qatar. His constant encouragement and support made this work successful.

I would also like to thank Professor Mohamed-Slim Alouini for his continuous collaboration and support. His valuable discussions and recommendations have tremendously contributed to my career as a researcher.

I am thankful to Dr. Mohamed Abdallah, Dr. Kamel Tourki, Dr. Hassan El-Sallabi, and several other group-mates for their collaborations and valuable discussions that are reflected in many of the results presented in this thesis.

I am also very thankful to all of my proposal and defense examination committee members for providing constructive comments that certainly improved the presentation of this thesis.

I would like to express my greatest and deepest appreciation to my family. My father and mother have always believed in me and have supported every endeavor of mine with full faith and confidence. My journey in accomplishing this work would not have been that easy without a faithful and supportive companion, I have always known that my wife is that best friend who was always there for me. With all the time she has provided, she was an exemplar mother for our kids Fatima, Idriss, and Anas. These little ones have always been a source of joy and tranquility for both of us. In reality, this thesis is partly theirs too.

Contents

List of Tables

List of Algorithms

List of Figures

List of Symbols

N_t number of transmit antennas

N_r number of receive antennas

Q peak interference constraint

L number of antennas verifying Q

S set of antennas verifying Q

$\mathbf{x}$ vector $\mathbf{x}$

$\mathbf{X}$ matrix $\mathbf{X}$

$\boldsymbol{\eta}$ AWGN noise

$\mathbf{H}$ MIMO channel matrix

$(\mathbf{x})^T$ transpose of vector $\mathbf{x}$

$(\mathbf{x})^H$ conjugate transpose of vector $\mathbf{x}$

$(\mathbf{x})^*$ complex conjugate of vector $\mathbf{x}$

$\|\mathbf{X}\|_{\mathrm{F}}$ Frobenius norm of a matix

$\mathrm{E}(a)$ expectation of random variable a

$|\mathcal{C}|$ cardinality of a set $\mathcal{C}$

$\mathrm{Pr}(a)$ probability of event a

$\Gamma(\cdot,\cdot)$ upper incomplete Gamma function

$\gamma(\cdot,\cdot)$ lower incomplete Gamma function

$F(\cdot)$ cumulative distribution function

$f(\cdot)$ probability density function

P_{out} outage probability

$P_{e,\mathrm{bit}}$ probability of bit error

$\Re(\cdot)$	real part of a complex variable
$\Im(\cdot)$	imaginary part of a complex variable
$\log_a(\cdot)$	the logarithm with base a
$\arg\max\limits_{x} f(x)$	a value of x that maximizes $f(x)$
$\arg\min\limits_{x} f(x)$	a value of x that minimizes $f(x)$
$\mathcal{N}(m, \sigma^2/2)$	Gaussian distribution of a random variable with mean m and varaiance $\sigma^2/2$
$\mathcal{CN}(m, \sigma^2)$	complex Gaussian distribution of a random variable having independent real and imaginary parts $\mathcal{N}(m, \sigma^2/2)$

List of Acronyms

ABER   Average bit error rate

ACT   Actual modulation variation

AM   Adaptive modulation

APM   Amplitude and phase modulation

APS   Adaptive power scheme

ASE   Average spectral efficiency

ASM   Adaptive spatial modulation

AWGN   Additive white Gaussian noise

BAS   Best antenna selection

BER   Bit error rate

CDF   Cumulative distribution function

CM   Coded modulation

CR   Cognitive Radio

CSI   Channel state information

FCC   Federal Communications Commission

FPS   Fixed power scheme

GSSK   Generalized space shift keying

I.i.d   Independent and identically distributed

IAS   Inter-antenna synchronization

IC   Interference constraint to the primary user

ICI	Inter-channel interference
ICSI	Interference link's channel state information
IEEE	Institute of Electrical and Electronics Engineers
INR	Interference-to-noise ratio
LOS	Line of sight
MGF	Moment generating function
MIMO	Multiple-input multiple-output
MIN	Minimum modulation variation
MISO	Multiple-input single-output
ML	Maximum likelihood
MRT	Maximum ratio transmission
MS	Minimum selection
MS-MRT	Minimum-selection maximum ratio transmission
OFDM	Orthogonal frequency division multiplexing
PDF	Probability density function
PA	Power adaptation
PEP	Pairwise error probability
PL	Primary link
PR	Primary receiver
PT	Primary transmitter
PU	Primary user
QAM	Quadrature amplitude modulation
QoS	Quality of Service
RA	Reconfigurable antenna
RF	Radio-Frequency
SE	Spectral efficiency
SINR	Signal-to-interference-and-noise ratio

SIMO	Single-input multiple output
SNR	Signal-to-noise ratio
SL	Secondary link
SCSI	Secondary link's channel state information
SM	Spatial modulation
SR	Secondary receiver
SSK	Space shift keying
ST	Secondary transmitter
STBC	Space time bloc code
SU	Secondary user
SWC	Scan and wait combining
TA	Transmit antenna
TAS	Transmit antenna selection
UB	Union bound
UWB	Ultra-WideBand

Chapter 1

Introduction

1.1 Cognitive Radio

Wireless communication systems are continuously evolving and growing, leading to an increasing need for spectrum resources. Although different spectrum bands are allocated to specific services, it has been identified that these bands are partially used or unoccupied most of the time [1,2]. Due to this underutilization, cognitive radio (CR) was proposed as one of the major solutions to enhance the spectrum usage efficiency. In underlay CR networks, also referred to as spectrum sharing systems, different wireless systems can coexist and cooperate in order to increase their spectral efficiency. In these systems, licensed primary users (PUs) and unlicensed secondary users (SUs) are allowed to coexist in the same frequency spectrum and transmit simultaneously as long as the interference of the SU to the PU stays below a predetermined threshold [3–5]. This interference constraint imposed by the PUs' receiver, also called interference temperature [1,6], guarantees reliable operation of the PUs regardless of the SUs' spectrum utilization and can badly affect the performance of the secondary link. In these settings, the SU can only transmit when the interference constraint is respected which makes the performance of the secondary link limited by the constraints set by the primary link. Consequently, maximizing the spectrum utilization, i.e., achieving the goals set by CR networks, needs to be addressed by minimizing the interference seen at the PU [7]. To this end, adaptive transmission techniques look to be very promising in these scenarios and need to be employed by CRs. Indeed, the choice of adaptive schemes perfectly matches

with the concept of CRs defined as being able to adapt their settings in order to provide wireless services most appropriate to the user needs and preferences [8].

1.2 Adaptive Transmission Techniques

In order to enhance the performance of spectrum sharing systems, several techniques have been considered in the literature. In this context, it was shown that switched diversity techniques are very helpful in improving the performance of the secondary link while respecting the interference constraint to the PU [9–11]. While the use of a single transmit antenna with these techniques minimizes the power consumption at the transmitter, it generates a loss in the average spectral efficiency (ASE). As a more spectrally-efficient solution, transmit beamforming was utilized in multiple-input multiple-output (MIMO) antenna systems in order to achieve both diversity and array gains in general wireless systems [12–14] and in CR systems in particular [15,16]. In [13], maximum ratio transmission (MRT) is proposed in order to maximize the received signal-to-noise ratio (SNR) assuming that full channel state information (CSI) is available at the transmitter. As a more practical implementation that can enhance the performance of spectrum sharing systems, multiple antenna systems can be employed to achieve full diversity order through space-time coding techniques such as space-time block codes (STBCs) [17]. STBCs offer simple maximum likelihood (ML) decoding using linear processing at the receiver. As a particular case with two transmit antennas, the Alamouti scheme [18] has been used with transmit antenna selection (TAS) as a systematic method to construct full-rate STBC with full diversity [19, 20]. Moreover, using STBC schemes with adaptive modulation (AM) yields significant performance enhancement compared to fixed modulation schemes [21] and have been efficiently implemented in several standard wireless networks, e.g. IEEE802.11, IEEE802.16. Based on multiple thresholds, AM [22–24] achieves high spectral efficiency in wireless communication systems and particularly provides much flexibility in spectrum sharing systems. The key idea of AM is to adapt the modulation parameters, such as constellation size, to the fading channel conditions while respecting the average bit error rate (ABER) requirements. AM has been recently used as a promising technique to improve the performance of CR systems [25, 26].

Although MIMO systems offer high data rates and high spectrally efficiency, several problems are encountered in the development of such systems [27–29]. These problems arise from several sources and include (i) high inter-channel interference (ICI) at the receiver due to the simultaneous transmission from multiple antennas using the same frequency, (ii) this high ICI increases the overall system complexity since complex receiver algorithms are needed, (iii) inter-antenna synchronization (IAS) is also needed at the transmitter, and (iv) multiple Radio-Frequency (RF) chains are used for each transmission which reduces the energy-efficiency of such systems [29]. In order to deal with these issues, the concepts of spatial modulation (SM) [30–32] and space-shift keying (SSK) [33, 34] are proposed as low-complexity and energy-efficient implementations of MIMO systems. Similar to SM, the key idea behind SSK is the use of a single Radio-Frequency (RF) chain during each transmission. Thus, only one antenna remains active during data transmission, which comes with the advantages of avoiding IAS and removing ICI. While SM and SSK offer this low overall system complexity, it has been shown that these modulation schemes can be implemented to offer better ABER performance as compared to that of some popular MIMO techniques including the vertical Bell Laboratories layered space-time (V-BLAST)and amplitude and phase modulation (APM) techniques as detailed in [33].

Even though the above energy-efficient implementations of MIMO techniques activate only one RF-chain for transmission, multiple RF-chains are still physically needed at the transmitter. Indeed, based on the incoming bits, the transmitter selects the chain to be activated during the next time slot. Thus, the transmitter in SM and SSK switches between RF chain from a transmission to another. This symbol-by-symbol RF switching is complex in terms of implementation and also impacts the performance of these techniques [35]. In order to address these issues, new multiple antenna designs based on parasitic antennas have been proposed in order to enable multiplexing gains with a single RF element [36, 37]. Thanks to the use of many passive antenna elements, the parasitic array in these techniques is capable of changing its radiation pattern on each symbol period and thus offering cost and energy effective solution for the implementation of MIMO systems. In more general settings, the concept of reconfigurable antennas (RAs), represents a new emerging technology that provides antennas with the ability of dynamically modifying their characteristics, such as

operating frequency, radiation pattern, and polarization [38]. This reconfiguration capability can be achieved via different approaches such as changing the physical structure of the antenna, altering the feed methods, and controlling the current density. Thanks to these techniques, the reconfigurable properties of RAs can be used as additional degrees of freedom in order to improve the performance of wireless communication systems including MIMO techniques [39–41].

1.3 Motivation

The importance of spectrum in wireless communication systems makes the concept of spectrum sharing systems a timely topic to investigate. Indeed, cognitive radio is expected to have a major role in many future wireless communication systems in order to address the problems of spectrum scarcity and underutilization [42]. In this context, taking advantage of this highly interesting topic, we aim at contributing to the optimization of the existing solutions, proposing new adaptive transmission schemes for underlay CR systems, and considering practical scenarios for the implementation of these techniques in future wireless communication systems.

Referring to the existing literature, we can find several adaptive techniques that have been considered in order to improve the performance of underlay cognitive radio systems. However, the effects of different adaptive solutions on the performance of these systems have been studied separately. While considering each of these techniques separately improves the performance of the secondary link, the performance improvement offered by their joint implementation in spectrum sharing systems needs to be investigated. In this context, based on specific design and optimization problems, we first identify the appropriate adaptive solutions to be used then we combine these solutions in an effort to reach the performance set by these problems. Taking advantage of the joint implementation of these adaptive transmission solutions, we can increase the number of available degrees of freedom which can exploited in order to enhance the performance of spectrum sharing systems.

While the transmission solutions discussed above offer a considerable improvement in the performance of spectrum sharing systems, they generally experience a high overall system

complexity and are not optimized to meet the tradeoff between spectral efficiency and energy efficiency. In order to address this issue, the proposed transmission techniques need to be designed while considering a tradeoff between spectral-efficiency and energy efficiency. Moreover, in more practical settings for their implementation in real communication systems, these techniques need to be cost-effective and to come with low complexity.

In light of the above, we aim at proposing new transmission schemes based on the joint use of a number of adaptive techniques in order to improve the performance of spectrum sharing systems. The main motivation behind this thesis is to make these transmission solutions appropriately designed in order to fit in the context of future wireless communication systems. To this end, these adaptive transmission schemes need to be jointly designed and optimized in terms of spectral efficiency, energy efficiency, implementation cost, and overall system complexity. This joint design will definitely address the requirements in order to be implemented in future wireless systems in general and in underlay cognitive radio systems in particular.

1.4   Thesis Contributions

Against the above motivations and apparent challenges, we propose in this thesis a number of adaptive transmission schemes aiming at improving the performance of spectrum sharing systems. Based on these proposed schemes and the related results, the contributions of the thesis can be summarized as follows:

- Under the scenario of spectrum sharing systems, we propose an adaptive transmission scheme using transmit power adaptation (PA), switched transmit diversity, and adaptive modulation [43]. Taking advantage of the channel reciprocity principle, we assume that the CSI of the interference link (denoted by ICSI) is available to the secondary transmitter (ST). This information is then used by the ST to adapt its transmit power, modulation constellation size, and used transmit branch. The goal of this joint adaptation is to minimize the average number of switched branches and the average system delay given the fading channel conditions, the required error rate performance, and a peak interference constraint to the primary receiver (PR). Confirming our previous

discussion, the joint use of three adaptive techniques in the proposed scheme offers considerable performance improvement when compared to selected existing schemes which separately use the same adaptive techniques.

- Although the PA schemes discussed above improves the performance of spectrum sharing systems, it requires perfect ICSI which can be impractical especially in CR networks. In order to address this, we propose a number of adaptive transmission techniques based on limited feedback from the PR [44,45]. In this case, only one bit is fed back by the PR to let ST know if the transmission from an antenna verifies the interference constraint or not. In this context, we first introduce the concept of minimum-selection maximum ratio transmission (MS-MRT) as an adaptive variation of the existing MRT technique. While in MRT all available antennas are used for transmission, MS-MRT uses the minimum subset of antennas verifying both the interference constraint to the PU and the ABER requirements. Similar to MRT, MS-MRT assumes that perfect CSI of the secondary link (SCSI) is available at the ST, which makes this scheme challenging from a practical point of view. To overcome this challenge, we propose another transmission technique based on STBC with transmit antenna selection. This technique uses the full-rate full-diversity Alamouti scheme in order to maximize the secondary's transmission rate. The performance of these techniques is analyzed in terms of the ASE, average number of transmit antennas, average delay, ABER, and outage performance. In order to give the motivation behind these analytical results, the tradeoffs offered by the proposed schemes are summarized and the advantages of using each adaptive scheme are highlighted.

- While the solutions discussed above offer a considerable improvement in the performance of the studied spectrum sharing systems, these techniques are not generally optimized for the tradeoff between spectral efficiency and throughput in one side vs. energy efficiency and low-complexity on the other side. Thus, we have to think about using new air-interface transmission technologies designed to find the best energy efficiency vs. spectral efficiency tradeoff. Motivated by the advantages of SM, we propose an adaptive transmission scheme using AM and SM, namely adaptive spatial modula-

tion (ASM) [46]. This proposed scheme improves the spectral efficiency of SM while offering a low energy consumption and a reduced system complexity. We have also extended ASM to spectrum sharing systems by proposing a number of ASM-CR schemes aiming at improving the performance of these systems in terms of spectral efficiency and energy efficiency. [47–49].

- In spite of the fact that ASM-CR schemes improve the performance of spectrum sharing system in terms of spectral efficiency and energy efficiency, they experience complexity and implementation due RF switching from symbol-to-symbol. In order to address this issue, we use the concept of reconfigurable antennas in an effort to improve the performance of SM and SSK by proposing a number of SSK-RA schemes [50,51]. Indeed, the reconfigurable properties of RAs can be used as additional degrees of freedom in order to enhance the performance of SM and SSK in terms of throughput, system complexity, and error performance. These SSK-RA schemes are also extended to spectrum sharing systems in order to improve the capacity of the secondary link while implementing an energy efficient and low-complexity secondary user.

1.5   Thesis Outline

The rest of thesis is organized as follows:

In Chapter 2, we present a brief background about the enabling techniques used in the proposed schemes for spectrum sharing systems. We start with an introduction to cognitive radio networks in general including spectrum sharing systems as a special case. Then we define each of the used techniques and the related work that was done in the literature. In this context, we first introduce the solutions proposed in order to maximize the spectral efficiency and the reliability of spectrum sharing systems. We then present the concept of single-RF MIMO including SM and SSK as main solutions to optimize the performance of communication systems in terms of the energy efficiency - spectral efficiency tradeoff. We finally introduce the concept of reconfigurable antennas and how can these antennas be used in order to improve the performance of future wireless communication systems in general and of spectrum sharing systems in particular.

In Chapter 3, we propose a number of adaptive transmission techniques offering different performance tradeoffs depending on the availability of the CSI at the ST. Assuming that the ICSI is fully available at the ST, we use PA jointly with adaptive modulation and switched transmit diversity in a first scheme. For limited ICSI, we introduce the MRT-CR technique as an extension of MRT to a spectrum sharing scenario. We then propose MS-MRT as a power saving implementation of MRT-CR. This novel adaptive transmission technique and its analysis including high SNR approximations are among the major contributions. While in MRT-CR and MS-MRT the ST requires full SCSI, we propose TAS/STBC in a more practical scenario to maximize the secondary user's capacity while only requiring a limited SCSI at the ST. We finally propose the hybrid scheme in order to reduce the delay experienced by the TAS/STBC scheme. In this chapter, the performance of these schemes in compared and confirmed via simulations and analysis.

In Chapter 4, we propose adaptive spatial modulation as an adaptive transmission scheme using AM and SM. This proposed scheme improves the spectral efficiency of SM while offering a low energy consumption and a reduced system complexity. In order to take advantage of ASM's promising performance, we also extend ASM in this chapter to spectrum sharing systems by proposing a number of ASM-CR schemes aiming at improving the performance of these systems in terms of spectral efficiency and energy efficiency based on a limited feedback from the primary user. In this chapter, we analyze the performance of these schemes in terms of ASE, average delay, and average bit error rate. We show that the proposed schemes offer tradeoffs in terms of the previously mentioned performance metrics, thus offering different options for applying ASM to CR systems. We also provide several simulation examples through which we corroborate the analytical results.

In Chapter 5, we use the concept of reconfigurable antennas in an effort to improve the performance of SM and SSK by proposing a number of SSK-RA schemes. In this context, we take advantage of reconfigurable properties of RAs as additional degrees of freedom in order to enhance the performance of SM and SSK in terms of throughput, system complexity, and error performance. Indeed, based on the variation of the Rician K-factor and the polarization correlation coefficients with different antenna states, the proposed schemes in this chapter jointly optimize the fading and correlation parameters in order to improve the performance

of SSK. These SSK-RA schemes are also extended to spectrum sharing systems in order to improve the capacity of the secondary link while implementing an energy efficient and low-complexity secondary user. The results presented in this chapter are confirmed via simulations and analysis.

In Chapter 6, we conclude our work with a brief summary about the proposed techniques and the major advantages of proposing these adaptive solutions. Based on this, we suggest some potential topics for future research.

Chapter 2

Background

In this chapter, we give a brief introduction about the enabling techniques used in our work. We start by introducing the concept of cognitive radio in general and the case of spectrum sharing systems in particular. Next, we introduce the solutions used in order to maximize the spectral efficiency and the reliability of these systems. In particular, we introduce the concepts of adaptive modulation, power adaptation, and switched transmit diversity. The particular choice of these techniques is due to their common *adaptive* property. Indeed, this property agrees with the concept of CR where a SU is defined as being able to adapt its properties to its surrounding environment. Thus, the use of adaptive techniques in a CR system offers much flexibility and justifies our focus on these solutions. However, many of the existing techniques are not optimized for the energy efficiency vs. spectral efficiency tradeoff which represents a main concern in the design of next-generation wireless networks. In order to come with a system having low overall complexity, high spectral efficiency, and reduced power consumption, the joint use of SM (equivalently SSK) with reconfigurable antennas seems to be very promising. In this context, the concepts of SM, SSK, and reconfigurable antennas are introduced in this chapter too.

2.1 Cognitive Radio

Wireless communication systems are continuously evolving and growing, leading to an increasing need for spectrum resources. Although different spectrum bands are allocated to

specific services, it was identified that these bands are unoccupied most of the time or partially used by the primary users [1, 2]. Thus, we need to do something in order to optimize the usage of this scarce spectrum resource. Cognitive radio was proposed as one of these solutions enhancing the spectrum usage efficiency. It is defined by the Federal Communications Commission (FCC) as a radio that can change its transmitter parameters according to the interactions with the environment in which it operates [1]. Depending on the ability of the SU to coexist and transmit simultaneously with the PR and on the spectrum usage, several strategies are considered.

2.1.1 Interweave CR

In interweave CR systems, also called opportunistic spectrum access systems, SUs are only allowed to use the spectrum when the PU is not active. Thus, no interference is tolerated by the PU. In opportunistic spectrum access, the SU exploits the *spectrum holes* left by the PU as shown in Fig. 2.1. In order to locate these spectrum holes and equivalently detect the PU's existence, *spectrum sensing* needs to be done by the CR. The main difculty in the interweave scheme is that of sensing and predicting the activity of the PU in several radio channels especially for highly dynamic PUs (i.e., PUs having a fast spectral activity change). Spectrum sensing performance depends also on the range of the secondary transmission. Indeed, the primary activity sensed by the secondary transmitter and secondary receiver may vary due to different primary signal's strengths. These factors decrease the correlation between the spectrum sensed at the transmitter and at the receiver which reduces the effectiveness of secondary spectrum utilization.
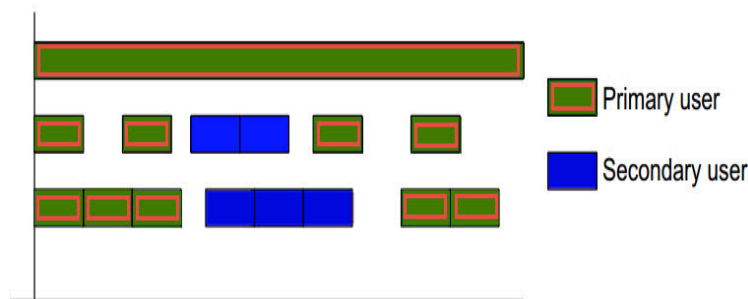
Figure 2.1: Interweave CR.

2.1.2 Spectrum Sharing Systems

In spectrum sharing systems (Fig. 2.2), also called underlay cognitive radio systems, the SU and PU can coexist simultaneously on the same spectrum as long as the SU ensures that the interference temperature of the primary user does not exceed a predefined limit. Rather than time and frequency agile radios, the SU needs to transmit at very low power and the secondary transceiver must be able to operate at very low SNR. This typically restricts underlay CR to low data rate applications or very short range applications such as personal area networks. Underlay CR has been adopted by regulatory bodies worldwide, and is allowed when SUs transmit using the Ultra-wideband (UWB) signal format. Due to the restrictive regulations, the applicability of UWB is limited to very short range applications, below 10m, but longer range operation, up to 300m, is possible but at very low data rates.
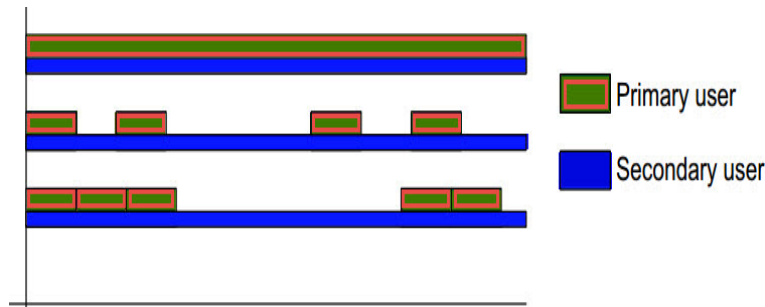
Figure 2.2: Underlay CR.

Unlike opportunistic CR systems, the ST in spectrum sharing systems adapts its transmission settings to the interference seen at the PR. While this comes with the advantage of removing the hardware required for spectrum sensing, it requires the existence of a coordination between the PR and the ST. This coordination can be done through a band-manager which can exchange control information between PUs and SUs [52]. Different levels of such coordination have been considered in the literature: while [11, 15, 16] assume that the interference link is perfectly known at the ST, [10, 53, 54] assume that the ST is only provided with partial knowledge of the interference channel. For the partial knowledge case, the authors in [10] assume that there is only a one bit ACK/NACK feedback process to let the ST know if a given antenna verifies or violates the interference temperature at the PR. One

practical model of spectrum sharing systems using coordination between the PR and the ST is cognitive femtocells networks which have been adopted in the 3GPP Long Term Evolution (LTE) standard [55, 56]. In this thesis, we propose spectrum sharing systems for both the case where full CSI about the interference link is available and the case where only a limited feedback exists between the PR and ST.

2.1.3 Overlay CR

In the overlay approach (Fig. 2.3), the SU have to pay a price in order to access the PU's spectrum. Indeed, the SU devotes part of its transmit power to enhance the primary signal and to facilitate its detection at the primary receiver. In exchange, the secondary may be allowed to increase the interference temperature level further and thus to achieves higher performance than the underlay approach. This help handed to the PU by the secondary and its contribution to improve the detection of the PU may also contribute to a higher acceptance of this technique by primary licensees. Thus, the overlay approach can be seen as an evolutionary step from the underlay technique, where a tighter degree of integration between primary and secondary users is necessary.
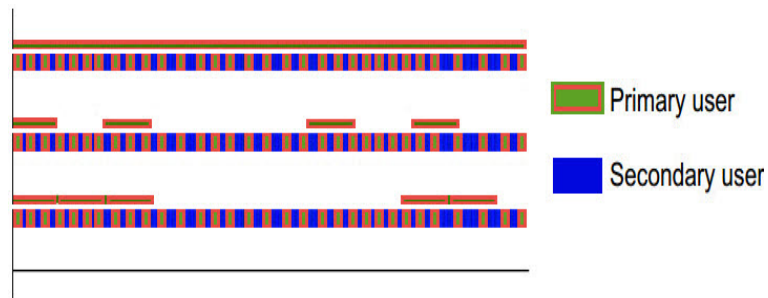
Figure 2.3: Overlay CR.

2.2 Adaptive Solutions

In this section, we introduce a couple of solutions used in our work in order to improve the performance of spectrum sharing systems. As pointed out before, the choice of adaptive techniques in CR systems offers much flexibility and justifies our focus on these solutions.

The discussed techniques are AM, PA, transmit diversity techniques, MRT, SM and SSK for MIMO systems, and RAs.

2.2.1 Rate and Power Adaptation

Based on multiple thresholds, AM can achieve high spectral efficiency in wireless communication systems and provides much flexibility in spectrum sharing systems. The key idea of AM is to adapt the modulation parameters, such as constellation size, to the fading channel conditions while respecting the bit error rate requirements [22–24]. Adaptive modulation has been used as a promising technique to improve the performance of CR systems [25, 26].

In addition to AM, PA techniques can be be useful in improving the performance of wireless communication systems in general and particulary the considered case of spectrum sharing systems where the secondary transmitter needs to verify the interference constraint [25]. Indeed, adaptive power control schemes, unlike schemes using a constant-power variable-rate setup, adapt the transmitted power to fading channels conditions while fullling the BER constraint [57, 58]. These schemes reduce the radiated power, and thus the potential interference to other systems/users which implies a signicant network capacity improvements.

Considering the case where the CSI of the interference link is perfectly known at the ST, PA was employed as an efficient solution to maximize the capacity of the secondary link while satisfying a peak/average interference constraint [7, 25]. While in [59], [60] rate adaptation is used with switched transmit diversity without PA, the authors in [25] use joint rate and PA in a typical spectrum-sharing system in order to maximize the SU's capacity. Considering the case of multiple antennas at the transmitter and that this latter is power limited, we can extend the schemes proposed in [59], [60] to a more practical scenario using joint power and rate adaptation. Thanks to PA, we can considerably reduce the average number of switched antennas experienced by the existing schemes.

2.2.2 Transmit Diversity Techniques

Another class of adaptive techniques that we use in order to increase the performance of the studied spectrum sharing systems is transmit diversity. In particular, switched diversity

techniques improve the reliability of wireless fading channels by adapting the transmitter structure to fading channel conditions and are very useful in mitigating the deleterious effect of fading [61]. In underlay CR, the performance of the secondary link can be badly affected because of the interference constraint to the primary user. In such scenarios, transmit diversity techniques are very helpful in improving the performance of the secondary link while respecting the interference constraint to the primary user [11, 59, 60]. Dual-antenna switch and stay (SSC) is one of these switching combining techniques that received a great deal of attention [62–65]. In this technique, the current antenna is used as long as the SNR is above a predetermined threshold, otherwise the transmitter switches and uses the second antenna. Switch and examine (SEC) has been proposed as alternative of SSC to take advantage of the additional diversity antennas [66]. The scan and wait (SWC) technique was then proposed in [67] in order to improve the performance of SEC and other traditional combining techniques at the expense of some time delay. In the SWC technique, the transmitter buffers data for a channel coherence time whenever none of the available diversity paths is able to reach a predetermined minimum quality requirement. The process of scanning and waiting is repeated indefinitely until an acceptable path is found. In the proposed schemes in this thesis, we use the same process as SWC if not enough antennas verify the interference constraint.

2.2.3 Maximum Ratio Transmission

Although the transmitter in the discussed transmit diversity techniques is equipped with multiple antennas, only one antenna is used for transmission which gives lower diversity efficiency than the case of multiple transmit antennas. More efficiently, multiple antenna systems can be employed to achieve full diversity order through space-time coding techniques such as OSTBCs [17]. These techniques offer simple ML decoding using linear processing at the receiver. As a particular case with two transmit antennas, the Alamouti scheme [18] has been used with TAS as a systematic method to construct full-rate STBC with a full diversity order [19]. Even more efficiently, assuming that perfect SCSI is available at the ST, the performance of multiple-antenna systems can be considerably improved through the usage of transmit beamforming. Indeed, transmit beamforming is used in general wireless systems [12–14] and in CR systems in particular [15, 16] and allows to achieve both diversity

and array gains. In [13], MRT is proposed in order to maximize the received SNR and was not studied in a spectrum sharing scenario. Thus the use of MRT is underlay CR systems can lead to a significant capacity improvement.

2.3 SM and SSK for MIMO Systems

Although the previously discussed solutions offer a considerable improvement in the performance of CR systems, these techniques are not generally optimized for the tradeoff between spectral efficiency and throughput in one side vs. energy efficiency and low-complexity in the other side. Indeed, these techniques either come with a high spectral efficiency at the expense of an increased system complexity and energy consumption or reduce the energy consumption at the expense of an increased complexity and/or a low spectral efficiency. Thus, to get advantage from the performance of MIMO systems, new air-interface transmission technologies need to be designed to find the best energy efficiency vs. spectral efficiency tradeoff mentioned above. Future networks using these technologies should be (i) heterogeneous with the use of small, inexpensive, and low power cells, (ii) throughput and energy optimized, (iii) cooperative in order to achieve better coverage and lower energy consumption, and (iv) using new transmission techniques increasing the energy efficiency and reducing the signal processing complexity.

2.3.1 MIMO Systems

MIMO systems use multiple antennas at both transmitter and/or receiver terminals in order to achieve higher throughput without increasing the amount of bandwidth and transmit power requirements. Indeed, MIMO technologies are at the origin of famous standards including WiMAX and LTE and considered to be very promising for the design of future wireless communications, including the fifth generation cellular networks (5G) [68]. While MIMO's spectral efficiency advantages are widely recognized, its energy efficiency needs to be more optimized. Indeed, MIMO shows modest energy efficiency for a high number of transmit antennas if realistic power consumption models are considered for the base stations [69]. Moreover, MIMO systems' implementation comes with an increased signal processing com-

plexity, stringent synchronization requirements among the transmit antennas, and multiple RF chains. In order to deal with these issues, the concept of single-RF MIMO is proposed as a promising research topic addressing MIMO concerns while achieving similar gains thanks to the use of a single activated antenna [70].

2.3.2 Spatial Modulation

SM in the Literature

The concept of SM was proposed in [30, 31] as a low-complexity and energy efficiency implementation of MIMO systems and falls under the family of single-RF MIMO discussed above. Before this, the principle of "spatial modulation" was discussed in the literature but with different meanings and scenarios. First discussed in [71], a version of SM that exploits the differences in the signals received from different transmit antennas to discriminate the transmitted information messages is introduced. Then, a multi-antenna modulation scheme where a number of bits equal to the number of transmit antennas is multiplexed in an orthogonal fashion is proposed in [72]. A channel hopping technique, known today as SM-MIMO, is also proposed in [73] where both the signal dimension and spatial dimensions are used to convey the information. Since it was first proposed, a lot of attention was given to SM as an enabling part of the future wireless communication systems which satisfies the spectral efficiency - energy efficiency tradeoff. An extensive research work is being done on the SM-MIMO concept [74]. For instance, SM performance in correlated and uncorrelated Nakagami fading channel is analysed in [75]. In [76] a soft-output maximum-likelihood detector for SM OFDM systems is proposed. Trellis coded SM (TCSM) and fractional bit encoded SM (FBE-SM) were also considered in [77] and [78] respectively.

SM Transmission

We consider the system model shown in Fig. 2.4 consisting of a MIMO wireless link with N_t transmit and N_r receive antennas. If antenna j is selected for transmission, then $m =$

Figure 2.4: SM System model.

$\log_2(M\,N_t)$ bits are grouped and mapped the constellation vector

$$\boldsymbol{x}_{jq} = [0 \ldots 0 \quad \underset{\underset{j^{th}\,\text{position}}{\uparrow}}{x_q} \quad 0 \ldots 0]^T.$$

The signal x_{jq} is then transmitted over an $N_r \times N_t$ wireless channel $\boldsymbol{H}$ and experiences an N_r-dim additive white Gaussian noise (AWGN) $\boldsymbol{\eta} = [\eta_1, \ \eta_1 \ldots, \ \eta_{N_r}]^T$. $\boldsymbol{H}$ and $\boldsymbol{\eta}$ have independent and identically distributed (i.i.d) entries according to $\mathcal{CN}(0,1)$. The output of the channel when x_q is transmitted from the jth antenna can be expressed as

$$\boldsymbol{y} = \sqrt{\rho}\,\boldsymbol{h}_j\,\boldsymbol{x}_q + \boldsymbol{\eta}, \tag{2.1}$$

where ρ is the average SNR at each receive antenna and $\boldsymbol{h}_j = [h_{j1} \ \ h_{j2} \ldots h_{jN_r}]^T$ denotes the jth column of $\boldsymbol{H}$.

An example of an SM mapper for $N_t = 4$ and $M = 2$ (i.e., 3 bits/s/Hz) is given in Table 2.1. Two information bits are used to select the transmit antenna and the third bits is mapped to a BPSK symbols.

Optimal SM Detection

The detector's main function is to find the antenna index used for transmission and the symbol sent by that antenna. Assuming equally likely channel inputs, this information can be jointly obtained using the optimal SM detector based on the ML principle proposed in [32]

$\boldsymbol{b}$	x	antenna j	$\boldsymbol{x}$
[0 0 0]	+1	1	$[1\ 0\ 0\ 0]^T$
[0 0 1]	-1	1	$[-1\ 0\ 0\ 0]^T$
[0 1 0]	+1	2	$[0\ 1\ 0\ 0]^T$
[0 1 1]	-1	2	$[0\ -1\ 0\ 0]^T$
[1 0 0]	+1	3	$[0\ 0\ 1\ 0]^T$
[1 0 1]	-1	3	$[0\ 0\ -1\ 0]^T$
[1 1 0]	+1	4	$[0\ 0\ 0\ 1]^T$
[1 1 1]	-1	4	$[0\ 0\ 0\ -1]^T$

Table 2.1: SM Mapper Rule Example

as

$$
\begin{aligned}
[\hat{j}, \hat{q}] &= \arg \max_{j,q} f_{\boldsymbol{Y}}(\boldsymbol{y}|\boldsymbol{x}_{jq}, \mathbf{H}) \\
&= \arg \min_{j,q} \sqrt{\rho}\|\boldsymbol{g}_{jq}\|_{\mathrm{F}}^2 - 2\Re\{\boldsymbol{y}^H \boldsymbol{g}_{jq}\},
\end{aligned}
\tag{2.2}
$$

where $\boldsymbol{g}_{jq} = \boldsymbol{h}_j \boldsymbol{x}_q,\ 1 \le j \le N_t,\ 1 \le q \le M$, and

$$
f_{\boldsymbol{Y}}(\boldsymbol{y}|\boldsymbol{x}_{jq}, \mathbf{H}) = \pi^{N_r} exp\left(-\|\boldsymbol{y} - \sqrt{\rho}\,\mathbf{H}\,\boldsymbol{x}_{jq}\|_{\mathrm{F}}^2\right)
\tag{2.3}
$$

is the probability density function (PDF) of the received signal conditioned on $\boldsymbol{x}_{jq}$ and $\mathbf{H}$.

2.3.3 Space Shift Keying

SSK in the Literature

Jeganathan *et al.* proposed SSK in [33] where antenna indices are used as the only mean to relay information. SSK can be seen as a subset of SM where the elimination of APM offers, including SM's advantages, lower detection complexity, equivalent performance to SM, less stringent receiver requirements, and easy integration within communication systems. A lot of research has been done in the study of these techniques. For instance, the performance of SSK has been studied in several scenarios including MISO correlated Nakagami-m channels with arbitrary correlation and fading parameters [79], MIMO correlated Rician fading channels [80], and MIMO Rayleigh fading channels with imperfect channel estimations [81]. SSK

was also used in the context of cooperative communications in order to enhance its spectral efficiency and network coverage. For instance, SSK with amplify-and-forward relaying is proposed and analysed in [82] and with multiple cooperative relays in [83] in an attempt to develop SSK-based systems achieving both transmit and receive diversity. SSK coded modulation (CM) was also proposed in [34] and demonstrates higher capacity results and much better ABER performance compared to APM-CM techniques. In [84], the authors extend SSK to a generalized version (GSSK) where more than one transmit antenna remain active in every channel use.

SSK Transmission

If antenna j is selected for transmission, then $m = \log_2(N_t)$ bits are grouped and mapped the constellation vector

$$\boldsymbol{x}_j = [0 \dots 0 \quad \underset{\substack{\uparrow \\ j^{th}\,\text{position}}}{1} \quad 0 \dots 0]^T.$$

An example of an SSK mapper for $N_t = 4$ (i.e., 2 bits/s/Hz) is given in Table 2.2.

$\boldsymbol{b} = [b_1 \ b_2]$	antenna j	$\boldsymbol{x}$
[0 0]	1	$[1\ 0\ 0\ 0]^T$
[0 1]	2	$[0\ 1\ 0\ 0]^T$
[1 0]	3	$[0\ 0\ 1\ 0]^T$
[1 1]	4	$[0\ 0\ 0\ 1]^T$

Table 2.2: SSK Mapper Rule Example

The received signal with SSK is $\boldsymbol{y} = \sqrt{\rho}\,\boldsymbol{h}_j + \boldsymbol{\eta}$, and the optimal ML detector finding the transmit antenna index is given by

$$
\begin{aligned}
\hat{j} &= \underset{j}{\arg\max} \ \ p_{\boldsymbol{Y}}(\boldsymbol{y}|\boldsymbol{x}_j, \boldsymbol{H}) \\
&= \underset{j}{\arg\min} \ \ \|\boldsymbol{y} - \sqrt{\rho}\,\boldsymbol{h}_j)\|_{\mathrm{F}}^2 \\
&= \underset{j}{\arg\max} \ \ \Re\left\{ \left(\boldsymbol{y} - \frac{\sqrt{\rho}}{2}\,\boldsymbol{h}_j\right)^H \boldsymbol{h}_j \right\}
\end{aligned}
\tag{2.4}
$$

2.4 Reconfigurable Antennas

Multiple antenna communication systems are based on conventional antenna theory in the sense that each antenna has fixed antenna characteristics. Conventional antennas typically have a fixed radiation pattern at a specific operating frequency and bandwidth. The interplay between the antenna directional response with the propagation channel determines the characteristics of radio channels. On the other hand, RAs is a new emerging technology that provides antennas with the capability of dynamically modifying their characteristics, such as operating frequency, radiation pattern, and polarization. This reconfiguration capability can be achieved via different approaches such as changing the physical structure of the antenna, altering the feed methods, and controlling the current density. The geometry of different paths for different current distributions determines how the antenna radiates its energy into a propagation channel and how the antenna receives radio frequency from this channel. The path geometry control is performed as internal mechanisms via different techniques including RF switches, varactors, and tunable materials [38]. RA technology is different from smart antenna technology since the reconfiguration process lies inside the antenna rather than in the external network as in beam-forming network. The most challenging part in antenna reconfiguration is the capability of the RA to tune several antenna parameters simultaneously such as resonance frequency, radiation pattern and polarization. For instance, the pattern reconfiguring of a dipole antenna takes place via its polarization parameter α. This parameters modifies the antenna gain pattern for both vertical and horizontal polarizations. These antenna gains can be written as follows [85]

$$G_v(\theta, \phi, \alpha) = 1.64 \Big(\cos\theta \cos\phi \sin\alpha - \sin\theta \cos\alpha \Big)^2 \frac{\cos^2(\pi\zeta/2)}{(1-\zeta^2)^2} \tag{2.5}$$

$$G_h(\theta, \phi, \alpha) = 1.64 \sin^2\phi \, \sin^2\alpha \, \frac{\cos^2(\pi\zeta/2)}{(1-\zeta^2)^2}, \tag{2.6}$$

where α is the angle between the antenna and the z-axis withe respect to the vertical zx-plane, $\zeta = \sin\theta \cos\phi \sin\alpha + \cos\phi \cos\alpha$, and the coefficient 1.64 corresponds to the directivity of the half-wavelength dipole antenna. The angles θ and ϕ are the elevation and azimuthal angles of the rays arriving from the dipole antennas dipole antenna with respect to the z-axis

and the x-axis, respectively.

In light of the above, the core idea of the wireless communication systems based on RAs relies on how to exploit the interplay between the impulse response of the propagation channel and different RAs' antenna radiation states. Indeed, each antenna radiation state may have different interplay with multipath components. Consequently, the radio channel characteristics are affected in different RF propagation domains, i.e., delay, angular and Doppler domains. For line of sight (LOS) communications, one of the important parameters that can be affected by the interplay results is the Rician channel K factor in line of sight radio channel channels. The interplay can increase and decrease is the Rician K factor and this variation can be exploited in order to improve the performance of wireless communication systems. The variability of K for different antenna radiation states can be given as [86]. In this context, the reconfigurable properties of RAs can be used as additional degrees of freedom in order to improve the performance of wireless communication systems including MIMO techniques [39–41].

2.5   Conclusion

Based on the background presented in this chapter, we come to the conclusion that the use of the discussed adaptive solutions in CR scenarios comes with a considerable performance improvement both in terms of spectral efficiency and energy efficiency. Moreover, the use of reconfigurable antennas seems to be promising in further improving spectrum sharing systems in terms of implementation complexity. In what follows, we present our proposed schemes based on the techniques defined above.

Chapter 3

Adaptive Solutions for MISO Spectrum Sharing Systems

3.1 Introduction

In this chapter, we propose a number of adaptive transmission techniques in order to improve the performance of the secondary link in a spectrum sharing system subject to the availability of the CSI at the ST. The first scheme uses power adaptation in order to verify the interference constraint to the PU and thus requires perfect knowledge of the interference link. In all other schemes, we assume a limited feedback from the PR to the ST. Indeed, the only information available to the ST is a single bit feedback indicating whether a transmit antenna verifies the interference constraint or not. On the other hand, the amount of CSI available to the ST about the secondary link varies from one scheme to another. In this context, each of the proposed schemes has its own pros and cons.

In the first proposed technique, we extend the concept of maximum ratio transmission (MRT) to an underlay CR scenario. This MRT-CR technique assumes that the ST has perfect CSI knowledge of the secondary link and comes as a variation of MRT adapted for underlay CR networks. MRT-CR maximizes the received signal-to-interference-and-noise ratio (SINR) at the secondary receiver (SR) employing transmit beamforming using all antennas verifying the interference constraint to the PR.

Inspired by the mode of operation of the minimum-selection generalized selection combin-

ing (MS-GSC) scheme [87], we propose another technique, referred to as minimum-selection MRT, which can be thought of as a power-saving implementation of MRT-CR. To this end, the ST adaptively selects the minimum subset of transmit antennas verifying the interference constraint and reaching the required SINR at the SR. The set of transmit antennas and the modulation constellation size in MS-MRT are adaptively determined to minimize the average number of transmit branches and to achieve the required ASE given the fading channel conditions, the required error performance, and a peak interference constraint.

The above two schemes assume perfect knowledge of the secondary link's CSI at the ST, which could be costly in terms of overhead and/or impractical. As an alternative, we propose an STBC scheme with TAS (TAS/STBC) where only a limited feedback from the SR is required at the ST. Based on this feedback, the ST selects two of the antennas verifying the interference constraint and maximizing the SINR at the SR, and transmits using the Alamouti scheme. While the TAS/STBC scheme offers high ASE, it experiences higher delay than other techniques since at least two antennas are needed for transmission (data is buffered for a channel coherence time if less than two antennas verify the interference constraint as detailed in the next section). In order to minimize this delay, we propose a hybrid scheme that uses TAS/STBC if more than two antennas are available for transmission and only one antenna if this latter is the only antenna verifying the interference constraint.

In light of the above, the contributions of this chapter and the tradeoffs offered by the proposed schemes may be summarized as follows:

- We introduce an adaptive scheme jointly using PA, AM, and switched transmit diversity. This scheme offers reduces the delay and the number of antenna switching of selected existing techniques. On the other hand, this scheme requires full CSI about the interference link (ICSI).

- Based on a limited ICSI, we introduce the MRT-CR technique as an extension of MRT to a spectrum sharing scenario. MRT-CR maximizes the SINR at the SR while using all antennas verifying the interference constraint for transmission.

- Inspired by the mode of operation of MS-GSC, we propose MS-MRT as a power saving implementation of MRT-CR. This novel adaptive transmission technique and its analy-

sis including high SNR approximations are among the major contributions. Compared to MRT-CR, MS-MRT minimizes the average number of antennas used for transmission at the expense of a lower received SINR.

- While in MRT-CR and MS-MRT the ST requires full CSI of the secondary link, we propose TAS/STBC in a more practical scenario to maximize the secondary user's capacity while only requiring a limited CSI at the ST. TAS/STBC has higher system delay than the previous techniques since it requires at least two antennas for communication.

- We finally propose the hybrid scheme in order to reduce the delay experienced by the TAS/STBC scheme.

The remainder of this chapter is organized as follows. We define the underlying system and channel models and describe the adaptive transmission system in Section 3.2. In Section 3.3, we first give the motivation and the mode of operation of the proposed techniques, then we derive expressions of the PDF and the cumulative distribution function (CDF) of their output SINR. We use these statistical results in Section 3.4 to analyze the performance of these techniques. We finally illustrate and confirm these results with selected numerical examples and compare their performance in Section 3.5.

3.2 Models and Adaptive Modulation

3.2.1 System and Channel Models

We consider the underlay cognitive system model shown in Fig. 3.1 where an $N_t \times 1$ multiple-input-single-output (MISO) secondary system aims to maximize its capacity in the presence of primary nodes equipped each with a single antenna. The SU is allowed to share the spectrum with the primary as long as an interference constraint with a peak value Q is respected. In all proposed schemes, the ST starts by sending a training sequence from each antenna in order to test it for the interference constraint. As described above, the PR sends a binary acknowledgment (ACK) to the ST through a reliable feedback channel whenever the interference constraint is satisfied, otherwise it sends a negative acknowledgment (NACK).

N_t feedback bits are required in order to test all the antennas and then obtain the subset S of antennas verifying the interference constraint. In all proposed schemes in this chapter, the ST needs to first find the set S before any communication with the SR can take place. Due to the limited knowledge about the interference link (except for the PA scheme where full ICSI is available at the ST), the ST uses the same transmit power in order to find S independently of the transmission technique and the number of transmit antennas used by each scheme. Thus, we have the same computational complexity for all schemes in terms of obtaining the set S which also provides a fair comparison between these schemes.
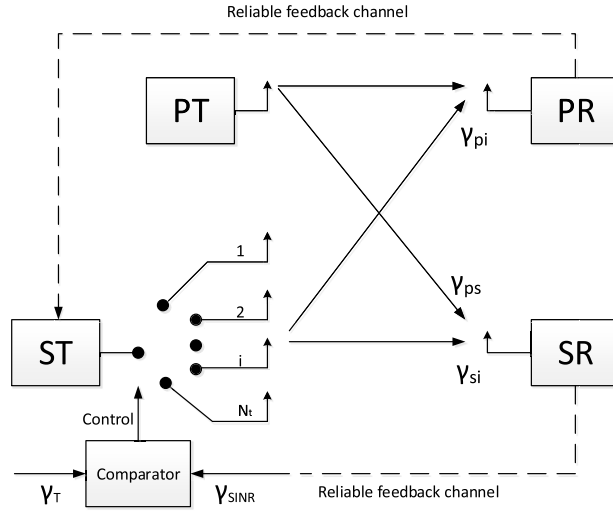
Figure 3.1: System model.

Let h_{s_i}, $i \in \{1, 2, \ldots, N_t\}$ be the channel coefficient between the ith antenna of the ST and the SR, h_{p_i} be the channel coefficient between the ith antenna of the ST and the PR, and h_{ps} be the channel coefficient between the primary transmitter (PT) and the SR[1]. We assume that these considered channels experience i.i.d Rayleigh fading. Assuming a secondary power P_t and a primary power P_p and a Gaussian noise with zero mean and variance N_0 on both the secondary and the interference channels, the received SNRs from the ith antenna at the SR and the PR are given respectively by $\gamma_{s_i} = \frac{P_t |h_{s_i}|^2}{N_0}$ and $\gamma_{p_i} = \frac{P_t |h_{p_i}|^2}{N_0}$ and the received interference-to-noise ratio (INR) from the PT is given by $\gamma_{ps} = \frac{P_p |h_{ps}|^2}{N_0}$. We define $\overline{\gamma}_s$ and

---

[1]Unlike the "Z-Channel" where the interference from the PT is ignored, the considered system, known as the "X-Channel", takes this interference into consideration and represents a more general and realistic scenario.

$\overline{\gamma}_p$ as the common average SNR per receive antenna at the SR and the PR, respectively. Under the assumption of frequency flat fading, we use a block-fading model and the feedback channels to the ST are assumed as follows:

Feedback from PR to ST we assume the presence of a reliable feedback channel between the PR and the ST. In this chapter, we only require a limited feedback to be sent from the PR to the ST. This feedback is used in order to let the ST know if a given antenna verifies or violates the interference temperature at the PR. As such, the PR sends a one bit message (ACK) to the ST through this channel whenever a transmit antenna satisfies the interference constraint, otherwise it sends a one bit NACK message.

Feedback from SR to ST we also assume that there is a reliable feedback channel between the SR and the ST. The amount of feedback sent though this channel depends on the used technique. While the MRT-CR and MS-MRT techniques require full CSI at the ST in order to maximize the received SINR, the TAS/STBC and hybrid schemes only require a limited feedback from the SR. Indeed, in this second set of schemes only a ranking of the transmit antennas according to their received SINR and the modulation mode that can be used with each antenna are required to be sent through this feedback channel.

3.2.2 Adaptive Transmission System

Cognitive radio is one of the most promising solutions for the existing spectrum scarcity problem. Similarly, adaptive modulation was shown to be very effective in increasing the spectral efficiency of communication systems over fading channels [22–24]. Thus, using adaptive modulation in spectrum sharing systems can provide much flexibility. Motivated by this potential, we consider the constant-power variable-rate uncoded M-ary quadrature amplitude modulation (M-QAM) [23] as an adaptive modulation system in a spectrum sharing scenario. With this adaptive modulator, the SNR range is divided into $N + 1$ fading regions and the constellation size $M = 2^n$ is assigned to the nth region ($n = 0, 1, \ldots, N$). The BER of coherent 2^n-QAM with two-dimensional Gray coding over an additive white Gaussian noise

channel with a SNR of γ can be well approximated as [24] by

$$P_{b_n}(\gamma) \simeq \frac{1}{5} \exp\left(\frac{-3\gamma}{2(2^n - 1)}\right). \tag{3.1}$$

Given a target instantaneous BER equal to P_{b_0}, the adaptive modulator switching thresholds γ_n for $n = 0, 1, \ldots, N$ are given by

$$\gamma_n = -\frac{2}{3} \ln(5 P_{b_0})(2^n - 1) \,; \, n = 0, 1, \ldots, N. \tag{3.2}$$

3.3 Proposed Techniques and Their Performance

Depending on the required secondary CSI at the ST, the proposed techniques can be classified into two sets (i) the set of techniques where full SCSI is required, namely the MRT-CR and the MS-MRT techniques, and (ii) the set of techniques where only a limited feedback from the SR is required at the ST, namely the TAS/STBC and the hybrid schemes. In this section, we give the motivation, the mode of operation, and the statistics of the output SINR at the SR for each of these techniques. While all scheme require limited CSI about the interference link, the scheme using PA requires full information about this link as detailed below.

3.3.1 Power Adaptation Scheme

Mode of Operation

Using the reciprocity principle [88], we assume that full ICSI is available to the ST. As such, the channel coefficients for the forward and the reverse directions can be assumed to be similar and the CSI experienced by the reverse link can be used for the forward link. Depending on the used SWC threshold γ_k, $k \in 1, \ldots, N$, we present different variations of the proposed scheme. While the case of $k = 1$ presents a variation of the switching efficient scheme (SES) offering the best delay and switching performance, the case of $k = N$ is a variation of the bandwidth efficient scheme (BES) scheme improving the delay performance and maintaining the spectral efficiency above a required level [10]. In the beginning of each data burst, the ST transmits a training sequence using its maximum power level P_{max}. Using SWC, the ST

cyclically switches between the N_t antennas in order to find the antenna that both verifies the interference constraint and reaches the required modulation threshold. The first antenna is then tested for the interference constraint Q; if this constraint is not respected then the transmit power is adapted to the interference channel and is set to $P^t = \frac{Q N_0}{|h_{p_1}|^2}$. This antenna is selected if its received SNR at SR is above γ_k else the next antenna is tested for the same process. If none of the N_t antennas satisfies constellation size k, the antenna with the highest γ_{s_j} is selected from S, where S is the set of antennas having an output SNR at the SR above γ_1. If S is empty, then the ST buffers the data and waits for a channel coherence time before going again through a scanning of the available antennas.

Statistics of the Output SNR

For analytical tractability, we assume that the effects of the PT's interference on the SR are neglected. Let γ_s denote the output SNR at the SR and let $P_k = \Pr[\gamma_s < \gamma_k]$ be the probability that the received SNR from a given antenna is below γ_k. The probability that no transmission occurs during a certain time slot is then given by $P_1^{N_t}$. Applying the mode of operation of the PA scheme, we derive the CDF of γ_s as

$$
F_{\gamma_s}^{\mathrm{PA}}(\gamma) = \begin{cases} \sum_{i=1}^{N_t} \frac{P_k^{i-1}}{1-P_1^{N_t}} \left(F_{\gamma_{s_i}}(\gamma) - F_{\gamma_{s_i}}(\gamma_k) \right) \\ + \sum_{i=1}^{N_t} \frac{P_1^{i-1}}{1-P_1^{N_t}} \left(F_{\gamma_{s_i}}(\gamma_k) - F_{\gamma_{s_i}}(\gamma_1) \right) F_{\gamma_{s_i}}^{N_t-i}(\gamma_k), & \gamma \geq \gamma_k; \\ \sum_{i=1}^{N_t} \frac{P_1^{i-1}}{1-P_1^{N_t}} \left(F_{\gamma_{s_i}}(\gamma) - F_{\gamma_{s_i}}(\gamma_1) \right) F_{\gamma_{s_i}}^{N_t-i}(\gamma), & \gamma_1 \leq \gamma < \gamma_k; \\ 0, & \gamma < \gamma_1, \end{cases}
\tag{3.3}
$$

where $F_{\gamma_{s_i}}(\cdot)$ can be obtained similar to [54] as

$$
\begin{aligned}
F_{\gamma_{s_i}}(\gamma) &= \Pr[\gamma_{s_i} \leq \gamma] = \Pr\left[\min\left(P_{\max}, \frac{Q N_0}{|h_{p_i}|^2} \right) \frac{|h_{s_i}|^2}{N_0} \leq \gamma \right] \\
&= 1 - \left(1 - \frac{\gamma}{\gamma + Q} e^{-\frac{Q}{\bar{\gamma}_p}} \right) e^{-\frac{\gamma}{\bar{\gamma}_s}}.
\end{aligned}
\tag{3.4}
$$

Differentiating (3.3) with respect to γ, the PDF of the received SNR for the proposed power adaptation scheme is obtained as

$$
f_{\gamma_s}^{\text{PA}}(\gamma) = \begin{cases} \sum_{i=1}^{N_t} \frac{P_k^{i-1}}{1-P_1^{N_t}} f_{\gamma_{s_i}}(\gamma), & \gamma \geq \gamma_k; \\[2mm] \sum_{i=1}^{N_t} \frac{P_1^{i-1}}{1-P_1^{N_t}} \Big((N_t - i + 1) F_{\gamma_{s_i}}^{N_t-i}(\gamma) \\[2mm] \quad - (N_t - i) F_{\gamma_{s_i}}(\gamma_1) F_{\gamma_{s_i}}^{N_t-i-1}(\gamma) \Big) f_{\gamma_{s_i}}(\gamma), & \gamma_1 \leq \gamma < \gamma_k; \\[2mm] 0, & \gamma < \gamma_1, \end{cases} \tag{3.5}
$$

where $f_{\gamma_{s_i}}(\cdot)$ is the PDF of the received SNR from one antenna.

3.3.2 MRT-CR

Motivation

The MRT-CR technique is proposed as an extension of MRT to spectrum sharing systems. While MRT uses all available antennas for transmission, MRT-CR uses only the subset of antennas verifying the interference constraint. Using optimal transmit beamforming introduced in [13], the MRT-CR technique maximizes the received SINR and can be seen as a benchmark for the other proposed techniques.

Mode of Operation

Before each data burst, the ST transmits a training sequence using power P_t. As a first step, the ST will determine the set of antennas satisfying the interference constraint (the L antennas receiving an ACK from the PR define the set S of antennas eligible to communicate with the SR). If S is empty (i.e., $L = 0$) no transmission takes place and data is buffered for a channel coherence time, otherwise all the antennas in S are used for transmission during the next data burst. Assuming that the ST has perfect knowledge of the CSI of the secondary channels, MRT with L transmit antennas is used as a transmission technique in order to maximize the received SINR at the SR. If this received SINR is below the threshold for the

lowest modulation mode (i.e., γ_1) then the SR declares outage.[2] At this stage, we note that the use of MRT maximizes the power in the direction of the SR and minimizes the beams in all other directions. Thus, in order to make sure that the interference constraint is still verified, we need to assume that the PR is not in the same direction of the SR. Indeed, in this special case the beamforming array factor is also maximized in the direction of the PR and the interference constraint to this latter may not be respected anymore.

Statistics of the Output SINR

The instantaneous received SINR with MRT-CR is given by $\gamma_{SINR} = \gamma_s/(1 + \gamma_{ps})$, where $\gamma_s = \overline{\gamma}_s \sum_{j=1}^{L} \gamma_j$ is the received SNR using MRT with the L antennas verifying the interference constraint and is given in [13, Eq.(11)], $\overline{\gamma}_s = \mathbb{E}[\gamma_j]$, $j = 1, 2, ..., L$ is the common average SNR per antenna, and γ_j is the instantaneous SNR of the jth antenna verifying Q.

PDF of the Received SINR   The PDF of the received SNR with MRT using L transmit antennas and one receive antenna is derived in [13] and is given by

$$f_{\gamma_s}^{\mathrm{MRT}}(x) = \frac{x^{L-1}e^{-\frac{x}{\overline{\gamma}_s}}}{(L-1)!\overline{\gamma}_s^L}. \tag{3.6}$$

Using the mode of operation of the MRT-CR technique and (3.6), the PDF of the received SNR γ_s can be obtained as

$$f_{\gamma_s}^{\mathrm{MRT-CR}}(x) = \frac{1}{1-P_1} \sum_{L=1}^{N_t} \binom{N_t}{L} \left(\Pr\left[\gamma_p \leq Q\right]\right)^L \left(\Pr\left[\gamma_p > Q\right]\right)^{N_t-L} \frac{x^{L-1}e^{-\frac{x}{\overline{\gamma}_s}}}{(L-1)!\overline{\gamma}_s^L}, \tag{3.7}$$

where $P_1 = \left(\Pr\left[\gamma_p > Q\right]\right)^{N_t} = e^{-\frac{N_t Q}{\overline{\gamma}_p}}$ is the probability that all antennas break the peak interference constraint . The term $1/(1-P_1)$ represents the possible events pertaining to how many times data is buffered before at least one antenna verifies the interference constraint. The sum from 1 to N_t considers all cases where L among the N_t available antennas verify the interference constraint $(L = 1, 2, ..., N_t)$.

---

[2]The only outage event occurs when the SINR at the SR is below γ_1. Data buffering caused by failure to verify the interference constraint is considered as a delay event and does not count as an outage event.

The PDF of the SINR can be obtained by averaging over the interference from the PT as

$$f_{\gamma_{SINR}}(x) = \int_0^\infty (1+u) f_{\gamma_s}\big((1+u)x\big) f_{\gamma_{ps}}(u) du,　\tag{3.8}$$

where $f_{\gamma_{ps}}(u) = 1/\overline{\gamma}_{ps} e^{-u/\overline{\gamma}_{ps}}$ is the PDF of the received INR. Using Binomial expansion in (3.7) and simple integration tools, $f_{\gamma_{SINR}}(\cdot)$ for MRT-CR is obtained from (3.8) as

$$
\begin{aligned}
f_{\gamma_{SINR}}^{\mathrm{MRT-CR}}(x) \;=\; & \frac{1}{1-e^{-\frac{N_t Q}{\overline{\gamma}_p}}} \sum_{L=1}^{N_t} \binom{N_t}{L} \left(1 - e^{-\frac{Q}{\overline{\gamma}_p}}\right)^L e^{-\frac{(N_t-L)Q}{\overline{\gamma}_p}} \\
& \times \; \frac{L\, x^{L-1} e^{-\frac{x}{\overline{\gamma}_s}}}{\overline{\gamma}_{ps}\,\overline{\gamma}_s^L} \sum_{l=0}^{L} \frac{1}{(L-l)!(x/\overline{\gamma}_s + 1/\overline{\gamma}_{ps})^{l+1}},
\end{aligned}
\tag{3.9}
$$

where $\overline{\gamma}_{ps} = \mathbb{E}[\gamma_{ps}]$ and $\overline{\gamma}_p = \mathbb{E}[\gamma_{p_j}]$, $j = 1, 2, ..., N_t$.

CDF of the Received SINR　The CDF of the received SNR with an $L \times 1$ MRT system can be obtained using a simple integration of (3.6) and is given by

$$F_{\gamma_s}^{\mathrm{MRT}}(x) = 1 - \sum_{k=0}^{L-1} \frac{1}{k!} \left(\frac{x}{\overline{\gamma}_s}\right)^k e^{-\frac{x}{\overline{\gamma}_s}}.　\tag{3.10}$$

Using the mode of operation of the MRT-CR technique and (3.10), the CDF of the received SNR can be obtained as

$$F_{\gamma_s}^{\mathrm{MRT-CR}}(x) = 1 - \frac{1}{1-P_1} \sum_{L=1}^{N_t} \binom{N_t}{L} (\mathrm{Pr}\,[\gamma_p \le Q])^L (\mathrm{Pr}\,[\gamma_p > Q])^{N_t-L} \sum_{k=0}^{L-1} \frac{1}{k!} \left(\frac{x}{\overline{\gamma}_s}\right)^k e^{-\frac{x}{\overline{\gamma}_s}}.$$
$$\tag{3.11}$$

The CDF of the SINR can be obtained by averaging over the PT's interference as

$$F_{\gamma_{SINR}}(x) = \int_0^\infty F_{\gamma_s}\big((1+u)x\big) f_{\gamma_{ps}}(u)\, du.　\tag{3.12}$$

Using Binomial expansion in (3.11) and simple integrations, $F_{\gamma_{SINR}}(\cdot)$ is obtained as

$$
\begin{aligned}
F_{\gamma_{SINR}}^{\text{MRT}-\text{CR}}(x) \;=\;& 1 - \frac{1}{1 - e^{-\frac{N_t Q}{\overline{\gamma}_p}}} \sum_{L=1}^{N_t} \binom{N_t}{L} \left(1 - e^{-\frac{Q}{\overline{\gamma}_p}}\right)^L \\
\times\;& e^{-\frac{(N_t - L)Q}{\overline{\gamma}_p}} \sum_{k=0}^{L-1}\sum_{l=0}^{k} \frac{1}{(k-l)!(x/\overline{\gamma}_s + 1/\overline{\gamma}_{ps})^{l+1}} \left(\frac{x}{\overline{\gamma}_s}\right)^k e^{-\frac{x}{\overline{\gamma}_s}}. \quad (3.13)
\end{aligned}
$$

3.3.3   MS-MRT

Motivation

The MS-MRT scheme is proposed in order to minimize the average number of antennas used for transmission. This can be done by selecting the minimum subset of transmit antennas satisfying both the interference to the PR and the BER requirements. This reduction in the number of transmit antennas minimizes the processing power consumption at the ST which comes at the expense of a reduction in the received SINR at the SR.

Mode of Operation

Similar to the MRT-CR scheme, the ST determines the set S of antennas satisfying the interference constraint. If S is empty, no transmission takes place and data is buffered for a channel coherence time, otherwise the antennas in S are ranked according to the quality of the channel with the SR. The strongest antenna, denoted by $\gamma_{1:L}$, is tested for a required output threshold γ_T. If the received SINR from this antenna is above γ_T then the ST transmits using only this antenna for the next data burst. If this antenna fails the output SINR condition, the ST tests if the SINR using MRT with the two strongest antennas is above γ_T. If this condition is verified then these two antennas are used with optimal transmit beamforming (i.e., MRT). Similarly, if these antennas are not enough to reach γ_T, the next strongest antenna is selected with the two first ones using MRT and this process is repeated till reaching the required threshold or till all antennas in S are tested. In this second case, we reduce to the MRT-CR technique where all antennas verifying the interference constraint are used for transmission.

Statistics of the Output SINR

The instantaneous received SINR is given by $\gamma_{SINR} = \gamma_s/(1 + \gamma_{ps})$, where $\gamma_s = \overline{\gamma}_s \sum_{k=1}^{i} \gamma_{k:L}$ is the received SNR using MRT with the i strongest antennas in S (i takes values between 1 and L with different probabilities) and $\gamma_{k:L}$, $k = 1, 2, ..., L$ is the instantaneous SNR of the kth strongest antenna among the L antennas verifying the interference constraint. Thanks to the full CSI available at the ST, we can see that the received SNR using MS-MRT with L antennas verifying the interference constraint is equivalent to the SNR received by an MS-GSC receiver equipped with L antennas. Based on this result, the analysis of MS-GSC with co-channel interference proposed by Daghfous *et. al* in [89] can be used to get closed-form expressions for MS-MRT in the presence of the PR's interference.

PDF of the Received SINR The adaptive number of antennas used for transmission in the MS-MRT technique is inspired by the mode of operation of MS-GSC. Thus, using the expression of the PDF of the output SNR with MS-GSC [90, Eq.(26)] and taking the interference constraint imposed by the PR into account, the PDF of the received SNR γ_s can be obtained as

$$
\begin{aligned}
f_{\gamma_s}(x) &= \frac{1}{1 - P_1} \sum_{L=1}^{N_t} \binom{N_t}{L} (\Pr[\gamma_p \leq Q])^L (\Pr[\gamma_p > Q])^{N_t - L} \\
&\times \left(\left[f_{\gamma_{s,1}}(x) + \sum_{j=2}^{L} f_{\gamma_{s,2,j}}(x) \left(\mathcal{U}(x - \gamma_T) - \mathcal{U}\left(x - \frac{j}{j-1}\gamma_T\right) \right) \right] \right. \\
&\times \left. \mathcal{U}(x - \gamma_T) + f_{\gamma_s}^{\mathrm{MRT}}(x) \left(\mathcal{U}(x) - \mathcal{U}(x - \gamma_T) \right) \right),
\end{aligned}
\tag{3.14}
$$

where $\mathcal{U}(\cdot)$ is the unit step function, and $f_{\gamma_{s,1}}(\cdot)$ and $f_{\gamma_{s,2,j}}(\cdot)$ are the distributions of the received SNR depending on the number of transmit antennas. Specifically,

$$
f_{\gamma_{s,1}}(x) = \frac{L}{\overline{\gamma}_s} \left(1 - e^{-\frac{x}{\overline{\gamma}_s}} \right)^{L-1} e^{-\frac{x}{\overline{\gamma}_s}},
\tag{3.15}
$$

represents the PDF of the output SNR when only the strongest antenna is used for transmission. $f_{\gamma_{s,2,j}}(\cdot)$ defines the case when j out of L antennas are used for transmission and it

is given in [90, Eq.(32)]. $f_{\gamma_s}^{\mathrm{MRT}}(\cdot)$ defines the case when all L antennas are used and is given in (3.6).

Using (3.8), the PDF of the SINR for MS-MRT can be derived from (3.14) as

$$
\begin{aligned}
f_{\gamma_{SINR}}^{\mathrm{MS-MRT}}(x) \;=\; & \frac{1}{1 - e^{-\frac{N_t Q}{\overline{\gamma}_p}}} \sum_{L=1}^{N_t} \binom{N_t}{L} \left(1 - e^{-\frac{Q}{\overline{\gamma}_p}}\right)^L e^{-\frac{(N_t - L)Q}{\overline{\gamma}_p}} \\
& \times \begin{cases}
f_{\gamma_{SINR,1}}(x) + f_{\gamma_{SINR,2}}(x) + f_{\gamma_{SINR,3}}(x), & x < \gamma_T; \\[2mm]
f_{\gamma_{SINR,4}}(x) + \sum_{j=2}^{L} f_{\gamma_{SINR,5,i}}(x) \\[2mm]
\quad \times \left(\mathcal{U}(x - \gamma_T) - \mathcal{U}(x - \frac{j}{j-1}\gamma_T)\right), & x \geq \gamma_T;
\end{cases}
\end{aligned}
\tag{3.16}
$$

where $f_{\gamma_{SINR,1}}(\cdot)$, $f_{\gamma_{SINR,2}}(\cdot)$, $f_{\gamma_{SINR,3}}(\cdot)$, $f_{\gamma_{SINR,4}}(\cdot)$, and $f_{\gamma_{SINR,5,i}}(\cdot)$ are derived below in closed-form using Binomial expansions and simple integrations.

$$
f_{\gamma_{SINR,1}}(x) = \frac{L}{\overline{\gamma}_s \overline{\gamma}_{ps}} \sum_{k=0}^{L-1} \binom{L-1}{k} (-1)^k \frac{\alpha_1(\alpha_2 + 1) + 1}{(\alpha_1)^2} e^{-\frac{(k+1)x}{\overline{\gamma}_s}} e^{-\alpha_1 \alpha_2}.
\tag{3.17}
$$

$$
\begin{aligned}
f_{\gamma_{SINR,2}}(x) = & \frac{1}{\overline{\gamma}_{ps}} \sum_{i=2}^{L} \left\{ \binom{L}{i} \frac{e^{-\frac{x}{\overline{\gamma}_s}}}{(i-1)! \overline{\gamma}_s^{\,i}} \sum_{k=0}^{i-1} \binom{i-1}{k} (i\,\gamma_T)^{i-k-1}(x - ix)^k \right. \\
& \times \sum_{n=0}^{k+1} \binom{k+1}{n} \frac{\gamma(n+1, \alpha_3\alpha_6) - \gamma(n+1, \alpha_3\alpha_2)}{(\alpha_3)^{n+1}} + \sum_{j=1}^{L-i} \binom{i}{j}^{i-1} \frac{L!(-1)^{j-i+1} e^{-\frac{(i+j)x}{i\overline{\gamma}_s}}}{(L-i-j)! j! i! \overline{\gamma}_s} \\
& \times \left[\frac{e^{-\alpha_4\alpha_2} - e^{-\alpha_4\alpha_6}}{\alpha_4} + \frac{(1 + \alpha_4\alpha_2)e^{-\alpha_4\alpha_2} - (1 + \alpha_4\alpha_6)e^{-\alpha_4\alpha_6}}{(\alpha_4)^2} \right. \\
& - e^{-\frac{j((i-1)x - i\gamma_T)}{i\overline{\gamma}_s}} \sum_{k=0}^{i-2} \frac{1}{k!} \left(\frac{j}{i\overline{\gamma}_s}\right)^k \sum_{n=0}^{k} \binom{k}{n} ((-1)i\,\gamma_T)^{k-n}(ix - x)^n \\
& \left. \left. \times \sum_{m=0}^{n+1} \binom{n+1}{m} \frac{\gamma(m+1, \alpha_5\alpha_6) - \gamma(m+1, \alpha_5\alpha_2)}{(\alpha_5)^{m+1}} \right] \right\}.
\end{aligned}
\tag{3.18}
$$

$$
f_{\gamma_{SINR,3}}(x) = \frac{x^{L-1} e^{-\frac{x}{\overline{\gamma}_s}}}{(L-1)! \overline{\gamma}_s^L \overline{\gamma}_{ps}} \sum_{k=0}^{L} \binom{L}{k} \frac{\gamma(k+1, \alpha_3\alpha_2)}{(\alpha_3)^{k+1}}.
\tag{3.19}
$$

$$f_{\gamma_{SINR,4}}(x) = \frac{L}{\overline{\gamma}_s \overline{\gamma}_{ps}} \sum_{k=0}^{L-1} \binom{L-1}{k} (-1)^k \frac{\alpha_1 + 1}{(\alpha_1)^2} e^{-\frac{(k+1)x}{\overline{\gamma}_s}}. \tag{3.20}$$

$$f_{\gamma_{SINR,5,i}}(x) =$$

$$\frac{1}{\overline{\gamma}_{ps}} \left\{ \binom{L}{i} \frac{e^{-\frac{x}{\overline{\gamma}_s}}}{(i-1)! \overline{\gamma}_s{}^i} \sum_{k=0}^{i-1} \binom{i-1}{k} (i\,\gamma_T)^{i-k-1}(x-ix)^k \sum_{n=0}^{k+1} \binom{k+1}{n} \frac{\gamma(n+1, \alpha_3\alpha_6)}{(\alpha_3)^{n+1}} \right.$$

$$+ \sum_{j=1}^{L-i} \left(\frac{i}{j}\right)^{i-1} \frac{L!(-1)^{j-i+1} e^{-\frac{(i+j)x}{i\overline{\gamma}_s}}}{(L-i-j)! j! i! \overline{\gamma}_s} \left[\frac{1 + \alpha_4 - (1 + \alpha_4 + \alpha_4\alpha_6)e^{-\alpha_4\alpha_6}}{(\alpha_4)^2} - e^{-\frac{j((i-1)x-i\gamma_T)}{i\overline{\gamma}_s}} \right.$$

$$\left. \times \sum_{k=0}^{i-2} \frac{1}{k!} \left(\frac{j}{i\overline{\gamma}_s}\right)^k \sum_{m=0}^{k} \binom{k}{m} ((-1)i\,\gamma_T)^{k-m}(ix-x)^m \sum_{n=0}^{m+1} \binom{m+1}{n} \frac{\gamma(n+1, \alpha_5\alpha_6)}{(\alpha_5)^{n+1}} \right] \right\}, \tag{3.21}$$

where $\gamma(n,x) = \int_0^x t^{n-1} e^{-t} dt$ is the lower incomplete Gamma function, and $\alpha_1, \ldots \alpha_6$ are given as follows $\alpha_1 = (k+1)x/\overline{\gamma}_s + 1/\overline{\gamma}_{ps}$, $\alpha_2 = (\gamma_T - x)/x$, $\alpha_3 = x/\overline{\gamma}_s + 1/\overline{\gamma}_{ps}$, $\alpha_4 = (i+j)x/i\overline{\gamma}_s + 1/\overline{\gamma}_{ps}$, $\alpha_5 = (j+1)x/\overline{\gamma}_s + 1/\overline{\gamma}_{ps}$, $\alpha_6 = (i\gamma_T/(i-1) - x)/x$.

For the very high average SNR range, using only the strongest antenna becomes sufficient to reach the required adaptive modulation threshold γ_T. In this regime, the MS-MRT technique behaves similar to the best antenna selection (BAS) scheme where the antenna having the highest received SINR and verifying the interference constraint is always selected for transmission [44].[3] Thus, for very high average SNR, (3.16) can be well approximated by the PDF of the BAS scheme given in [44] by

$$f_{\gamma_{SINR}}^{\text{BAS}}(x) = \frac{1}{1 - e^{-\frac{N_t Q}{\overline{\gamma}_p}}} \sum_{L=1}^{N_t} \binom{N_t}{L} \left(1 - e^{-\frac{Q}{\overline{\gamma}_p}}\right)^L e^{-\frac{(N_t - L)Q}{\overline{\gamma}_p}}$$

$$\times \frac{L}{\overline{\gamma}_s \overline{\gamma}_{ps}} \left(\sum_{j=0}^{L-1} \binom{L-1}{j} (-1)^j \left(\frac{\alpha_j(x) + 1}{\alpha_j(x)^2}\right) e^{-\frac{(j+1)x}{gs}} \right), \tag{3.22}$$

where $\alpha_j(x) = (j+1)x/\overline{\gamma}_s + 1/\overline{\gamma}_{ps}$.

---

[3]This approximation will be confirmed via simulations in Section 3.5.

CDF of the Received SINR Using the mode of operation of the MS-MRT schemes and [90, Eq.(20)], the CDF of the received SNR at the SR is given by

$$
\begin{aligned}
F_{\gamma_s}(x) \;=\; & \frac{1}{1 - e^{-\frac{N_t Q}{\bar{\gamma}_p}}} \sum_{L=1}^{N_t} \binom{N_t}{L} \left(1 - e^{-\frac{Q}{\bar{\gamma}_p}}\right)^L e^{-\frac{(N_t - L)Q}{\bar{\gamma}_p}} \\
& \times \; \left(\left[F_{\gamma_{s,1}}(x) - F_{\gamma_{s,1}}(\gamma_T) + \sum_{j=2}^{L} F_{\gamma_{s,2,j}}(x) + F_{\gamma_s}^{\mathrm{MRT}}(\gamma_T)\right]\right. \\
& \times \; \left.\mathcal{U}(x - \gamma_T) + F_{\gamma_s}^{\mathrm{MRT}}(x)\Big(\mathcal{U}(x) - \mathcal{U}(x - \gamma_T)\Big)\right),
\end{aligned}
\tag{3.23}
$$

where $F_{\gamma_{s,1}}(x) = \int_0^x f_{\gamma_{s,1}}(u)du = (1 - e^{-\frac{x}{\bar{\gamma}_s}})^L$ is the CDF of the output SNR when the strongest antenna is used for transmission. $F_{\gamma_{s,2,j}}(\cdot)$ defines the case when j out of L antennas are used for transmission and is given in [90, Eq.(23)]. $F_{\gamma_s}^{\mathrm{MRT}}(\cdot)$ defines the case when all L antennas are used and is given in (3.10).

The CDF of the output SINR is derived from (3.23) considering the interference from the PT using (3.12) and can be expressed as

$$
\begin{aligned}
F_{\gamma_{SINR}}^{\mathrm{MS-MRT}}(x) \;=\; & \frac{1}{1 - e^{-\frac{N_t Q}{\bar{\gamma}_p}}} \sum_{L=1}^{N_t} \binom{N_t}{L} \left(1 - e^{-\frac{Q}{\bar{\gamma}_p}}\right)^L e^{-\frac{(N_t - L)Q}{\bar{\gamma}_p}} \\
& \times \begin{cases}
\begin{aligned}
& F_{\gamma_{SINR,1}}(x) + F_{\gamma_{SINR,2}}(x) \\
& + \sum_{l=2}^{L}\left(F_{\gamma_{SINR,3,l}}(x) + G_{\gamma_{SINR,l}}(x)\right),
\end{aligned} & x < \gamma_T; \\[2em]
\begin{aligned}
& F_{\gamma_{SINR,4}}(x) + \sum_{l=2}^{L}\left(F_{\gamma_{SINR,5,l,0}}(x) + G_{\gamma_{SINR,l}}(x)\right. \\
& \left. + \sum_{i=2}^{l-1}\left(F_{\gamma_{SINR,5,i,1}}(x) + G_{\gamma_{SINR,i}}(x)\right)\right) \\
& \times \left(\mathcal{U}(x - \tfrac{l+1}{l}\gamma_T) - \mathcal{U}(x - \tfrac{l}{l-1}\gamma_T)\right),
\end{aligned} & x \ge \gamma_T;
\end{cases}
\end{aligned}
\tag{3.24}
$$

where $F_{\gamma_{SINR,1}}(\cdot)$, $F_{\gamma_{SINR,2}}(\cdot)$, $F_{\gamma_{SINR,3,i}}(\cdot)$, $F_{\gamma_{SINR,4}}(\cdot)$, $F_{\gamma_{SINR,5,i,u}}(\cdot)$, and $G_{\gamma_{SINR,i}}(x)$ are obtained with the help of [89] and are given in closed-form as

$$F_{\gamma_{SINR,1}}(x) = 1 - e^{-\frac{\alpha_2}{\overline{\gamma}_{ps}}} - \frac{e^{-\frac{x}{\overline{\gamma}_s}}}{\overline{\gamma}_{ps}} \sum_{k=0}^{L-1} \frac{1}{k!} \left(\frac{x}{\overline{\gamma}_s}\right)^k \sum_{n=0}^{k} \binom{k}{n} \frac{\gamma(n+1,\alpha_2\alpha_3)}{(\alpha_3)^{n+1}} \tag{3.25}$$

$$F_{\gamma_{SINR,2}}(x) = L\,e^{-\frac{\alpha_2}{\overline{\gamma}_{ps}}} - L\,\frac{e^{-\frac{x}{\overline{\gamma}_s}}e^{-\alpha_2\alpha_3}}{\alpha_3\overline{\gamma}_{ps}} + \sum_{j=1}^{L-1}(-1)^j \binom{L}{j+1}\left[e^{-\frac{\alpha_2}{\overline{\gamma}_{ps}}} - \frac{e^{-\frac{(j+1)x}{\overline{\gamma}_s}}e^{-\alpha_2\alpha_5}}{\alpha_5\overline{\gamma}_{ps}}\right] \tag{3.26}$$

$$F_{\gamma_{SINR,3,l}}(x) = \begin{cases} \beta_L(\gamma_T)\left[e^{-\alpha_2} - e^{-\frac{L/(L-1)\gamma_T - x}{x}}\right], & l = L; \\ \beta_l(\gamma_T)\left[e^{-\frac{(l+1)/l\gamma_T - x}{x}} - e^{-\frac{l/(l-1)\gamma_T - x}{x}}\right], & l \neq L; \end{cases} \tag{3.27}$$

$$F_{\gamma_{SINR,4}}(x) = L\left(1 - \frac{e^{-\frac{x}{\overline{\gamma}_s}}}{\alpha_3\overline{\gamma}_{ps}}\right) + \sum_{j=1}^{L-1}(-1)^j\binom{L}{j+1}\left[1 - \frac{e^{-\frac{(j+1)x}{\overline{\gamma}_s}}}{\alpha_5\overline{\gamma}_{ps}}\right] \tag{3.28}$$

$$F_{\gamma_{SINR,5,i,u}}(x) = \begin{cases} \beta_i(\gamma_T)\left[1 - e^{-\frac{\alpha_6}{\overline{\gamma}_{ps}}}\right], & u = 0; \\ \beta_i(\gamma_T)\left[e^{-\frac{(i+1)/i\gamma_T - x}{\overline{\gamma}_{ps}\,x}} - e^{-\frac{\alpha_6}{\overline{\gamma}_{ps}}}\right], & u = 1; \end{cases} \tag{3.29}$$

where $\beta_i(\gamma_T) = P_{\Gamma_i}(x) - F_{\gamma_{SINR,1}}(x)$ where $P_{\Gamma_i}(\cdot)$ is the CDF of the case where i antennas are used for transmission and is given in [90, Eq.(17)].

$$G_{\gamma_{SINR,i}}(x) =$$

$$\frac{L!}{(L-i)!(i-1)!} \sum_{k=0}^{i-2} \frac{(1-i)^k}{(i-2-k)!} \sum_{m=0}^{k} \frac{1}{\overline{\gamma}_s^{\,i-1-k+m}} \sum_{l=0}^{m} \frac{(-1)^l}{(m-l)!l!} \frac{\gamma_T^{\,i-1-k+l}}{i-1-k+l}$$

$$\times \left\{ e^{-\frac{\gamma_T}{\overline{\gamma}_s}} \gamma_T^{m-l}\left(1 - \left(\frac{i-1}{i}\right)^{i-1-k+l}\right)\left(e^{-\frac{a}{\overline{\gamma}_{ps}}} - e^{-\frac{b}{\overline{\gamma}_{ps}}}\right) \right.$$

$$- e^{-\frac{x}{\overline{\gamma}_s}} x^{m-l}\left(\sum_{n=0}^{m-l}\binom{m-l}{n}\frac{\gamma(n+1,\alpha_3 b) - \gamma(n+1,\alpha_3 a)}{\overline{\gamma}_{ps}(\alpha_3)^{n+1}}\right)$$

$$\left. - \left(\frac{(i-1)x}{i\overline{\gamma}_s}\right)^{i-1-k+l} \sum_{n=0}^{i-1-k+m}\binom{i-1-k+m}{n}\frac{\gamma(n+1,\alpha_3 b) - \gamma(n+1,\alpha_3 a)}{\overline{\gamma}_{ps}(\alpha_3)^{n+1}}\right)\right\}$$

$$+ \sum_{j=1}^{L-i} \frac{(-1)^j L!}{(L-i-j)!(i-1)!j!\overline{\gamma}_s^{\,i}} \sum_{k=0}^{i-2} \frac{(1-i)^k}{(i-2-k)!} \sum_{m=0}^{k}\left(\frac{j+1}{\overline{\gamma}_s}\right)^{m-k-1}$$

$$\times \sum_{l=0}^{m} \frac{(-1)^l(i-2-k+l)!}{(m-l)!l!}\left(-\frac{\overline{\gamma}_s}{j}\right)^{i-1-k+l} \cdots$$

$$
\times \left\{ \gamma_T^{m-l} \left(e^{-\frac{(i+j)\gamma_T}{i\overline{\gamma}_s}} \sum_{n=0}^{i-2-k+l} \frac{1}{n!} \left(-\frac{(i-1)j\gamma_T}{i\overline{\gamma}_s} \right)^n - e^{-\frac{\gamma_T}{\overline{\gamma}_s}} \sum_{n=0}^{i-2-k+l} \frac{1}{n!} \left(-\frac{j\gamma_T}{\overline{\gamma}_s} \right)^n \right) \left(e^{-\frac{a}{\overline{\gamma}_{ps}}} - e^{-\frac{b}{\overline{\gamma}_{ps}}} \right) \right.
$$

$$
- x^{m-l} \left(e^{-\frac{(i+j)x}{i\overline{\gamma}_s}} \sum_{n=0}^{i-2-k+l} \frac{1}{n!} \left(-\frac{(i-1)jx}{i\overline{\gamma}_s} \right)^n \sum_{u=0}^{m+n-l} \binom{m+n-l}{u} \frac{\gamma(u+1, \alpha_7 b) - \gamma(u+1, \alpha_7 a)}{\overline{\gamma}_{ps}(\alpha_7)^{u+1}} \right.
$$

$$
\left. \left. - e^{-\frac{(j+1)x - j\gamma_T}{\overline{\gamma}_s}} \sum_{n=0}^{i-2-k+l} \frac{1}{n!} \left(-\frac{j\gamma_T}{\overline{\gamma}_s} \right)^n \sum_{u=0}^{m-l} \binom{m-l}{u} \frac{\gamma(u+1, \alpha_5 b) - \gamma(u+1, \alpha_5 a)}{\overline{\gamma}_{ps}(\alpha_5)^{u+1}} \right) \right\}
$$

$$
- \sum_{j=0}^{L-i} \frac{(-1)^j L!}{(L-i-j)!(i-1)!j!\overline{\gamma}_s^i} \sum_{k=0}^{i-2} \frac{(1-i)^k}{(i-2-k)!} \sum_{m=0}^{k} \frac{(i-2-k+m)!}{m!(i-1)^m} \left(\frac{j+1}{\overline{\gamma}_s} \right)^{m-k-1}
$$

$$
\times \left(\frac{(i-1)\overline{\gamma}_s}{i+j} \right)^{i-1-k+m} \left(e^{-\frac{(i+j)\gamma_T}{i\overline{\gamma}_s}} \sum_{n=0}^{i-2-k+m} \frac{1}{n!} \left(\frac{(i+j)\gamma_T}{i\overline{\gamma}_s} \right)^n \left(e^{-\frac{a}{\overline{\gamma}_{ps}}} - e^{-\frac{b}{\overline{\gamma}_{ps}}} \right) \right.
$$

$$
\left. - e^{-\frac{(i+j)x}{i\overline{\gamma}_s}} \sum_{n=0}^{i-2-k+m} \frac{1}{n!} \left(\frac{(i+j)x}{i\overline{\gamma}_s} \right)^n \sum_{u=0}^{n} \binom{n}{u} \frac{\gamma(u+1, \alpha_7 b) - \gamma(u+1, \alpha_7 a)}{\overline{\gamma}_{ps}(\alpha_7)^{u+1}} \right), \tag{3.30}
$$

where $\alpha_7 = (i+j)x/\overline{\gamma}_s + 1/\overline{\gamma}_{ps}$.

For the very high average SNR range, (3.24) can also be well approximated by the CDF of the BAS scheme given in [44] by

$$
F_{\gamma_{SINR}}^{\text{BAS}}(x) = \frac{1}{1 - e^{-\frac{N_t Q}{\overline{\gamma}_p}}} \sum_{L=1}^{N_t} \binom{N_t}{L} \left(1 - e^{-\frac{Q}{\overline{\gamma}_p}} \right)^L e^{-\frac{(N_t - L)Q}{\overline{\gamma}_p}}
$$

$$
\times \sum_{j=0}^{L-1} \binom{L}{j+1} (-1)^j \left(1 - \frac{e^{-\frac{(j+1)x}{gs}}}{\overline{\gamma}_{ps} \alpha_j(x)} \right). \tag{3.31}
$$

3.3.4 TAS/STBC Scheme

Motivation

While the MRT-CR and MS-MRT techniques require full CSI of the secondary link, the ST in the TAS/STBC scheme requires only a feedback about which antennas and the modulation mode to used with each antenna. Thus, the TAS/STBC scheme is proposed as a more practical implementation of a MISO system in an underlay CR scenario.

Mode of Operation

Similar to the previous techniques, the ST starts by finding the subset of antennas satisfying the interference constraint. If S is empty or contains only one antennas (i.e., $L = 0$ or $L = 1$), no transmission takes place and data is buffered for a channel coherence time. Otherwise, the SR feeds back the indices of the antennas ordered in terms of their received SINR and the modulation mode to be used. The two strongest antennas in the set S are then used for transmission during the next data burst using the Alamouti scheme. If the output SINR from these antennas is below γ_1, then the SR declares outage.

Statistics of the Output SINR

The instantaneous received SNR for the TAS/STBC scheme is given by $\gamma_s = \frac{\overline{\gamma}_s}{2}\left[\gamma_{1:L} + \gamma_{2:L}\right]$, where $\gamma_{1:L}$ and $\gamma_{2:L}$ are the instantaneous SNRs from the two strongest antenna verifying the interference constraint and the $1/2$ coefficient is due to the equal power allocation between the two selected antennas.

PDF of the Received SINR Using the mode of operation of the TAS/STBC scheme and [19, Eq.(13)] for $L_t = 2$ and $L_r = 1$, the PDF of the received SNR γ_s can be obtained as

$$
\begin{aligned}
f_{\gamma_s}(x) &= \frac{2}{1 - P_2} \sum_{L=2}^{N_t} \binom{N_t}{L} \left(\Pr\left[\gamma_p \leq Q\right]\right)^L \left(\Pr\left[\gamma_p > Q\right]\right)^{N_t - L} \\
&\times \frac{L(L-1)}{\overline{\gamma}_s} \left(\frac{x}{\overline{\gamma}_s} + \sum_{k=1}^{L-2} \frac{(-1)^k}{k} \binom{L-2}{k} \left(1 - e^{-\frac{kx}{\overline{\gamma}_s}}\right)\right) e^{-\frac{2x}{\overline{\gamma}_s}},
\end{aligned} \tag{3.32}
$$

where $P_2 = \left(N_t - (Nt-1)e^{-\frac{Q}{\overline{\gamma}_p}}\right)e^{-\frac{(N_t-1)Q}{\overline{\gamma}_p}}$ is the probability that the number of antennas verifying the interference constraint is strictly less than two which represents the case when data is buffered for the TAS/STBC scheme.

Averaging over the interference from the PT, the PDF of the SINR can be derived as

$$
\begin{aligned}
f_{\gamma_{SINR}}^{\text{TAS/STBC}}(x) = {} & \frac{2}{1-P_2} \sum_{L=2}^{N_t} \frac{N_t!\left(1-e^{-\frac{Q}{\overline{\gamma}_p}}\right)^L e^{-\frac{(N_t-L)Q}{\overline{\gamma}_p}}}{(L-2)!(N_t-L)!} \\
& \times \left(\frac{4\overline{\gamma}_{ps}{}^2 x^3 + 4\overline{\gamma}_s\overline{\gamma}_{ps}(1+\overline{\gamma}_{ps})x^2 + \overline{\gamma}_s{}^2\left(1+2\overline{\gamma}_{ps}(1+\overline{\gamma}_{ps})\right)x}{\overline{\gamma}_s(\overline{\gamma}_s + 2\,\overline{\gamma}_{ps}\,x)^3} \right. \\
& + \sum_{k=1}^{L-2} \frac{(-1)^k}{k}\binom{L-2}{k}\left[\frac{\overline{\gamma}_s(1+\overline{\gamma}_{ps}) + (k+2)\overline{\gamma}_{ps}x}{(\overline{\gamma}_s + (k+2)\overline{\gamma}_{ps}x)^2}e^{-\frac{kx}{\overline{\gamma}_s}} - \frac{\overline{\gamma}_s(1+\overline{\gamma}_{ps}) + 2\,\overline{\gamma}_{ps}x}{(\overline{\gamma}_s + 2\overline{\gamma}_{ps}x)^2}\right] \left. \right)e^{-\frac{2x}{\overline{\gamma}_s}}.
\end{aligned}
\tag{3.33}
$$

CDF of the Received SINR The CDF of γ_s is derived with the help of [19, Eq.(11)] as

$$
\begin{aligned}
F_{\gamma_s}(x) = {} & \frac{1}{1-P_2} \sum_{L=1}^{N_t} \binom{N_t}{L}L(L-1)\left(1-e^{-\frac{Q}{\overline{\gamma}_p}}\right)^L e^{-\frac{(N_t-L)Q}{\overline{\gamma}_p}} \\
& \times \left(\frac{1}{2} - \left(\frac{1}{2} + \frac{x}{\overline{\gamma}_s}\right)e^{-\frac{2x}{\overline{\gamma}_s}} + \sum_{k=1}^{L-2}(-1)^k\binom{L-2}{k} \right. \\
& \times \left. \left(\frac{1}{k+2} + \frac{2}{k(k+2)}e^{-\frac{(k+2)x}{\overline{\gamma}_s}} - \frac{1}{k}e^{-\frac{2x}{\overline{\gamma}_s}}\right)\right).
\end{aligned}
\tag{3.34}
$$

The CDF of the SINR is obtained from (3.34) using (3.12) as

$$
\begin{aligned}
F_{\gamma_{SINR}}^{\text{TAS/STBC}}(x) = {} & \frac{1}{1-P_2} \sum_{L=2}^{N_t} \frac{N_t!\left(1-e^{-\frac{Q}{\overline{\gamma}_p}}\right)^L e^{-\frac{(N_t-L)Q}{\overline{\gamma}_p}}}{(L-2)!(N_t-L)!} \\
& \times \left(\frac{1}{2} - \frac{e^{-\frac{2x}{\overline{\gamma}_s}}}{2 + \frac{4\overline{\gamma}_{ps}x}{\overline{\gamma}_s}} - xe^{-\frac{2x}{\overline{\gamma}_s}}\frac{\overline{\gamma}_s(1+\overline{\gamma}_{ps}) + 2\overline{\gamma}_{ps}x}{(\overline{\gamma}_s + 2\overline{\gamma}_{ps}x)^2} + \sum_{k=1}^{L-2}\frac{(-1)^k}{k+2} \right. \\
& \times \left. \binom{L-2}{k}\left(1 + \frac{2\,e^{-\frac{(k+2)x}{\overline{\gamma}_s}}}{k\left(1+\frac{(k+2)\overline{\gamma}_{ps}}{\overline{\gamma}_s}x\right)} - \frac{(k+2)e^{-\frac{2x}{\overline{\gamma}_s}}}{k\left(1+\frac{2\overline{\gamma}_{ps}}{\overline{\gamma}_s}x\right)}\right)\right).
\end{aligned}
\tag{3.35}
$$

3.3.5 Hybrid Scheme

Motivation

In the TAS/STBC scheme, data is buffered whenever less than two antennas verify the interference constraint. Thus, the TAS/STBC experiences more delay than MS-MRT. The hybrid scheme is proposed in order to minimize the delay experienced by TAS/STBC scheme

while sacrificing a minor ASE loss at high average SNRs.

Mode of Operation

In this scheme, data is buffered only if all antennas fail the interference constraint. If $L = 1$, the ST transmits using only one antenna, otherwise if $L \geq 2$ the best two antennas are selected for transmission using the TAS/STBC scheme.

Statistics of the Output SINR

PDF of the Received SINR   Depending on the number of antennas verifying the interference constraint, the PDF of the received SNR with the hybrid scheme is derived using the previous results as

$$
f_{\gamma_s}(x) = \frac{1}{1 - P_1} \left(N_t \Big(\Pr\left[\gamma_p \leq Q\right] \Big) \Big(\Pr\left[\gamma_p > Q\right] \Big)^{N_t - 1} \frac{1}{\overline{\gamma}_s} e^{-\frac{x}{\overline{\gamma}_s}} + (1 - P_2) f_{\gamma_s}^{\mathrm{TAS/STBC}}(x) \right),
$$

(3.36)

where $f_{\gamma_s}^{\mathrm{TAS/STBC}}(\cdot)$ is given in (3.32), the first part of the sum represents the case when only one antenna verifies the interference constraint, and the second part represents the case when more than two antennas verify the constraint (i.e., the TAS/STBC scheme is used).

Using (3.8) and (3.36), the PDF of the SINR is derived as

$$
\begin{aligned}
f_{\gamma_{SINR}}(x) &= \frac{1}{1 - P_1} \left(N_t \Big(1 - e^{-\frac{Q}{\overline{\gamma}_p}} \Big) e^{-\frac{(N_t - 1)Q}{\overline{\gamma}_p}} \right. \\
&\quad \times \left. \frac{\overline{\gamma}_s + \overline{\gamma}_{ps}\overline{\gamma}_s + \overline{\gamma}_{ps}x}{(\overline{\gamma}_s + \overline{\gamma}_{ps}x)^2} e^{-\frac{x}{\overline{\gamma}_s}} + (1 - P_2) f_{\gamma_{SINR}}^{\mathrm{TAS/STBC}}(x) \right).
\end{aligned}
$$

(3.37)

CDF of the Received SINR   Based on the mode of operation of the hybrid scheme, the CDF of the received SNR is given by

$$
\begin{aligned}
F_{\gamma_s}(x) &= \frac{1}{1 - P_1} \left(N_t \Big(1 - e^{-\frac{Q}{\overline{\gamma}_p}} \Big) e^{-\frac{(N_t - 1)Q}{\overline{\gamma}_p}} \Big(1 - e^{-\frac{x}{\overline{\gamma}_s}} \Big) \right. \\
&\quad + \left. (1 - P_2) F_{\gamma_s}^{\mathrm{TAS/STBC}}(x) \right),
\end{aligned}
$$

(3.38)

where $F_{\gamma_s}^{\text{TAS/STBC}}(\cdot)$ is given in (3.34).

Using simple integration tools, the CDF of the SINR for the hybrid scheme can be derived from (3.12) and (3.38) as

$$
\begin{aligned}
F_{\gamma_{SINR}}(x) &= \frac{1}{1-P_1}\left(N_t\left(1-e^{-\frac{Q}{\bar{\gamma}_p}}\right)e^{-\frac{(N_t-1)Q}{\bar{\gamma}_p}}\right. \\
&\times \left.\left(1-\frac{e^{-\frac{x}{\bar{\gamma}_s}}}{1+\frac{\bar{\gamma}_{ps}}{\bar{\gamma}_s}x}\right)+(1-P_2)F_{\gamma_{SINR}}^{\text{TAS/STBC}}(x)\right).
\end{aligned}
\tag{3.39}
$$

3.4 Performance Analysis

Using the SINR statistics derived in the previous section, we analyse in what follows the performance of each scheme. In order to highlight the motivation behind these performance results, we present the tradeoffs offered by different schemes at the end of this section. In this context, the main purpose of these derived results is to present the pros and cons of these schemes and to confirm their related tradeoffs.

3.4.1 Average Spectral Efficiency

For the considered adaptive modulation scheme, the modulation mode n is used if the output SINR falls between the switching thresholds γ_n and γ_{n+1}. Thus the ASE is given by the sum of the data rates (n) of each of the $N+1$ regions, weighted by the probability that the output SINR falls in the nth region. Equivalently, the ASE of our adaptive modulation system is given as in [23, Eq.(33)] by $\eta = \sum_{i=1}^{N} n\, p_n$, where $p_n = F_{\gamma_{SINR}}(\gamma_{n+1}) - F_{\gamma_{SINR}}(\gamma_n)$ denotes the probability that the nth constellation is used. Using the expressions of the CDF of the output SINR derived in Section 3.3, we get the ASE of each proposed technique as

$$
\eta = N - \sum_{n=2}^{N} F_{\gamma_{SINR}}(\gamma_n).
\tag{3.40}
$$

3.4.2 Average Number of Transmit Antennas

The average power consumption of the studied system can be quantified in terms of the average number of transmit antennas $\overline{N}$. While the TAS/STBC scheme always uses two antennas for transmission, $\overline{N}$ for the other techniques is derived as follows.

MRT-CR

Since MRT-CR uses all antennas verifying the interference constraint for transmission, $\overline{N}$ for this technique can be easily obtained as

$$\overline{N}^{\text{MRT}-\text{CR}} = \frac{1}{1-P_1} \sum_{L=1}^{N_t} L \binom{N_t}{L} \left(1 - e^{-\frac{Q}{\overline{\gamma}_p}}\right)^L e^{-\frac{(N_t-L)Q}{\overline{\gamma}_p}}. \tag{3.41}$$

MS-MRT

Based on the mode of operation of MS-MRT, $\overline{N}$ can be expressed as

$$\overline{N}^{\text{MS}-\text{MRT}} = \frac{1}{1-P_1} \sum_{L=1}^{N_t} \binom{N_t}{L} \left(1 - e^{-\frac{Q}{\overline{\gamma}_p}}\right)^L e^{-\frac{(N_t-L)Q}{\overline{\gamma}_p}} \overline{N}_L, \tag{3.42}$$

where $\overline{N}_L$ is given by

$$\begin{aligned}
\overline{N}_L &= \sum_{l=1}^{L} l \Pr[N=l] = 1 + \sum_{i=1}^{L-1} \binom{L}{i} \Bigg\{ 1 - \frac{e^{\frac{1}{\overline{\gamma}_{ps}}}}{\overline{\gamma}_{ps}} \sum_{k=0}^{L-1} \frac{1}{k!} \left(\frac{\gamma_T}{\overline{\gamma}_s}\right)^k \frac{\Gamma(k+1, \frac{\gamma_T}{\overline{\gamma}_s} + \frac{1}{\overline{\gamma}_{ps}})}{(\frac{\gamma_T}{\overline{\gamma}_s} + \frac{1}{\overline{\gamma}_{ps}})^{k+1}} \\
&\quad + \sum_{l=1}^{L-i} (-1)^{i+l-1} \binom{L-i}{l} \left(\frac{i}{j}\right)^{i-1} \left[\left(1+\frac{l}{i}\right)^{-1} \left[1 - \frac{e^{-\left(1+\frac{l}{i}\right)\frac{\gamma_T}{\overline{\gamma}_s}}}{1 + \left(1+\frac{l}{i}\right)\frac{\gamma_T \overline{\gamma}_{ps}}{\overline{\gamma}_s}}\right] \right. \\
&\quad \left. - \sum_{m=0}^{i-2} \left(-\frac{l}{i}\right)^m \left(1 - \frac{e^{\frac{1}{\overline{\gamma}_{ps}}}}{\overline{\gamma}_{ps}} \sum_{k=0}^{m} \frac{1}{k!} \left(\frac{\gamma_T}{\overline{\gamma}_s}\right)^k \frac{\Gamma(k+1, \frac{\gamma_T}{\overline{\gamma}_s} + \frac{1}{\overline{\gamma}_{ps}})}{(\frac{\gamma_T}{\overline{\gamma}_s} + \frac{1}{\overline{\gamma}_{ps}})^{k+1}}\right) \right] \Bigg\},
\end{aligned} \tag{3.43}$$

where $\Gamma(n,x) = \int_x^\infty t^{n-1} e^{-t} dt$ is the upper incomplete Gamma function.

Hybrid Scheme

The average number of transmit antennas for the hybrid scheme is given by

$$
\begin{aligned}
\overline{N}^{\text{Hybrid}} &= \frac{1}{1-P_1}\left(1 \times \Pr\left[L=1\right] + 2 \times \sum_{L=2}^{N_t}\binom{N_t}{L}\left(1-e^{-\frac{Q}{\overline{\gamma}_p}}\right)^L e^{-\frac{(N_t-L)Q}{\overline{\gamma}_p}}\right) \\
&= \frac{1}{1-P_1}\left(2\left(1-e^{-\frac{N_t Q}{\overline{\gamma}_p}}\right) - N_t\left(1-e^{-\frac{Q}{\overline{\gamma}_p}}\right)e^{-\frac{(N_t-1)Q}{\overline{\gamma}_p}}\right),
\end{aligned} \tag{3.44}
$$

where one antenna is used if $\Pr\left[L=1\right]$ (i.e., only one antenna verifies the interference constraint) and two antenna are used if $\Pr\left[L \geq 2\right]$.

3.4.3 Average Delay

In the TAS/STBC scheme, data is buffered if strictly less than two antennas verify the interference constraint to the PR. On the other hand, all the other schemes can communicate using a single antenna and data is buffered only when all the N_t antennas break the interference constraint. The probability of data buffering, P, is given by P_2 for the TAS/STBC scheme and by P_1 for the for all the other schemes where P_1 and P_2 were previously defined. The average delay can be expressed in terms of the number of slot times that the system waits until a transmission occurs. Let N_w denote this number, thus N_w is a standard Geometric random variable with probability mass function (PMF) given by

$$
\Pr\left[N_w = n\right] = P^n\left(1-P\right). \tag{3.45}
$$

Mean and Variance

Derived from the properties of the Geometric random variable, the mean $\overline{N}_w$ and the variance $\text{Var}\left[N_w\right]$ of N_w are respectively given by

$$
\overline{N_w} = \frac{P}{1-P}, \tag{3.46}
$$

and

$$\text{Var}\,[N_w] = \frac{P}{(1-P)^2}. \tag{3.47}$$

Dropping Probability

Another metric showing the effect of delay is the probability of dropping data. Indeed, for delay sensitive applications data may be dropped if the waiting time before transmission is above a given threshold $N_{w_{\text{th}}}$. This threshold depends on the type of delay-sensitive application and presents an important quality of service measure. The dropping probability P_{drop} is defined as

$$P_{\text{drop}} = \text{Pr}\,[N_w > N_{w_{\text{th}}}] = \left[P^L\right]^{N_{w_{\text{th}}}+1}. \tag{3.48}$$

3.4.4 Average BER

The average BER for the used adaptive modulation system is given in [23, Eq.(35)] as

$$\overline{P}_b = \frac{1}{\eta} \sum_{n=1}^{N} n\, \overline{P}_{b_n}, \tag{3.49}$$

where $\overline{P}_{b_n}$ is the average BER for constellation size n, and is given by

$$\overline{P}_{b_n} = \begin{cases} \int_0^{\gamma_2} P_{b_1}\,(x)\; f_{\gamma_{SINR}}\,(x)\; dx, & n = 1; \\ \int_{\gamma_n}^{\gamma_{n+1}} P_{b_n}\,(x)\; f_{\gamma_{SINR}}\,(x)\; dx, & n > 1; \end{cases} \tag{3.50}$$

where $P_{b_n}(\cdot)$ is given in (3.1) and $f_{\gamma_{SINR}}(\cdot)$ was derived for each proposed technique in Section 3.3.

Due to the considered adaptive modulation system, it becomes very challenging to derive closed-form or simplified expressions of the average BER expression for the proposed techniques. Indeed, the used of finite integration $\left(\int_{\gamma_n}^{\gamma_{n+1}}\right)$ over complex integrands including the high power denominator components caused by the interference from the PT are at the origin of these challenges.

3.4.5 Tradeoffs

In order to highlight the motivation behind the analysis derived above, we present in what follows the main tradeoffs between the proposed schemes. These tradeoffs can be classified in terms of efficiency, reliability, delay, and system complexity.

Efficiency

The MRT-CR scheme is proposed in order to maximize the ASE of the considered system while assuming perfect knowledge of the secondary link's CSI. On the other hand, this scheme uses all antennas verifying the interference constraint for transmission which requires activating multiple RF-chains and thus comes with an additional power consumption. In order to address this, MS-MRT is proposed as a tradeoff scheme between spectral efficiency and energy efficiency. Indeed, MS-MRT transmits using the minimum number of antennas satisfying a certain ASE. The TAS/STBC is also an energy-efficient scheme that always uses two transmit antennas. This scheme comes with the highest ASE at high average SNRs while only requiring a limited feedback from the SR.

Reliability

In terms of reliability, MRT-CR has the best BER performance in the low average SNR range where most antennas verify the interference constraint. At high average SNRs, the TAS/STBC scheme uses two transmit antennas and thus achieves better BER than other schemes transmitting with a single antenna at this range. Similarly, these schemes experience the same behavior in terms of the outage performance.

Delay

The ASE and reliability improvements offered by TAS/STBC at high average SNR come with an additional delay. Indeed, while the TAS/STBC scheme needs at least two antennas verifying the interference constraint in order to transmit, all other techniques can transmit using a single antenna. In order to alleviate this delay experienced by the TAS/STBC scheme, the Hybrid scheme is proposed as a delay-capacity tradeoff scheme. In this scheme, a single-

antenna transmission happens if only one antenna verifies the interference constraint and a two-antennas transmission takes place using TAS/STBC if more than two antennas are available for transmission. The Hybrid scheme offers lower delay at high average SNRs with a slight degradation in the ASE, BER, and outage performances.

Complexity

While all schemes have the same complexity in terms of feedback from the PR, they come with different complexities with regard to the secondary link and to the required feedback from the SR. Indeed, MS-MRT and MRT-CR experience the highest complexity since they require full knowledge of the secondary channel. Moreover, MS-MRT has the highest computational complexity since it needs to find the minimum subset of antennas verifying a certain ASE while MRT-CR transmits as soon as it gets the list of antennas verifying the interference constraint. In a more practical scenario, the TAS/STBC scheme offers a much lower complexity since it only requires a feedback of the indices and the modulation modes of the antennas selected for transmission. The Hybrid scheme experiences similar computational complexity and required the same amount of feedback as the TAS/STBC scheme.
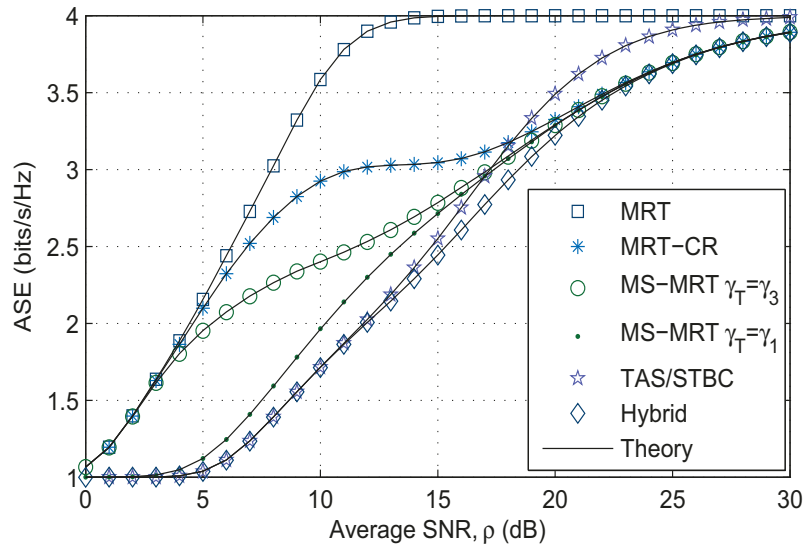

Figure 3.2: ASE versus ρ for $\overline{\gamma}_{ps} = $ -5 dB and $Q_{\mathrm{dB}} = 10$ dB.

3.5   Numerical Examples

The performance of the proposed scheme is illustrated in this section for $N_t = 8$, $N = 4$, and $P_{b_0} = 10^{-3}$. These numerical examples are obtained by Monte-Carlo simulations and confirmed analytically. For the average BER simulations, we first find the ASE for each channel realisation using Monte-Carlo simulations then we derive the BER corresponding to the equivalent constellation size using (3.1). In the figures presented in this section the curves in continuous lines represent the results obtained by analysis and the curves with symbols represent the simulation results.

While the common average SNR per receive antenna at the SR and the PR, respectively denoted by $\overline{\gamma}_s$ and $\overline{\gamma}_p$, are generally different, we assume that $\overline{\gamma}_s = \overline{\gamma}_p = \rho$ when presenting the numerical results for the proposed schemes.[4] This assumption is only for performance comparison simplification and does not impact the performance results presented here.

3.5.1   Average Spectral Efficiency

In Fig. 3.2, we depict the ASE as a function of the common average SNR per antenna ρ for all proposed techniques. In this figure, we only consider successful transmissions, data buffering and the related delay performance is separately presented in Fig. 3.6. As a benchmark, we also present the ASE for the existing MRT technique [13] with interference from the PT. The MRT technique, where all the N_t antennas are always used for transmission (i.e., non-cognitive scenario), has the highest capacity and can be seen as a benchmark for the performance of the proposed techniques. The curve for "MRT with interference" shows the degradation of the ASE due to the effect of the PT's interference.

Among the proposed techniques, MRT-CR offers the best secondary's capacity in the low and medium average SNR range and has lower performance than MRT since only the subset of antennas verifying the interference constraint is used for transmission. MS-MRT uses only the subset of antennas allowing to reach the required modulation mode and offers lower performance for lower values of γ_T. For high average SNRs, the MRT-CR and MS-

---

[4]More efficiently, $\overline{\gamma}_s$ and $\overline{\gamma}_p$ can be expressed as a function of the distance separating ST and the secondary and primary receivers in order to take the path-loss into consideration.

MRT techniques offer the same ASE since in this range fewer antennas verify the interference constraint and data is either buffered or only one antenna is used for transmission for both techniques. In a more practical scenario, the TAS/STBC scheme offers lower ASE in the low average SNR regime, but for high average SNRs it outperforms the other techniques since it uses two antennas with high output SINR and then offers better performance than the case when only one antenna is used. The hybrid scheme offers the same performance as the TAS/STBC scheme for low average SNR since it is more likely that more than two antennas verify the interference constraint. On the other hand, for high average SNR, fewer branches verify the interference and the hybrid scheme is similar to MS-MRT.

3.5.2 Average Number of Transmit Antennas
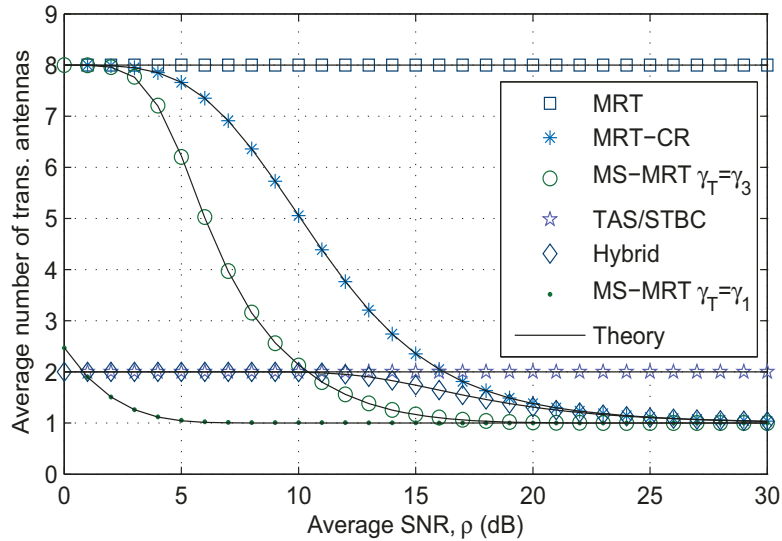
Figure 3.3: Average number of transmit antennas versus ρ for $\overline{\gamma}_{ps}$ = -5 dB and Q_{dB} = 10 dB.

In Fig. 3.3, we present the average number of transmit antennas as a function of ρ. The proposed MS-MRT technique reduces the average number of transmit antennas and thus offers better processing power consumption than MRT-CR. Indeed, while in the MRT-CR technique all the antennas in S need to be used for transmission, MS-MRT offers a considerable power saving by transmitting only with the antennas achieving the required modulation mode. Thus, a lower number of antennas is required for transmission which

shows the advantage of MS-MRT especially for $\gamma_T = \gamma_1$. The TAS/STBC scheme always uses two transmit antennas which comes at the expense of an additional delay (as shown in 3.5.5). On the other hand, the hybrid scheme uses two antennas at the low average SNR range and one antenna when this latter is the only antenna verifying the interference constraint.
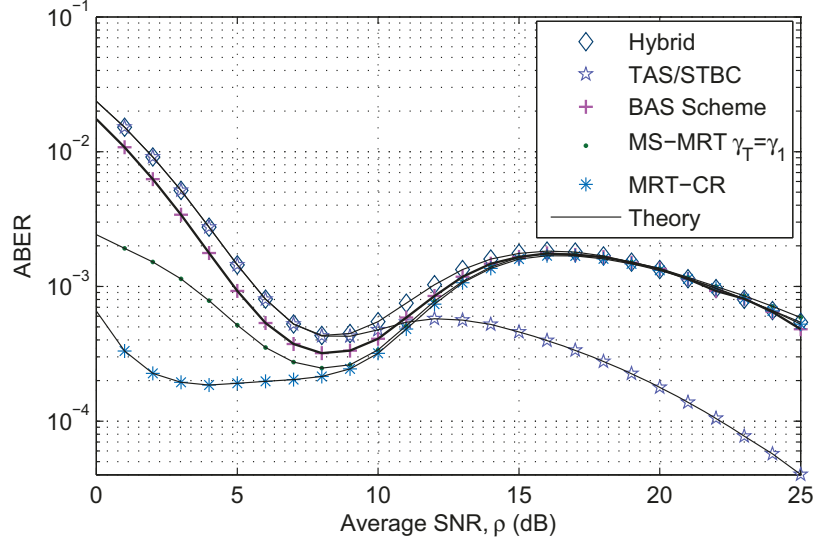
Figure 3.4: Average BER versus ρ.

3.5.3 Average BER Performance

In Fig. 3.4, we depict the BER as a function of ρ for an average INR $\overline{\gamma}_{ps} = $ -5 dB and a peak interference constraint $Q_{\mathrm{dB}} = 10$ dB. For low average SNR, the antennas used for transmission are not able to reach the threshold γ_1 for the lowest modulation mode which breaks the BER requirements at this range. While the shape of the average BER curves looks unusual, it is typical to the considered adaptive system where different number of transmit antennas and different modulation schemes are used at different average SNR ranges [10, 43]. Indeed, the reduction of the number of antennas verifying the interference constraint for higher values of ρ is behind the counterintuitive degradation in the average BER experienced in the medium average SNR range. This generates a lower output SINR at the SR and thus generates higher average error rates. At the high average SNR, the TAS/STBC scheme achieves better average BER performance than other schemes since two antennas are always used for transmission.

At high average SNR, we can also validate from this figure the approximations given in (3.22) and (3.31). Indeed, we have a close match for average SNRs above 10 dB between the MS-MRT scheme and the BAS scheme where the best antenna verifying the interference constraint is selected for transmission.

3.5.4 Outage Performance

Fig. 3.5 shows the outage probability of the proposed schemes as a function of ρ for $Q_{\mathrm{dB}} = 10$ dB. For low average SNR, more antennas are able to verify the peak interference constraint but fail to reach the threshold for the minimum modulation mode which generates an outage event. The TAS/STBC scheme offers better performance especially in the high average SNR range since it uses the best two antennas for transmission. In the low average SNR range, MRT-CR has the best outage performance since most antennas verify the interference constraint and all these antennas are used for transmission. For medium average SNR less antennas verify the interference which generates a decrease in the output SINR and thus an increase in the outage probability.
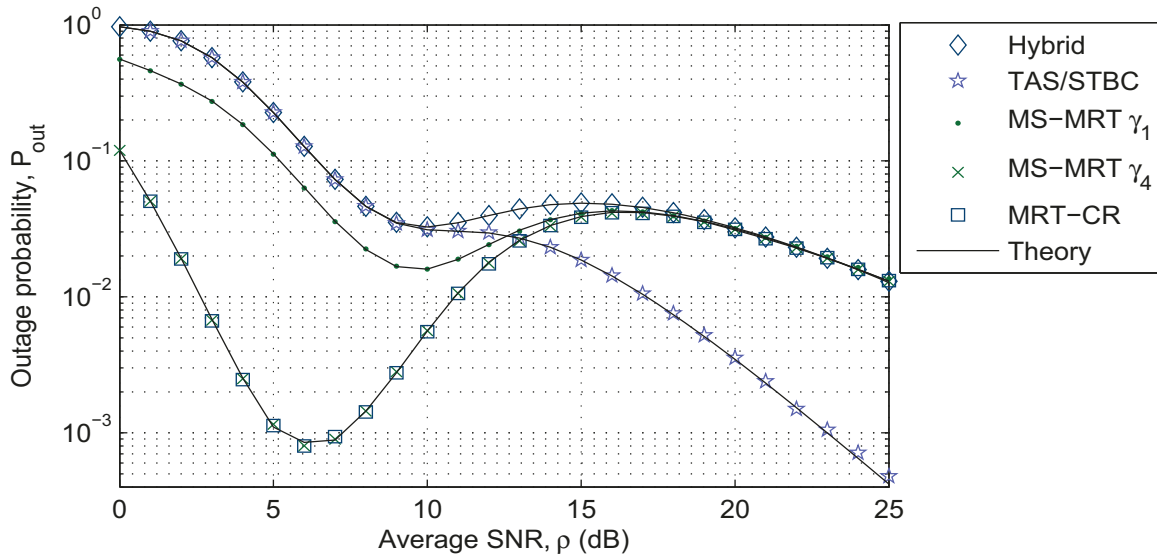
Figure 3.5: Outage probability versus ρ.

3.5.5   Average Delay Performance

The performance improvements introduced by the TAS/STBC scheme come at the expense of an additional time delay since data is buffered even when only one antenna verifies the interference constraint. In Fig. 3.6, we depict the average number of time slots required before finding an acceptable branch versus the peak interference level when $\rho = 10$ dB. From this figure, we can see that the lower the value of Q (i.e., more stringent interference constraint) the higher the delay. Indeed, in this case, fewer antennas verify the interference constraint which makes the ST wait for a longer time before transmitting. For higher values of Q, more antennas verify the interference constraint, which minimizes the average delay. This figure also shows the effect of the number of available antennas at the ST on the delay performance. The higher N_t the lower delay experienced by the proposed techniques. In the proposed schemes, we need to buffer data since the ST does not know the channel gains to the PR. If we assume that the ST has full knowledge of the interference channel, PA can be used in order to minimize the average delay [43].
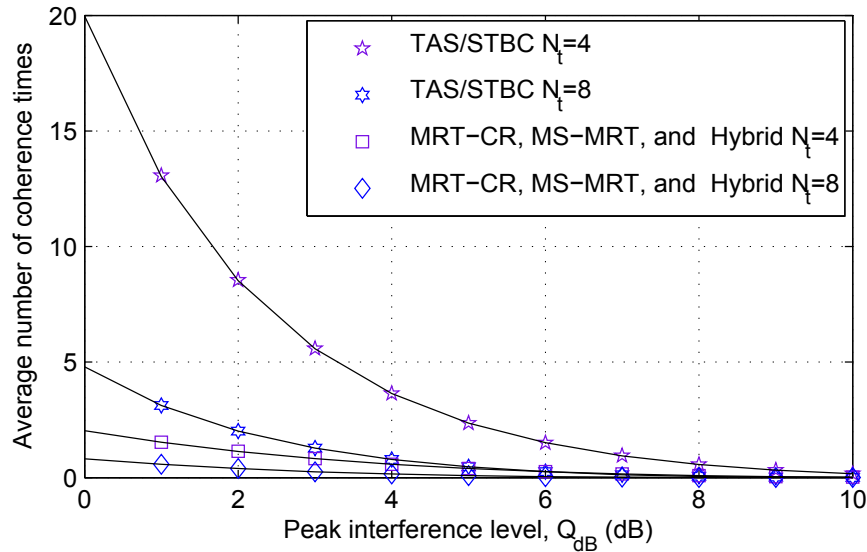
Figure 3.6: Average number of time slots required before finding an acceptable antenna versus the peak interference Q_{dB} for $\rho = 10$ dB and for different values of N_t.

3.6   Conclusion

Inspired by the mode of operation of MS-GSC, we proposed in this chapter the concept of MS-MRT as an adaptive variation of the existing MRT technique in an underlay CR scenario. It was shown that, when the CSI of the secondary link is available at the ST, the proposed techniques improve the ASE of the existing switched diversity schemes by using adaptive transmit beamforming employing the antennas verifying the interference constraint. It was also shown that the MS-MRT technique considerably improves the processing power consumption performance of the MRT technique by minimizing the average number of transmit antennas. In a more practical scenario and based on a limited CSI at the transmitter, the TAS/STBC scheme was shown to offer improved spectral performance at the expense of an additional delay for high average SNR. The hybrid scheme was proposed as a capacity-delay tradeoff between the MS-MRT and the TAS/STBC schemes. These tradeoffs offered by the proposed schemes represent the main motivation behind the derived analytical results and are confirmed in this chapter thanks to selected numerical examples.

Chapter 4

Adaptive Spatial Modulation (ASM) for Spectrum Sharing Systems

4.1 Introduction

In this chapter, we introduce ASM for multiple antenna systems, with the aim of improving the energy efficiency through SM and improving the ASE through AM [46]. Under the scenario of spectrum sharing systems, we extend the concept of ASM to cognitive radio systems in an effort to improve the secondary system's performance in terms of energy efficiency and ASE. To this end, we propose two ASM schemes, one referred to as fixed power scheme (FPS) and the other as adaptive power scheme (APS). In both schemes, the ST has limited knowledge of the CSI of the interference link. The difference between the two schemes, however, lies in the way the limited CSI is used to adapt the transmit power and/or modulation. As a benchmark, we also consider the case in which the ST has perfect knowledge of the CSI. For all cases, we analyze the performance in terms of ASE, average delay, and average bit error rate. We show that the proposed schemes offer tradeoffs in terms of the previously mentioned performance metrics, thus offering different options for applying ASM to CR systems. We also provide several simulation examples through which we corroborate the analytical results.

We show that the full CSI scheme takes advantage of the availability of CSI at the secondary transmitters and does transmit power adaptation. Consequently, data buffering is avoided. On the other hand, the impracticality of the full CSI assumption and the limitation

of the transmit power at high average SNR are the main drawbacks of this technique. As for the FPS scheme, it is proposed in order to minimize the feedback from the PU to the secondary nodes. While this scheme offers ABER and ASE performance improvements compared to the ideal case, it experiences high delays since a transmit antenna can be used only if it verifies the interference constraint to the PU since no power adaptation is allowed. The APS scheme, on the other hand, uses quantized PA and thus offers a delay-ABER trade-off in comparison with the FPS and the full CSI schemes.

The remainder of the chapter is organized as follows. Section 4.2 presents the system and channel models and defines the used adaptive modulation system and the optimal ASM-CR Detector. Section 4.3 gives the motivation and the details behind the mode of operation of each proposed technique. Section 4.4 analyses the performance of different schemes and Section 4.5 illustrates and confirms this performance via selected numerical results. Finally, Section 4.6 concludes the chapter.

4.2   System and Channel Models

4.2.1   System Model

We consider the system model shown in Fig. 4.1, which consists of a MIMO wireless link with N_t transmit and N_r receive antennas in a spectrum sharing system. Under this scenario, the ST is allowed to share the spectrum with a single-antenna PU as long as an interference constraint to this latter with a peak value Q is respected. All feedback links presented in the system model are assumed to be reliable and carry different levels of feedback information between the PU and the secondary nodes. Based on this feedback information, the SR determines the list of antennas eligible for transmission and the modulation mode that can be used by each antenna. Depending on both the number of antennas verifying the interference and their achieved modulation modes, the SR provides the ST with the list of antennas and the modulation mode that can be used for the next coherent time. The mode of operation for each proposed technique and the information carried through the reliable feedback channels are given in details in Section 4.3.
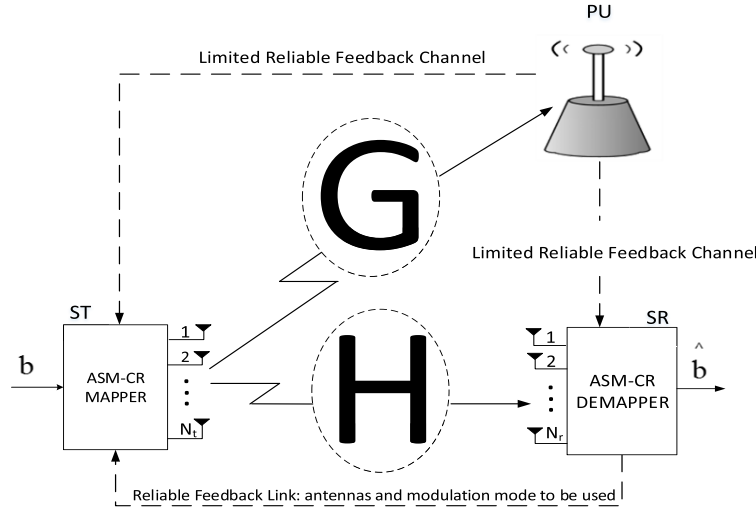
Figure 4.1: ASM-CR System model.

4.2.2 Channel Model

Let $h_{s_{ji}}$, $i \in \{1, 2, \ldots, N_t\}$ and $j \in \{1, 2, \ldots, N_r\}$ be the channel coefficient between the ith antenna of the ST and jth antenna of the SR and let g_{p_i} be the channel coefficient between the ith antenna of the ST and the PU. While the proposed schemes and analytical framework are applicable to generic fading scenarios, we assume for this study that the received signal from each antenna experiences i.i.d Rayleigh fading. Let $\mathbf{G}$ be the $1 \times N_t$ wireless channel matrix between the ST and PU. The $N_r \times N_t$ wireless channel matrix between the ST and SR is denoted by $\mathbf{H}$ and the transmitted signal through this channel experiences an N_r-dim AWGN $\boldsymbol{\eta} = [\eta_1, \ \eta_2 \ldots, \ \eta_{N_r}]^T$. $\mathbf{G}$, $\mathbf{H}$, and $\boldsymbol{\eta}$ have i.i.d entries according to a complex Gaussian distribution with zero mean and unit variance, i.e., $\mathcal{CN}(0, 1)$. Assuming a secondary power $P_t \leq P_{\max}$, where $P_{\max}$ is the maximum power that can be used by the ST, the received SNRs from the ith antenna at the SR and the PU are given respectively by $\gamma_{s_i} = P_t \sum_{j=1}^{N_r} |h_{s_{ji}}|^2$ and $\gamma_{p_i} = P_t |g_{p_i}|^2$. We define $\overline{\gamma}_s$ and $\overline{\gamma}_p$ as the common average SNR per receive antenna at the SR and the PR, respectively. Assuming frequency flat fading for all links, and that the links' gains have similar statistics, the interference and secondary links experience on average the same SNR during each channel coherence time. In this context, we assume that $\overline{\gamma}_s = \overline{\gamma}_p = \rho$ when analysing the performance and presenting the numerical results for the proposed ASM-CR schemes.

4.2.3   Adaptive Transmission System

We consider the constant-power variable-rate uncoded M-ary QAM (M-QAM) [23] as an adaptive modulation system. With this adaptive modulator, the SNR range is divided into $m_t + 1$ fading regions and the constellation size $M = 2^m$ is assigned to the mth region ($m = 0, 1, \ldots, m_t$). The BER of coherent 2^m-QAM with two-dimensional Gray coding over an AWGN channel with an SNR of γ can be well approximated as [23]

$$P_{b_m}(\gamma) \simeq \frac{1}{5} \exp\left(\frac{-3\gamma}{2(2^m - 1)}\right). \tag{4.1}$$

Given a target instantaneous BER equal to P_{b_0}, the adaptive modulator switching thresholds are given by

$$\gamma_m = -\frac{2}{3} \ln(5\, P_{b_0})(2^m - 1)\,;\ m = 1, 2, \ldots, m_t. \tag{4.2}$$

In order to satisfy the BER requirement, modulation mode $m = m_j$ or lower can be used for antenna j if the received SNR from that antenna is above γ_m but below γ_{m+1}. In all proposed schemes, we present two variations when deciding on the modulation mode to be used by each antenna. These variations are proposed to compromise between ASE in one side and ABER and system complexity on the other side.

Actual Modulation Variation (ACT): In this option, we aim at achieving the maximum possible ASE while keeping the ABER below a certain threshold. Based on the SR's feedback, the antenna selected for transmission uses the highest achievable modulation mode. While this option maximizes the throughput, an antenna index detection error may cause the receiver to select symbols from a constellation other than the one that the transmit symbol is drawn from. Moreover, this option comes with an additional receiver's complexity since the detector uses different constellations to decide on the symbol and antenna that were used for transmission. To alleviate this, we propose next a second modulation selection variation.

Minimum Modulation Variation (MIN): In this second option, we aim at improving the ABER experienced by the first scheme at the expense of a slight loss in the average throughput. While in the ACT variation, different transmit antennas can send symbols

drawn from different constellations depending on their received SNR at the SR, the antennas in the MIN variation use a common constellation. Indeed, the receiver in this option only feeds back the minimum modulation mode that can be achieved by all antennas. This way, the same modulation mode is used by all selected antennas for a given time slot. Thus, the decoder decides on the transmitted symbol and used antenna using a single constellation, which reduces the detection complexity.

4.2.4 Optimal ASM-CR Detection

In all proposed techniques, the ST obtains the list of antennas selected for transmission and the modulation modes to be used with each antenna based on the feedback from the PU and the SR. Let N denote the number of selected antennas and $m_1, m_2, \ldots, m_N$ be the modulation modes reached by each of them. The first $\log_2(N)$ bits in the random sequence of independent bits $\mathbf{b}$ are used to determine the antenna to be active for transmission for the next time slot. If antenna j is selected for transmission, then the next $\log_2(M_j)$ bits are used to draw the symbol x_q from an adaptive M_j-ary QAM constellation, where $M_j = 2^{m_j}$ for the ACT variation, and $M_j = 2^{m_{\min}}$ for the MIN variation where $m_{\min} = \min_{i=1\ldots N} m_i$. These $\log_2(N\,M_j)$ bits are then mapped to the constellation vector

$$\boldsymbol{x}_{jq} = [0 \ldots 0 \quad \underset{\substack{\uparrow \\ j^{th}\,\text{position}}}{x_q} \quad 0 \ldots 0]^T.$$

The signal x_{jq} is then transmitted using only antenna j over the wireless channel $\mathbf{H}$ and the output of the channel can be expressed as

$$\boldsymbol{y} = \sqrt{\rho}\,\boldsymbol{h}_j\,\boldsymbol{x}_q + \boldsymbol{\eta}, \tag{4.3}$$

where $\boldsymbol{h}_j$ denotes the jth column of $\mathbf{H}$ and ρ was defined above as the common average faded SNR per antenna for the secondary and interference links.

The detector's main task is to find the antenna index used for transmission and the symbol sent by that antenna. Assuming equally likely channel inputs, this information can be jointly

obtained using the optimal ASM detector based on the ML principle presented in [46] as

$$[\hat{j}, \hat{q}] = \arg\max_{j,q} f_{\boldsymbol{Y}}(\boldsymbol{y}|\boldsymbol{x}_{jq}, N, m, \mathbf{H}) = \arg\min_{j,q} \sqrt{\rho}\|\boldsymbol{g}_{jq}\|_{\mathrm{F}}^2 - 2\mathrm{Re}\{\boldsymbol{y}^H\boldsymbol{g}_{jq}\}, \qquad (4.4)$$

where $\boldsymbol{g}_{jq} = \boldsymbol{h}_j\boldsymbol{x}_q$, $1 \leq j \leq N$, $1 \leq q \leq 2^m$, $m = \log_2(M_j)$, and $f_{\boldsymbol{Y}}(\boldsymbol{y}|\boldsymbol{x}_{jq}, \mathbf{H}) = \pi^{N_r}\exp\left(-\|\boldsymbol{y} - \sqrt{\rho}\,\mathbf{H}\,\boldsymbol{x}_{jq}\|_{\mathrm{F}}^2\right)$ is the PDF of the received signal conditioned on $\boldsymbol{x}_{jq}$ and $\mathbf{H}$. The selected j and q are different from a time slot to another and are a function of (i) the number of antennas verifying the interference, (ii) the received SNR from these antennas, (iii) and the values of the incoming bits.

4.3 Motivation and Mode of Operation

Depending on the level of the required interference link's CSI at the ST, the techniques presented in this chapter can be classified into two sets (i) the ideal case where full CSI is required at the secondary transmitter, and (ii) the proposed techniques where only limited feedback from the PU is required at the secondary nodes, namely the fixed power and adaptive power schemes. The ideal case is presented as a benchmark to the limited feedback schemes. In this section, we first present the motivation behind each of the proposed techniques then we give their modes of operation.

4.3.1 Perfect CSI (Benchmark)

Motivation: This technique is proposed as a benchmark for the schemes with limited feedback from the PU. In this technique, the ST has perfect knowledge of the CSI of the interference link. Thanks to this knowledge, the ST uses PA with each transmit antenna in order to respect the interference constraint. While this comes with the advantage of removing extra delays due to the failure of verifying the interference constraint, the transmit power in this case is limited by the interference level seen at the PU which leads to a degradation in the ASE and ABER performance. Moreover, the perfect CSI assumption could be costly in terms of overhead and/or impractical.

Mode of Operation: Since the ST has perfect CSI of the interference link, PA is used in order to respect the interference seen at the PU. Indeed, if the peak interference constraint level Q caused by antenna j is verified, then that antenna can be used with $P_t = P_{\max}$. If, on the other hand, this constraint is not respected then the transmit power is adapted to the interference channel and is set to $P_t = \frac{Q}{|h_{p_j}|^2}$, where h_{p_j} is the channel coefficient between the jth antenna of the ST and the PU. Once the transmit power from each antenna is determined and assumed to be available to the SR, this latter finds the modulation mode that can be used by each antenna depending on wether the ACT or MIN variation is used. While using the actual modulation achieved by each antenna seems to be more efficient in terms of ASE, this case comes with an additional complexity and worse ABER performance. The mode of operation of the ideal case with both variations is summarised by Algorithm 1 below.

Algorithm 1 Ideal Case

1: Find P_{t_j} for antenna j, $j = 1, 2, \ldots, N_t$; if $P_{\max} \times |h_{p_j}|^2 \leq Q \Rightarrow P_{t_j} = P_{\max}$ else $P_{t_j} = \frac{Q}{|h_{p_j}|^2}$.
2: Let $\gamma_{s_j} = P_{t_j} \times \sum_{j=1}^{Nr} |h_{s_{ji}}|^2$ be the received SNR from antenna j.
3: Find modulation mode m_j reached by antenna j; If $\gamma_m \leq \gamma_{s_j} < \gamma_{m+1} \Rightarrow m_j = m$.
4: $\log_2(N_t)$ input bits are used to select transmit antenna j.
5: ACT $\Rightarrow$ use 2^m-QAM where $m = m_j$ is the modulation reached by antenna j (step 3).
6: MIN $\Rightarrow$ use 2^m-QAM where $m = m_{\min}$ and $m_{\min} = \min\{m_1, m_2, \ldots, m_{N_t}\}$.
7: Transmit m bits from antenna j using 2^m-QAM.

4.3.2 Fixed Power Scheme (FPS)

Motivation: The FPS scheme is proposed to minimize the amount of feedback required by the secondary system. Indeed, the only information fed back to the secondary nodes about a given antenna is whether that antenna verifies the interference constraint or not. Thus, a one bit feedback from the PU is enough to know if a given antenna is eligible for transmission. This way, all antennas selected for transmission use a fixed power equal to $P_{\max}$. While this maximum power increases the ASE and improves the ABER performance, the FPS scheme experiences a high delay for high average SNRs since data is buffered if less than two antennas verify the interference constraint to the PU.

Mode of Operation: Before transmission takes place, the ST tests all its N_t antennas for the interference constraint by broadcasting some pilot signals. Let N_Q be the number of

antennas verifying the interference level Q. The number of antennas that can be used for transmission with the FPS scheme needs to be lower or equal to N_Q and also needs to be a power of two. Let N be the largest integer verifying both of these conditions. In response to the same pilot signals, the SR determines the modulation mode achieved by each transmit antenna and ranks these antennas according to their received SNRs. At this stage, the SR selects the N best antennas among N_Q for transmission. Then, the indices of these antennas and the modulation mode to be used are sent to the ST through a reliable feedback channel. In the ACT variation, each antenna selected for transmission can use the maximum modulation that it can reach. On the other hand, in the MIN variation, the minimum modulation mode reached by the N selected antennas is used by all selected transmit antennas.

If N_Q is strictly lower than two, then data is buffered for a channel coherence time. This requirement increases the time that the delay especially in the high average SNR range. The mode of operation of the FPS scheme is summarised by Algorithm 2 below.

Algorithm 2 FPS Scheme

1: Find N_Q, while $N_Q < 2 \Rightarrow$ buffer data.
2: If $N_Q \geq 2 \Rightarrow$ SR ranks these antennas according to their SNRs: $\gamma_{1:N_Q} \geq \gamma_{2:N_Q} \geq \ldots \geq \gamma_{N_Q:N_Q}$.
3: Let $n = \lfloor \log_2(N_Q) \rfloor$ and $N = 2^n \Rightarrow$ the best N antennas among N_Q are available for transmission.
4: n input bits are used to select transmit antenna j.
5: ACT $\Rightarrow$ use 2^m-QAM if $\gamma_m \leq \gamma_{j:N_Q} < \gamma_{m+1}$.
6: MIN $\Rightarrow$ use 2^m-QAM if $\gamma_m \leq \gamma_{N:N_Q} < \gamma_{m+1}$.
7: Transmit m bits from antenna j using 2^m-QAM.

4.3.3 Adaptive Power Scheme (APS)

Motivation: Similar to the FPS scheme, the APS scheme only requires a limited knowledge about the interference link. While FPS uses $P_{\max}$ with the antennas verifying the interference constraint and buffers data otherwise, APS uses PA if the interference to the PU falls in a certain range above Q. In this context, APS is proposed as a tradeoff scheme between the ideal case and the FPS scheme, offering a trade-off between ASE and average system delay. Indeed, the APS scheme minimizes the delay experienced by the FPS scheme with a slight decrease in ASE due to the use of PA.

Mode of Operation: In the ideal PA case, the transmitted power can be varied continuously to accurately follow the channel variations. For practical scenarios, the resolution of PA is limited, e.g., for Universal Mobile Telecommunications System (UMTS) systems, power control step sizes on the order of 1 dB are proposed [91]. Thus, in the APS scheme, we present a discrete PA scenario between the PU and the secondary nodes. Let δ be the used power control step size and $\Delta_{\max}$ be the maximum amount of power that can be reduced by the ST. When PA is required, PU sends $N_b = \lceil \log_2(\Delta_{\max}/\delta) \rceil$ bits to let the ST know the number of steps required in order to verify the interference constraint. This information is also sent to the SR in order to find the modulation mode that can be reached by each transmit antenna. In order to maximize the ASE of the secondary link, $\Delta_{\max}$ is designed to increase the probability that the modulation mode reached by a given antenna before and after PA remains the same. Thus, $\Delta_{\max}$ should be limited by the minimum ratio between the switching thresholds defined in (4.2) and is given by

$$\Delta_{\max} \leq \min_{1 \leq m \leq m_t} \frac{\gamma_{m+1}}{\gamma_m}. \tag{4.5}$$

Before each transmission, ST tests all its N_t antennas for the interference constraint by broadcasting some pilot signals. The selected antennas and the transmit power that can be used by each of these antennas are obtained according to the three following scenarios; (i) if the interference caused by a given antenna is below Q, that antenna can be used for transmission with power $P_t = P_{\max}$, (ii) if the interference γ_p is greater than Q but lower than $Q \times \Delta_{\max}$, PA is used in order to satisfy the interference constraint Q. To achieve this, the transmit power is reduced to $P_t = P_{\max}/\delta^k$ if $Q \times \delta^{k-1} < \gamma_p \leq Q \times \delta^k$ where k takes values between 1 and $K_{\max}$, where $K_{\max} = \lceil \Delta_{\max}/\delta \rceil$ is the maximum number of power steps that can be reduced by the ST, and (iii) if the caused interference by a ST's antenna is above $Q \times \Delta_{\max}$ then that antenna can not be used for transmission during the current coherence time. Let $N_{Q'}$ be the number of antennas verifying the interference level $Q' = Q \times \Delta_{\max}$. The number of antennas that can be selected for transmission with the APS scheme needs to be lower or equal to $N_{Q'}$ and also needs to be a power of two. Let N be the largest integer verifying both of these conditions. Thanks to the N_b bits sent from the PU,

the SR determines the modulation mode achieved by each transmit antenna and ranks these antennas according to their received SNRs. At this stage, the SR selects the N best antennas among $N_{Q'}$ for transmission. Then, the indices of these antennas and the modulation mode to be used are sent to the ST through a reliable feedback channel. In the ACT variation, each antenna selected for transmission can use the actual modulation that it can reach. On the other hand, in the MIN variation, the minimum modulation mode reached by the N transmit antennas is used by the selected transmit antenna.

If $N_{Q'}$ is strictly lower than two, then data is buffered for a channel coherence time. This requirement increases the average delay that the ST needs to wait before transmission especially in the high average SNR range. The mode of operation of the APS scheme is summarised by Algorithm 3 below.

Algorithm 3 APS Scheme

1: Find $N_{Q'}$; defined as the number of antennas verifying $\gamma_p \leq Q \times \Delta_{\max}$.
2: While $N_{Q'} < 2 \Rightarrow$ buffer data.
3: If $N_{Q'} \geq 2 \Rightarrow$ find P_t for each of these antennas.
4: If $\gamma_p \leq Q \Rightarrow P_t = P_{\max}$; if $Q \times \delta^{k-1} < \gamma_p \leq Q \times \delta^k \Rightarrow P_t = P_{\max}/\delta^k$, $1 \leq k \leq K_{\max}$.
5: SR ranks these antennas according to their SNRs: $\gamma_{1:N_{Q'}} \geq \gamma_{2:N_{Q'}} \geq \ldots \geq \gamma_{N_Q:N_{Q'}}$.
6: Let $n = \lfloor \log_2(N_{Q'}) \rfloor$ and $N = 2^n \Rightarrow$ the best N antennas among $N_{Q'}$ are available for transmission.
7: n input bits are used to select transmit antenna j.
8: ACT $\Rightarrow$ use 2^m-QAM if $\gamma_m \leq \gamma_{j:N_{Q'}} < \gamma_{m+1}$.
9: MIN $\Rightarrow$ use 2^m-QAM if $\gamma_m \leq \gamma_{N:N_{Q'}} < \gamma_{m+1}$.
10: Transmit m bits from antenna j using 2^m-QAM.

4.4   Performance Analysis

In this section, we analyse the performance of each of the proposed schemes in terms of the ASE, average delay, effective throughput, and ABER. For analytical tractability, the derived results are given for a single receive antenna. In selected special cases, we derive general expressions as a function of N_r.

In the presented ASE performance, we only account for successful transmissions and the time slots where data is buffered are not considered. Thus, the ASE only reflects the throughput when enough antennas are available for transmission. In order to show the effect

of data buffering, we also analyse the average delay experienced by the proposed schemes. Combining the ASE and average delay results, we also present the effective throughput performance where data buffering is considered as zero throughput.

4.4.1 Perfect CSI

In this ideal case, the ST transmits with its maximum power P_{max} if the interference constraint at the PU is verified. If, on the other hand, this constraint is violated, PA is employed by the ST. Thus, based on the received SNR at the PU, ST selects its transmit power as

$$P_t \;=\; \min\left(P_{\text{max}}, \frac{Q}{|h_{p_i}|^2}\right). \tag{4.6}$$

The CDF and the PDF of the received SNR from the jth antenna are respectively given for $N_r = 1$ as in [43] by

$$
\begin{aligned}
F_{\gamma_{s_j}}(x) = \Pr\left[\gamma_{s_j} \le x\right] &= \Pr\left[\min\left(P_{\text{max}}, \frac{Q}{|h_{p_j}|^2}\right) \times |h_{s_j}|^2 \le x\right] \\
&= 1 - \left(1 - \frac{x}{x+Q} e^{-\frac{Q}{\rho}}\right) e^{-\frac{x}{\rho}},
\end{aligned} \tag{4.7}
$$

and

$$f_{\gamma_{s_j}}(x) \;=\; \frac{(Q+x)\left((Q+x)e^{\frac{Q}{\rho}} - x\right) + \rho\, Q}{\rho(Q+x)^2} e^{-\frac{x+Q}{\rho}}. \tag{4.8}$$

ASE: The total ASE of the proposed ASM-CR techniques is given by the sum of the throughput obtained by the spatial dimension (SD) and the AM dimension denoted by η_{SD} and η_{AM}, respectively. For the perfect CSI scenario, all N_t antennas in the ST are eligible for transmission thanks to the use of PA. Thus, no data buffering is required and the ASE is equal to the effective throughput η_{eff}. Moreover, the ASE achieved by the SD is constant and is given by $\eta_{\text{SD}} = log_2(N_t)$.

For the considered AM system, modulation mode m is used if the output SNR falls between thresholds γ_m and γ_{m+1}. Thus, the average link spectral efficiency is given by the sum of the data rates (i.e., m) of each of the $m_t + 1$ regions, weighted by the probability that

the output SNR falls in the mth region. Equivalently, the ASE of the AM system is given by [23, Eq.(33)]

$$\eta_{\text{AM}} = \sum_{m=1}^{m_t} m \, p_m, \tag{4.9}$$

where p_m denotes the probability that the mth constellation is selected and depends on whether the ACT or MIN modulation selection variation is used.

ACT Variation: In this variation, the antenna selected for transmission uses the actual modulation mode it can reach. Thus, constellation mode m is used by antenna j if the received SNR γ_{s_j} from that antenna falls between thresholds γ_m and γ_{m+1}. Based on this, p_m for the ACT variation is given by

$$p_m^{\text{ACT}} = \Pr\left[\gamma_m \leq \gamma_{s_j} < \gamma_{m+1}\right] = F_{\gamma_{s_j}}\left(\gamma_{m+1}\right) - F_{\gamma_{s_j}}\left(\gamma_m\right), \tag{4.10}$$

where $F_{\gamma_{s_j}}(\cdot)$ is given by (4.7). Substituting (4.10) in (4.9) and letting $\gamma_{m_t+1} = +\infty$ (i.e., $F_{\gamma_{s_j}}\left(\gamma_{m_t+1}\right) = 1$), the ASE of the signal dimension for the ACT option is given by

$$\eta_{\text{AM}}^{\text{ACT}} = m_t - \sum_{m=2}^{m_t} F_{\gamma_{s_j}}\left(\gamma_m\right). \tag{4.11}$$

MIN Variation: In this variation, the antenna selected for transmission uses the minimum modulation mode that can be reached by the set of transmit antennas. Thus, constellation mode m is used by antenna j if the minimum output SNR from all antenna falls between γ_m and γ_{m+1}. Based on this, p_m for this second option is given by

$$p_m^{\text{MIN}} = \Pr\left[\gamma_m \leq \min_{i=1...N_t}\gamma_{s_i} < \gamma_{m+1}\right] = \left(1 - F_{\gamma_{s_j}}\left(\gamma_m\right)\right)^{N_t} - \left(1 - F_{\gamma_{s_j}}\left(\gamma_{m+1}\right)\right)^{N_t}. \tag{4.12}$$

The ASE of the signal dimension for the MIN variation is then given by

$$\eta_{\text{AM}}^{\text{MIN}} = 1 + \sum_{m=2}^{m_t} \left(1 - F_{\gamma_{s_j}}\left(\gamma_m\right)\right)^{N_t}. \tag{4.13}$$

Finally, the total ASE and the effective throughput for the ideal case are given by

$$\eta = \eta_{\text{eff}} = \eta_{\text{SD}} + \eta_{\text{AM}} = \log_2(N_t) + \begin{cases} m_t - \sum_{m=2}^{m_t} F_{\gamma_{s_j}}(\gamma_m), & \text{ACT variation;} \\ 1 + \sum_{m=2}^{m_t} \left(1 - F_{\gamma_{s_j}}(\gamma_m)\right)^{N_t}. & \text{MIN variation;} \end{cases} \quad (4.14)$$

4.4.2 Fixed Power Scheme

In the FPS scheme, transmission occurs only if two or more antennas verify the peak interference constraint Q. Otherwise (i.e., $N_Q < 2$), data is buffered for a channel coherence time. The probability of data buffering for the FPS scheme is then given by

$$\begin{aligned} P_{\text{buf}}^{\text{FPS}} &= \Pr[N_Q < 2] = \Pr[N_Q = 1] + \Pr[N_Q = 0] \\ &= N_t \Pr[\gamma_p \le Q] \left(\Pr[\gamma_p > Q]\right)^{N_t - 1} + \left(\Pr[\gamma_p > Q]\right)^{N_t} \\ &= N_t \left(1 - e^{-\frac{Q}{\rho}}\right) e^{-\frac{(N_t - 1)Q}{\rho}} + e^{-\frac{N_t Q}{\rho}} = \left(N_t - (N_t - 1)e^{-\frac{Q}{\rho}}\right) e^{-\frac{(N_t - 1)Q}{\rho}}, \quad (4.15) \end{aligned}$$

where $\Pr[\gamma_p > Q]$ is the probability that one antenna fails to verify the peak interference constraint Q.

Given that N_Q antennas verify the interference constraint and based on the mode of operation of the FPS scheme, the PDF of the received SNR from antenna j is given for a single receive antenna by

$$\begin{aligned} f_{\gamma_{s_j}}^{\text{FPS}}(x) &= \frac{1}{1 - P_{\text{buf}}^{\text{FPS}}} \sum_{N_Q = 2}^{N_t} \binom{N_t}{N_Q} \left(\Pr[\gamma_p \le Q]\right)^{N_Q} \left(\Pr[\gamma_p > Q]\right)^{N_t - N_Q} \frac{1}{N} \sum_{i=1}^{N} f_{\gamma_{i:N_Q}}(x) \\ &= \frac{1}{1 - P_{\text{buf}}^{\text{FPS}}} \sum_{N_Q = 2}^{N_t} \binom{N_t}{N_Q} \left(1 - e^{-\frac{Q}{\rho}}\right)^{N_Q} e^{-\frac{(N_t - N_Q)Q}{\rho}} \frac{1}{N} \sum_{i=1}^{N} f_{\gamma_{i:N_Q}}(x), \quad (4.16) \end{aligned}$$

where the term $1/(1 - P_{\text{buf}}^{\text{FPS}})$ represents the possible events on how many times data is buffered before at least two antennas verify the interference constraint. The sum from 2 to N_t considers the cases where N_Q among the N_t available antennas verify the peak interference constraint to the PU. N represents the number of antennas selected for transmission ($N = 2^n$, where $n = \lfloor \log_2(N_Q) \rfloor$). $f_{\gamma_{i:N_Q}}(\cdot)$ is the PDF of the received SNR from the ith strongest antenna

among the N_Q verifying the interference constraint and is derived using [92, page 41] as

$$
\begin{aligned}
f_{\gamma_{i:N_Q}}(x) &= \frac{N_Q!}{(N_Q - i)!(i - 1)!}\left(F_{\exp}(x)\right)^{N_Q - i}\left(1 - F_{\exp}(x)\right)^{i-1} f_{\exp}(x) \\
&= \frac{N_Q!}{(N_Q - i)!(i - 1)!\rho}\left(1 - e^{-\frac{x}{\rho}}\right)^{N_Q - i} e^{-\frac{ix}{\rho}},
\end{aligned}
\tag{4.17}
$$

where $F_{\exp}(\cdot)$ and $f_{\exp}(\cdot)$ are respectively the CDF and PDF of the received SNR from each antenna before ordering and represent the statistics of an Exponential random variable.

For $N_t = 2$ and arbitrary N_r, the received SNR with the FPS scheme is a χ^2-distributed random variable with $2 \times N_r$ degrees of freedom. The PDF of γ_{s_j} in this case is given by [93, Eq. 2.1-110]

$$
f_{\gamma_{s_j}}^{\mathrm{FPS}}(x) = \frac{x^{N_r - 1}}{(N_r - 1)!\rho^{N_r}}e^{-\frac{x}{\rho}}.
\tag{4.18}
$$

The CDF of the received SNR for the FPS scheme is given for a single receive antenna by

$$
\begin{aligned}
F_{\gamma_{s_j}}^{\mathrm{FPS}}(x) &= \frac{1}{1 - P_{\mathrm{buf}}^{\mathrm{FPS}}}\sum_{N_Q=2}^{N_t}\binom{N_t}{N_Q}\left(\Pr\left[\gamma_p \leq Q\right]\right)^{N_Q}\left(\Pr\left[\gamma_p > Q\right]\right)^{N_t - N_Q}\frac{1}{N}\sum_{i=1}^{N}F_{\gamma_{i:N_Q}}(x) \\
&= \frac{1}{1 - P_{\mathrm{buf}}^{\mathrm{FPS}}}\sum_{N_Q=2}^{N_t}\binom{N_t}{N_Q}\left(1 - e^{-\frac{Q}{\rho}}\right)^{N_Q}e^{-\frac{(N_t - N_Q)Q}{\rho}}\frac{1}{N}\sum_{i=1}^{N}F_{\gamma_{i:N_Q}}(x),
\end{aligned}
\tag{4.19}
$$

where $F_{\gamma_{i:N_Q}}(\cdot)$ is the CDF of the SNR of the ith strongest antenna among the N_Q antennas verifying the interference and is obtained from (4.17) using Binomial expansion and simple integrations as

$$
F_{\gamma_{i:N_Q}}(x) = \frac{N_Q!}{(i - 1)!}\sum_{k=0}^{N_Q - i}(-1)^k \frac{1 - e^{-\frac{(k+i)x}{\rho}}}{k!(N_Q - k - i)!(k + i)}.
\tag{4.20}
$$

For $N_t = 2$ and arbitrary N_r, the CDF of γ_{s_j} is given by [93, Eq. 2.1-114]

$$
F_{\gamma_{s_j}}^{\mathrm{FPS}}(x) = 1 - \sum_{k=0}^{N_r - 1}\frac{1}{k!}\left(\frac{x}{\rho}\right)^k e^{-\frac{x}{\rho}}.
\tag{4.21}
$$

ASE: The total ASE of the FPS scheme is the sum of the throughput obtained by the

SD and AM dimensions denoted by η_{SD} and η_{AM}, respectively. While for the ideal case the spatial dimension's ASE is always given by $n_t = \log_2(N_t)$, η_{SD} for the FPS scheme depends on the number of antennas verifying the interference and is given by $\sum_{n=1}^{n_t} n\, q_n$, where q_n is the probability that $N = 2^n$ antennas are available for transmission and is given by

$$q_n = \frac{1}{1 - P_{\text{buf}}^{\text{FPS}}} \sum_{N=2^n}^{\min(2^{n+1}-1, N_t)} \binom{N_t}{N} \left(1 - e^{-\frac{Q}{\rho}}\right)^N e^{-\frac{(N_t - N)Q}{\rho}}. \tag{4.22}$$

The ASE of the AM system for the FPS scheme is given by

$$\eta_{\text{AM}} = \sum_{m=1}^{m_t} m\, p_m, \tag{4.23}$$

where p_m depends on which variation is used in the selection of the modulation mode for each antenna.

ACT Variation: In this variation, antenna j uses modulation mode m if the received SNR γ_{s_j} from that antenna falls between thresholds γ_m and γ_{m+1}. Based on this, p_m for the ACT variation is given by

$$p_m^{\text{ACT}} = \Pr\left[\gamma_m \leq \gamma_{s_j} < \gamma_{m+1}\right] = F_{\gamma_{s_j}}^{\text{FPS}}(\gamma_{m+1}) - F_{\gamma_{s_j}}^{\text{FPS}}(\gamma_m). \tag{4.24}$$

The ASE of the signal dimension for the ACT option is then given by

$$\eta_{\text{AM}}^{\text{ACT}} = m_t - \sum_{m=2}^{m_t} F_{\gamma_{s_j}}^{\text{FPS}}(\gamma_m). \tag{4.25}$$

MIN Variation: In this variation, modulation mode m is used by antenna j if the minimum output SNR from all antennas falls between γ_m and γ_{m+1}. Given that N_Q antennas verify the interference constraint and that N antennas are selected for transmission, p_m for this second option is given by

$$\begin{aligned} p_m^{\text{MIN}} &= \Pr\left[\gamma_m \leq \min_{i=1,\dots,N} \gamma_{i:N_Q} < \gamma_{m+1}\right] \\ &= \Pr\left[\gamma_m \leq \gamma_{N:N_Q} < \gamma_{m+1}\right] = F_{\gamma_{N:N_Q}}(\gamma_{m+1}) - F_{\gamma_{N:N_Q}}(\gamma_m). \end{aligned} \tag{4.26}$$

The ASE of the signal dimension for MIN variation is then given by

$$\eta_{\text{AM}}^{\text{MIN}} = m_t - \frac{1}{1 - P_{\text{buf}}^{\text{FPS}}} \sum_{N_Q=2}^{N_t} \binom{N_t}{N_Q} \left(1 - e^{-\frac{Q}{\rho}}\right)^{N_Q} e^{-\frac{(N_t - N_Q) Q}{\rho}} \sum_{m=2}^{m_t} F_{\gamma_{N:N_Q}}(\gamma_m). \quad (4.27)$$

Finally, the total ASE for the FPS scheme is given by

$$\begin{aligned}
\eta^{\text{FPS}} = \eta_{\text{SD}} + \eta_{\text{AM}} &= \frac{1}{1 - P_{\text{buf}}^{\text{FPS}}} \sum_{n=1}^{n_t} n \sum_{N=2^n}^{\min(2^{n+1}-1,N_t)} \binom{N_t}{N} \left(1 - e^{-\frac{Q}{\rho}}\right)^N e^{-\frac{(N_t-N)Q}{\rho}} \\
&\quad + m_t - \frac{1}{1 - P_{\text{buf}}^{\text{FPS}}} \sum_{N_Q=2}^{N_t} \binom{N_t}{N_Q} \left(1 - e^{-\frac{Q}{\rho}}\right)^{N_Q} e^{-\frac{(N_t-N_Q)Q}{\rho}} \\
&\quad \times \begin{cases} \frac{1}{N} \sum_{i=1}^{N} \sum_{m=2}^{m_t} F_{\gamma_{i:N_Q}}(\gamma_m), & \text{ACT}; \\ \sum_{m=2}^{m_t} F_{\gamma_{N:N_Q}}(\gamma_m). & \text{MIN}; \end{cases}
\end{aligned} \quad (4.28)$$

While the above expression of ASE reflects the system's throughput limited to successful transmissions (i.e, the ASE is not affected by data buffering), the effective throughput can be obtained by considering the buffering time slots as zero throughput. Thus, the effective throughput for the FPS can be obtained from (4.28) as

$$\eta_{\text{eff}}^{\text{FPS}} = \eta^{\text{FPS}} \times \left(1 - P_{\text{buf}}^{\text{FPS}}\right), \quad (4.29)$$

where $1 - P_{\text{buf}}^{\text{FPS}}$ represents the probability of successful transmission with the FPS scheme (i.e., $N_Q \geq 2$).

4.4.3 Adaptive Power Scheme

While in the FPS scheme an antenna can be used only if Q is verified, the PU in the APS scheme tolerates an interference level up to $Q' = Q \times \Delta_{\max}$. Thus, data is buffered in this scheme if less than two antennas verify Q'. The probability of data buffering for the APS scheme is then given by

$$P_{\text{buf}}^{\text{APS}} = \left(N_t - (Nt - 1)e^{-\frac{Q \Delta_{\max}}{\rho}}\right) e^{-\frac{(N_t - 1)Q \Delta_{\max}}{\rho}}. \quad (4.30)$$

Based on the mode of operation of the APS scheme, the PDF of the receive SNR from antenna j for this scheme can be written as

$$f_{\gamma_{s_j}}^{\text{APS}}(x) = \frac{1}{1 - P_{\text{buf}}^{\text{APS}}} \sum_{N_{Q'}=2}^{N_t} \binom{N_t}{N_{Q'}} \left(1 - e^{-\frac{Q\,\Delta_{\max}}{\rho}}\right)^{N_{Q'}} e^{-\frac{(N_t - N_{Q'})\,Q\,\Delta_{\max}}{\rho}} \frac{1}{N} \sum_{i=1}^{N} f_{\gamma_{i:N_{Q'}}}(x), \quad (4.31)$$

where $f_{\gamma_{i:N_{Q'}}}(\cdot)$ represents the PDF of the SNR of the ith strongest antenna among the $N_{Q'}$ antennas verifying Q' and is given by

$$f_{\gamma_{i:N_{Q'}}}(x) = \frac{N_{Q'}!}{(N_{Q'} - i)!(i - 1)!} \left(F_{\gamma_s}(x)\right)^{N_{Q'} - i} \left(1 - F_{\gamma_s}(x)\right)^{i-1} f_{\gamma_s}(x), \quad (4.32)$$

where $F_{\gamma_s}(\cdot)$ and $f_{\gamma_s}(\cdot)$ are respectively the common CDF and PDF of the received SNR from any transmit antenna verifying the interference constraint to the PU (i.e., $\gamma_p \leq Q\,\Delta_{\max}$) before ordering and are respectively given by

$$
\begin{aligned}
F_{\gamma_s}(x) &= \frac{1}{F_{\gamma_p}(Q\,\Delta_{\max})} \left(F_{\gamma_p}(Q) F_{\exp}(x) + \sum_{k=1}^{K_{\max}} \left(F_{\exp}(\delta^k Q) - F_{\exp}(\delta^{k-1} Q) \right) F_{\exp}(\delta^k x) \right) \\
&= \frac{1}{1 - e^{-\frac{Q\,\Delta_{\max}}{\rho}}} \left((1 - e^{-\frac{Q}{\rho}})(1 - e^{-\frac{x}{\rho}}) + \sum_{k=1}^{K_{\max}} \left(e^{-\frac{\delta^{k-1}Q}{\rho}} - e^{-\frac{\delta^k Q}{\rho}} \right) \left(1 - e^{-\frac{\delta^k x}{\rho}} \right) \right),
\end{aligned}
$$

$$ (4.33) $$

and

$$
\begin{aligned}
f_{\gamma_s}(x) &= \frac{1}{F_{\gamma_p}(Q\,\Delta_{\max})} \left(F_{\gamma_p}(Q) f_{\exp}(x) + \sum_{k=1}^{K_{\max}} \delta^k \left(F_{\exp}(\delta^k Q) - F_{\exp}(\delta^{k-1} Q) \right) f_{\exp}(\delta^k x) \right) \\
&= \frac{1}{\rho(1 - e^{-\frac{Q\,\Delta_{\max}}{\rho}})} \left((1 - e^{-\frac{Q}{\rho}}) e^{-\frac{x}{\rho}} + \sum_{k=1}^{K_{\max}} \delta^k \left(e^{-\frac{\delta^{k-1}Q}{\rho}} - e^{-\frac{\delta^k Q}{\rho}} \right) e^{-\frac{\delta^k x}{\rho}} \right),
\end{aligned}
$$

$$ (4.34) $$

where the sum from 1 to $K_{\max}$ defines the case where the interference to the PU falls between Q and $Q \times \Delta_{\max}$ and thus PA with step δ is used in this case.

For $N_t = 2$ and arbitrary N_r, the PDF of the received SNR with the APS scheme is

derived as

$$
\begin{aligned}
f_{\gamma_{s_j}}^{\mathrm{APS}}(x) &= \frac{1}{1 - e^{-\frac{Q\,\Delta_{\max}}{\rho}}} \Bigg((1 - e^{-\frac{Q}{\rho}}) \left(\frac{x^{N_r-1}}{(N_r-1)!\rho^{N_r}} e^{-\frac{x}{\rho}} \right) \\
&+ \sum_{k=1}^{K_{\max}} \left(e^{-\frac{\delta^{k-1}Q}{\rho}} - e^{-\frac{\delta^k Q}{\rho}} \right) \left(\frac{\delta^{N_r\,k}\, x^{N_r-1}}{(N_r-1)!\rho^{N_r}} e^{-\frac{\delta^k\,x}{\rho}} \right) \Bigg).
\end{aligned}
\tag{4.35}
$$

Similarly, the CDF of the received SNR from antenna j for APS is obtained as

$$
F_{\gamma_{s_j}}^{\mathrm{APS}}(x) = \frac{1}{1 - P_{\mathrm{buf}}^{\mathrm{APS}}} \sum_{N_{Q'}=2}^{N_t} \binom{N_t}{N_{Q'}} \left(1 - e^{-\frac{Q\,\Delta_{\max}}{\rho}} \right)^{N_{Q'}} e^{-\frac{(N_t-N_{Q'})\,Q\,\Delta_{\max}}{\rho}} \frac{1}{N} \sum_{i=1}^{N} F_{\gamma_{i:N_{Q'}}}(x),
\tag{4.36}
$$

where $F_{\gamma_{i:N_{Q'}}}(\cdot)$ represents the CDF of the SNR of the ith strongest antenna among the $N_{Q'}$ antennas verifying the interference constraint and is given by

$$
F_{\gamma_{i:N_{Q'}}}(x) = 1 - \sum_{n=i}^{N_{Q'}} \binom{N_{Q'}}{n} \left(F_{\gamma_s}(x) \right)^{N_{Q'}-n} \left(1 - F_{\gamma_s}(x) \right)^{n}.
\tag{4.37}
$$

For $N_t = 2$ and arbitrary N_r, the CDF of the received SNR with APS is given by

$$
\begin{aligned}
F_{\gamma_{s_j}}^{\mathrm{APS}}(x) &= \frac{1}{1 - e^{-\frac{Q\,\Delta_{\max}}{\rho}}} \Bigg((1 - e^{-\frac{Q}{\rho}}) \left(1 - \sum_{i=0}^{N_r-1} \frac{1}{i!} \left(\frac{x}{\rho} \right)^{i} e^{-\frac{x}{\rho}} \right) \\
&+ \sum_{k=1}^{K_{\max}} \left(e^{-\frac{\delta^{k-1}Q}{\rho}} - e^{-\frac{\delta^k Q}{\rho}} \right) \left(1 - \sum_{i=0}^{N_r-1} \frac{1}{i!} \left(\frac{\delta^k\,x}{\rho} \right)^{i} e^{-\frac{\delta^k\,x}{\rho}} \right) \Bigg).
\end{aligned}
\tag{4.38}
$$

ASE: Similar to the two previous techniques, the total ASE of the APS scheme is the sum of the throughput obtained by the spatial dimension and the signal dimension. Equivalent to the FPS scheme, η_{SD} for the APS scheme depends on the number of antennas verifying the interference constraint. The main advantage with the APS scheme is that the PU can tolerate an interference level up to $Q\,\Delta_{\max}$ and PA is used in order to reduce the ST's interference below Q. Thus, η_{SD} for the APS scheme is given by $\sum_{n=1}^{n_t} n\, q_n$, where q_n is the probability that $N = 2^n$ antennas are selected for transmission and is given by

$$
q_n = \frac{1}{1 - P_{\mathrm{buf}}^{\mathrm{APS}}} \sum_{N=2^n}^{\min(2^{n+1}-1,\,N_t)} \binom{N_t}{N} \left(1 - e^{-\frac{Q\,\Delta_{\max}}{\rho}} \right)^{N} e^{-\frac{(N_t-N)Q\,\Delta_{\max}}{\rho}}.
\tag{4.39}
$$

The ASE of the AM system for the APS scheme is given by

$$\eta_{\text{AM}} = \sum_{m=1}^{m_t} m \, p_m. \tag{4.40}$$

ACT Variation: In this variation, modulation mode m is used by antenna j if the received SNR γ_{s_j} after PA falls between thresholds γ_m and γ_{m+1}. Based on this, p_m for the ACT variation is given by

$$p_m^{\text{ACT}} = \Pr\left[\gamma_m \le \gamma_{s_j} < \gamma_{m+1}\right] = F_{\gamma_{s_j}}^{\text{APS}}(\gamma_{m+1}) - F_{\gamma_{s_j}}^{\text{APS}}(\gamma_m). \tag{4.41}$$

The ASE of the signal dimension for the ACT option is then given by

$$\eta_{\text{AM}}^{\text{ACT}} = m_t - \sum_{m=2}^{m_t} F_{\gamma_{s_j}}^{\text{APS}}(\gamma_m). \tag{4.42}$$

MIN Variation: In this variation, modulation mode m is used by antenna j if the minimum output SNR from all antennas after PA falls between γ_m and γ_{m+1}. Given $N_{Q'}$ antennas verifying the constraint and N antennas selected for transmission, p_m for this second option is given by

$$
\begin{aligned}
p_m^{\text{MIN}} &= \Pr\left[\gamma_m \le \min_{i=1,\dots,N} \gamma_{i:N_{Q'}} < \gamma_{m+1}\right] \\
&= \Pr\left[\gamma_m \le \gamma_{N:N_{Q'}} < \gamma_{m+1}\right] = F_{\gamma_{N:N_{Q'}}}(\gamma_{m+1}) - F_{\gamma_{N:N_{Q'}}}(\gamma_m).
\end{aligned} \tag{4.43}
$$

The ASE of the signal dimension for the MIN variation is then given by

$$\eta_{\text{AM}}^{\text{MIN}} = m_t - \frac{1}{1 - P_{\text{buf}}^{\text{APS}}} \sum_{N_{Q'}=2}^{N_t} \binom{N_t}{N_{Q'}} \left(1 - e^{-\frac{Q\,\Delta_{\max}}{\rho}}\right)^{N_{Q'}} e^{-\frac{(N_t - N_{Q'})\,Q\,\Delta_{\max}}{\rho}} \sum_{m=2}^{m_t} F_{\gamma_{N:N_{Q'}}}(\gamma_m). \tag{4.44}$$

Finally, the total ASE of the APS scheme is given by

$$
\begin{aligned}
\eta^{\mathrm{APS}} = \eta_{\mathrm{SD}} + \eta_{\mathrm{AM}} = {} & \frac{1}{1 - P_{\mathrm{buf}}^{\mathrm{APS}}} \sum_{N=2^n}^{\min(2^{n+1}-1, N_t)} \binom{N_t}{N} \left(1 - e^{-\frac{Q\,\Delta_{\max}}{\rho}}\right)^N e^{-\frac{(N_t - N)Q\,\Delta_{\max}}{\rho}} \\
& + m_t - \frac{1}{1 - P_{\mathrm{buf}}^{\mathrm{APS}}} \sum_{N_{Q'}=2}^{N_t} \binom{N_t}{N_{Q'}} \left(1 - e^{-\frac{Q\,\Delta_{\max}}{\rho}}\right)^{N_{Q'}} e^{-\frac{(N_t - N_{Q'})\,Q\,\Delta_{\max}}{\rho}} \\
& \times \begin{cases} \frac{1}{N} \sum_{i=1}^{N} \sum_{m=2}^{m_t} F_{\gamma_{i:N_{Q'}}}(\gamma_m), & \mathrm{ACT}; \\ \sum_{m=2}^{m_t} F_{\gamma_{N:N_{Q'}}}(\gamma_m), & \mathrm{MIN}; \end{cases}
\end{aligned} \tag{4.45}
$$

Similar to the FPS scheme, the effective throughput for the APS is given by

$$
\eta_{\mathrm{eff}}^{\mathrm{APS}} = \eta^{\mathrm{APS}} \times \left(1 - P_{\mathrm{buf}}^{\mathrm{APS}}\right), \tag{4.46}
$$

where $1 - P_{\mathrm{buf}}^{\mathrm{APS}}$ represents the probability of successful transmission with the APS scheme (i.e., $N_{Q'} \geq 2$).

4.4.4 Average Delay

The main advantage of the perfect CSI case is the fact that it comes without transmission delays. In the limited CSI schemes, however, data is buffered for a channel coherence time if less than two antennas verify the interference constraint set by the PU. This is similar to the idea of scan and wait combining [67] where the average delay for these schemes can be expressed in terms of the number of time slots that the ST needs to wait until a transmission occurs (i.e., until two or more antennas verify the constraint). Let N_w denote this number, thus N_w is a standard Geometric random variable with probability mass function given by

$$
\Pr\left[N_w = n\right] = P_{\mathrm{buf}}^n \left(1 - P_{\mathrm{buf}}\right), \tag{4.47}
$$

where P_{buf} is given for the FPS and APS schemes by (4.15) and (4.30), respectively.

Mean and Variance: Derived from the properties of the Geometric random variable, the mean $\overline{N}_w$ and the variance $\mathrm{Var}\,[N_w]$ of N_w are respectively given by

$$\overline{N_w} = \frac{P_{\text{buf}}}{1 - P_{\text{buf}}}, \tag{4.48}$$

and

$$\mathrm{Var}\,[N_w] = \frac{P_{\text{buf}}}{\left(1 - P_{\text{buf}}\right)^2}. \tag{4.49}$$

Dropping Probability: Another metric showing the effect of delay is the probability of dropping data. Indeed, for delay sensitive applications data may be dropped if the waiting time before transmission is above a given threshold $N_{w_{\text{th}}}$. This threshold depends on the type of delay-sensitive application and presents an important quality of service measure. The dropping probability P_{drop} is defined as

$$P_{\text{drop}} = \mathrm{Pr}\,[N_w > N_{w_{\text{th}}}] = [P_{\text{buf}}]^{N_{w_{\text{th}}}+1}. \tag{4.50}$$

4.4.5   ABER

We derive in what follows an asymptotic performance bound for the proposed techniques under i.i.d Rayleigh flat fading channel conditions. Following the steps of [94] and knowing that the ABER is a function of both the antenna index detection and the constellation symbol detection, the overall bit error probability can be bounded as

$$P_{e,\text{bit}} \geq P_a + P_s - P_a\,P_s, \tag{4.51}$$

where P_a is defined in [46] as the bit error probability of transmit antenna index estimation given that the symbol is perfectly detected and P_s is defined as the bit error probability of symbol estimation given that the transmit antenna index is perfectly detected. It was shown in [94] that the lower bound given in (4.51) is very tight in spite of the assumption of independent estimation processes of the active antenna index and the transmitted symbol.

BER of Symbol Estimation: Assuming perfect antenna index estimation, P_s represents the ABER of the considered adaptive modulation system over Rayleigh fading channels. P_s is then given as [23, Eq.(35)]

$$P_s = \frac{1}{\eta_{\text{AM}}} \sum_{m=1}^{m_t} m \, \overline{P}_{b_m},$$

(4.52)

where $\overline{P}_{b_m}$ is the ABER for constellation size m, and is given by

$$\overline{P}_{b_m} = \begin{cases} \int_0^{\gamma_2} P_{b_1}(x) \, f_{\gamma_{s_j}}(x) \, dx, & m = 1; \\ \int_{\gamma_m}^{\gamma_{m+1}} P_{b_m}(x) \, f_{\gamma_{s_j}}(x) \, dx, & m > 1; \end{cases}$$

(4.53)

where $f_{\gamma_{s_j}}(\cdot)$ is the PDF of the received SNR from antenna j and was previously derived for all proposed schemes and $P_{b_m}(\cdot)$ is given by (4.1).

BER of Antenna Index Estimation: The expression of the BER for the antenna index estimation can be obtained by averaging over possible used modulation and antennas as

$$P_a = \sum_{n=1}^{n_t} \sum_{m=1}^{m_t} p_{n,m} \, P_{a|n,m},$$

(4.54)

where $p_{n,m} = p_n \, p_m$ is the probability that 2^n antennas are available for transmission and modulation mode m is used, and $P_{a|n,m}$ denotes the antenna index detection's error rate given that modulation mode m and 2^n antennas are used for transmission. An asymptotic performance bound of $P_{a|n,m}$ for 2^m-QAM and 2^n antennas with optimal detection is derived in [94, Eq.(13)] using the union bound (UB) [93, p. 261-262] as

$$P_{a|n,m} \leq \sum_{j=1}^{2^n} \sum_{\hat{j}=1}^{2^n} \sum_{q=1}^{2^m} \frac{N(j,\hat{j}) P(x_{jq} \to x_{\hat{j}q})}{2^{n+m}},$$

(4.55)

where $N(j,\hat{j})$ is the number of bits in error between antenna index j and estimated antenna index $\hat{j}$ and $P(x_{jq} \to x_{\hat{j}q})$ is the pairwise error probability of choosing signal x_{jq} given that

$x_{\hat{j}q}$ was transmitted and is given by

$$P(x_{jq} \to x_{\hat{j}q}) = \gamma_{\text{ASM}}^{N_r} \sum_{w=0}^{N_r-1} \binom{N_r + w - 1}{w} (1 - \gamma_{\text{ASM}})^w, \tag{4.56}$$

where $\gamma_{\text{ASM}} = \frac{1}{2} \left(1 - \sqrt{\frac{\rho|x_q|^2/2}{1+\rho|x_q|^2/2}} \right)$.

4.5 Numerical Examples

The performance of the proposed schemes is illustrated in this section for a maximum modulation mode $m_t = 4$ (i.e., the modulation that can be used by the ST varies from BPSK to 16-QAM) and an ABER constraint $P_{b_0} = 10^{-3}$. These numerical examples, obtained by Monte-Carlo simulations and confirmed with analytical results, are illustrated in terms of ASE, average delay, effective throughput, and ABER.
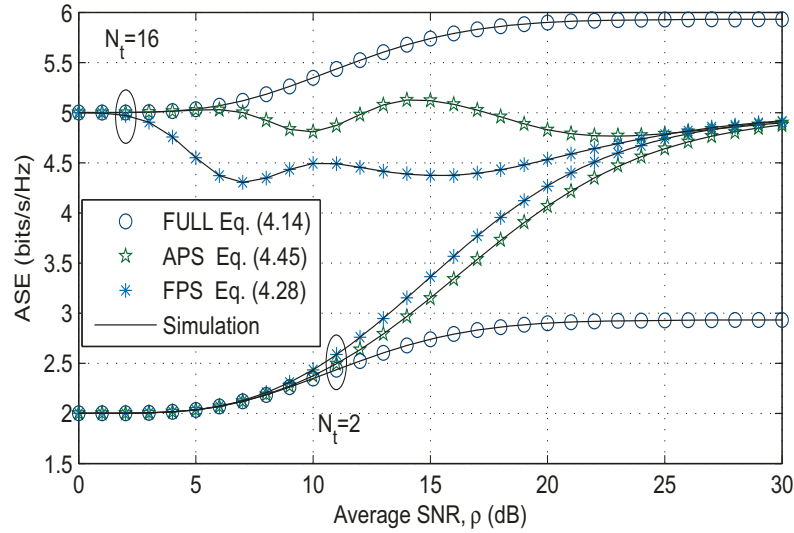

Figure 4.2: Total ASE for all schemes with the ACT variation versus ρ for $Q_{\text{dB}} = 10$ dB, $N_r = 1$, and $N_t = 2$ and 16.

4.5.1 Average Spectral Efficiency

Fig. 4.2 depicts the total ASE for the proposed schemes as a function of the average SNR per receive antenna ρ using the ACT variation for $N_r = 1$ and for $N_t = 2$ and 16. For the low average SNR range, most antennas verify the interference constraint which increases the ASE for all schemes. Thus, the more transmit antennas are available at the ST, the higher is the ASE in that range. This ASE enhancement is mainly due to the spatial constellation generated by the use of spatial modulation. The highest signal dimension's ASE is offered by the Full CSI technique where all antennas are available for transmission thanks to the use of PA. For high average SNRs, the ASE improves thanks to the use of adaptive modulation. In this range, data is either buffered or two antennas are available which makes the ASE for the FPS and APS technique converge to 5 bits/s/Hz (i.e., $\log_2(2 \times 16)$). For the Full CSI technique, $\log_2(N_t)$ bits/s/Hz are generated by the spatial dimension but the signal dimension for this technique is lower than the limited feedback techniques since PA makes the transmit power very small for high average SNRs.
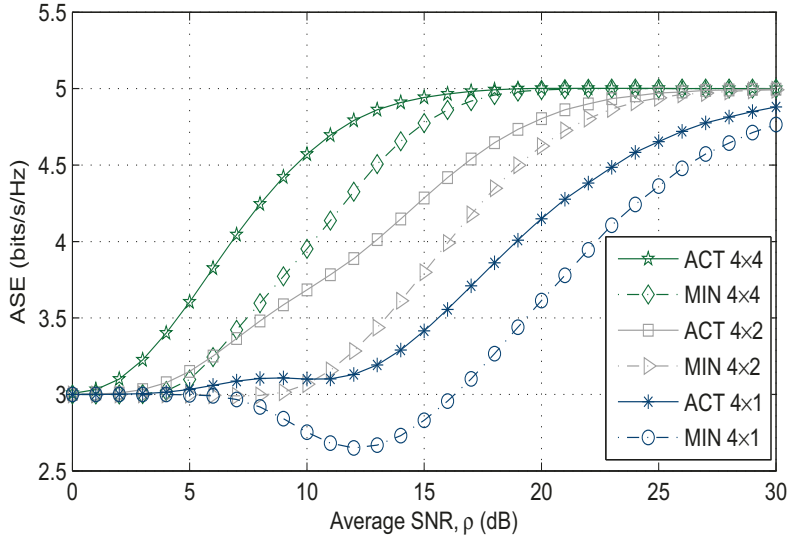

Figure 4.3: Total ASE for the APS scheme with the ACT and MIN variations versus ρ for $Q_{\mathrm{dB}} = 10$ dB, $N_t = 4$ and different N_r.

For $N_t = 2$, the FPS and APS schemes offer the same η_{SD}, which is 1 bit/s/Hz. Still, the FPS scheme offers slightly higher total ASE in the medium and high average SNR range

since it always uses power $P_{\max}$ while the APS uses a lower power due to PA. For high values of N_t, on the other hand, the APS scheme offers better ASE performance than the FPS scheme especially in the medium average SNR range. Indeed, while the FPS scheme buffers all antennas causing an interference above Q to the PU, the latter can tolerate an interference up to $Q \times \Delta_{\max}$ for the APS scheme. Consequently, more antennas are available for transmission and thus the ASE generated by the spatial dimension for the APS scheme outperforms that of the FPS scheme.

Fig. 4.3 compares the ASE for the APS scheme with the ACT and the MIN variations for $N_t = 4$, $Q_{\mathrm{dB}} = 10$ dB, $\delta_{\mathrm{dB}} = 0.25$ dB, $\Delta_{\max_{\mathrm{dB}}} = 3.75$ dB[1], and different number of receive antennas. In the low average SNR range, both variations achieve the same ASE of 3 bits/s/Hz. Indeed, in this range all antennas verify the interference level $Q \times \Delta_{\max}$ and BPSK is used for transmission. Thus, η_{SD} and η_{AM} are given by $\log_2(4)$ and $\log_2(2)$, respectively. In the medium and high average SNR range, the ACT variation offers better ASE since the actual modulation achieved by each antenna is used in this variation. Fig. 4.3 also shows the improvement in the ASE with the use of a higher number of receive antennas at the SR.
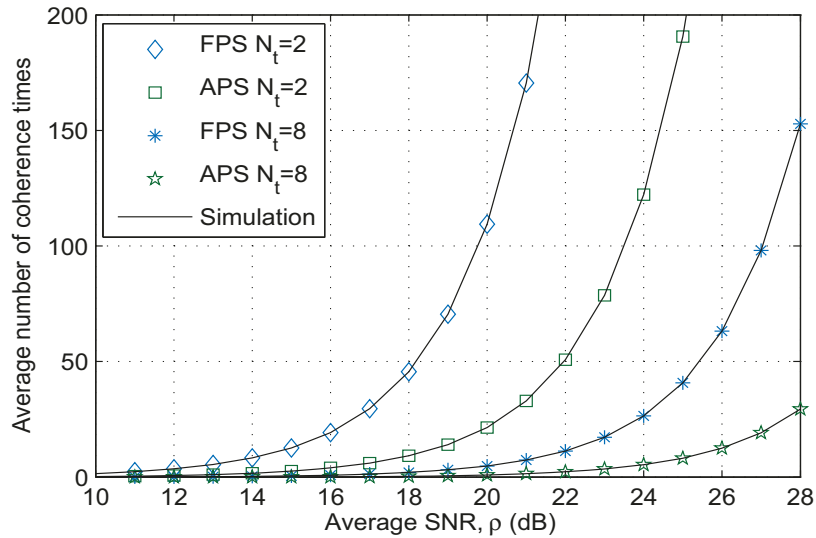

Figure 4.4: Average number of waiting time slots required before transmission versus ρ for $Q_{\mathrm{dB}} = 10$ dB and for $N_t = 2$ and 8.

---

[1]$\Delta_{\max_{\mathrm{dB}}}$ is chosen by taking equality in (4.5). In this case, the maximum number of PA steps is $K_{\max} = 15$. Thus $N_b = 4$ bits are required to let the ST know the number of needed PA steps in order to reduce the interference to below Q.

4.5.2 Average Delay Performance

The ASE performance improvement introduced by the limited CSI schemes in the high average SNR range comes at the expense of an additional time delay since data is buffered if less than two antennas verify the interference constraint to the PU. In Fig. 4.4, we depict the average number of time slots required before finding two acceptable antennas as a function of ρ for $Q_{dB} = 10$ dB. From this figure, we can see that the higher the average SNR the more time ST needs to wait before transmitting. Indeed, in this case, fewer antennas verify the constraint which makes the ST wait for a longer time. This figure also shows the effect of the number of available antennas at the ST on the delay performance. The higher N_t the lower the delay experienced by the proposed techniques since the probability of having at least two antennas verifying the constraint increases with N_t. Moreover, Fig. 4.4 shows the advantage of APS over FPS in terms of delay. Indeed, the PU in the APS scheme tolerates an interference level up to $Q \times \Delta_{max}$ (before using power adaptation) which reduces the probability of data buffering. While data needs to be buffered in the limited CSI schemes, the full CSI technique uses the perfect knowledge about the interference channel and performs PA in order to avoid data buffering.
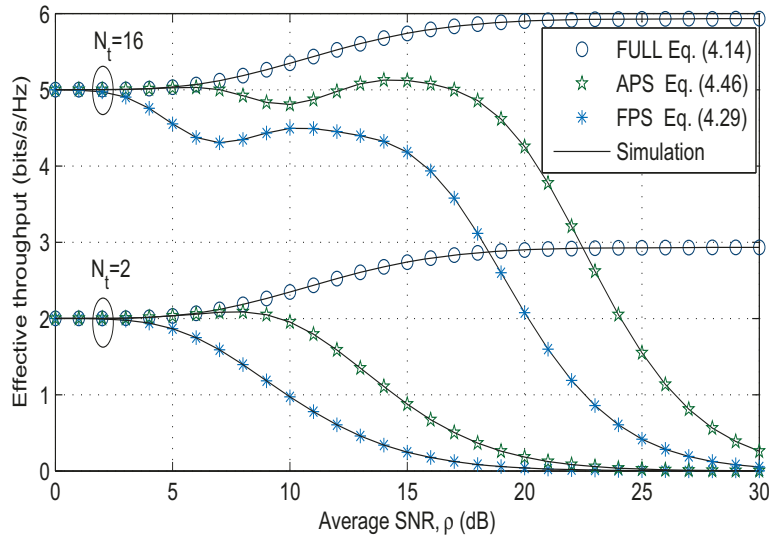

Figure 4.5: Effective throughput comparison for all three proposed techniques versus ρ for $Q_{dB} = 10$ dB, $N_r = 1$, and for $N_t = 2$ and 16.

4.5.3 Effective Throughput

Fig. 4.5 depicts the effective throughput as a function of ρ using the ACT variation for $N_r = 1$ and for $N_t = 2$ and 16. This figure combines the previously presented ASE and delay results by counting data buffering as zero throughput events. Thus, for high average SNRs, it becomes very challenging to find antennas verifying the interference constraint which vanishes the effective throughput. Fig. 4.5 shows that the APS scheme has better performance than the FPS scheme thanks to the use of PA. It also shows that the full CSI has the best η_{eff} since this scheme does not experience data buffering.
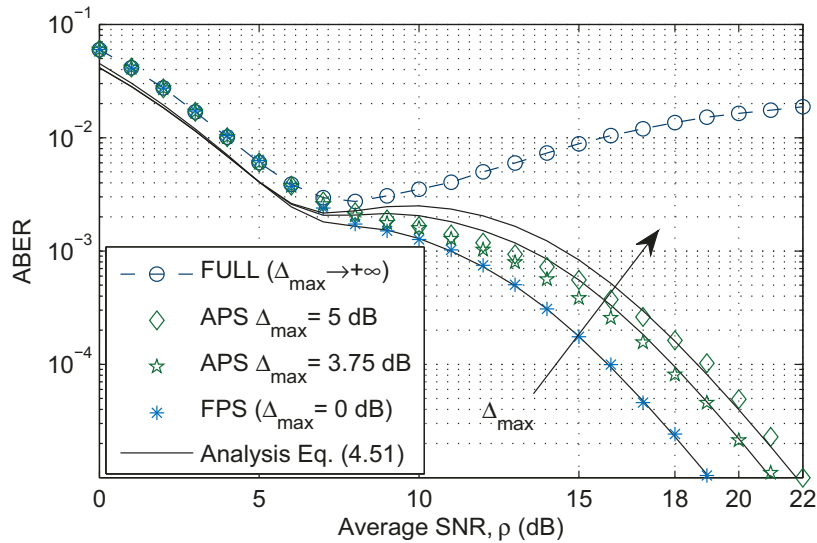

Figure 4.6: ABER comparison for all schemes with the MIN variation as a function of ρ for $Q_{\text{dB}} = 10$ dB, $N_t = 2$, and $N_r = 4$.

4.5.4 Average Bit Error Rate

The effective throughput improvement gained by the full CSI technique comes at the expense of a lower ABER performance compared to the limited CSI schemes as shown in Fig. 4.6. Indeed, PA minimizes the transmit power for the ideal case especially in the high average SNR range. The FPS scheme offers the best error performance since the selected transmit antenna always uses its maximum transmit power P_{max} when enough antennas are available for transmission. Fig. 4.6 also confirms that the APS scheme can be seen as a delay-ABER

tradeoff scheme between the ideal and the FPS techniques. Indeed, depending on the values taken by $\Delta_{\max}$, the APS scheme converges to one of other techniques. In this context, for very high values of $\Delta_{\max}$ the APS scheme is equivalent to the ideal case where data buffering is not required and the ABER converges to an error floor. For very small values of $\Delta_{\max}$, an improvement in the ABER performance is observed at the expense of higher average delay and APS converges to FPS.
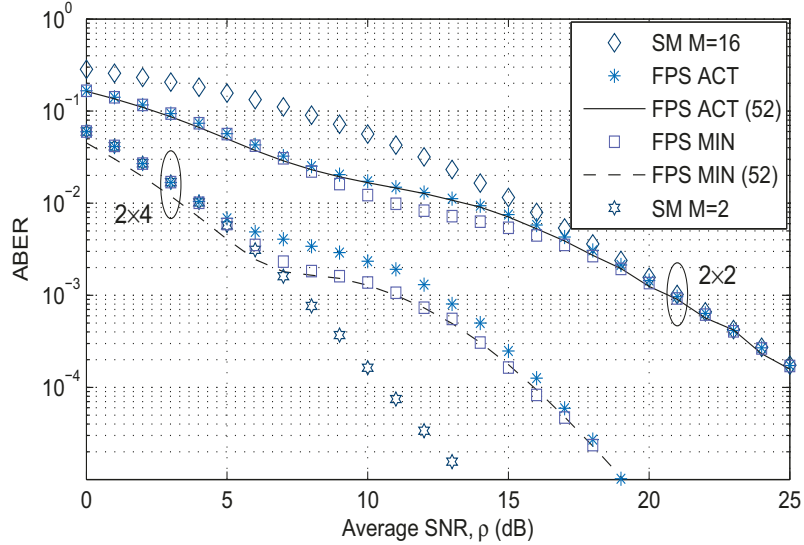

Figure 4.7: ABER comparison for the FPS scheme for both variations and the SM technique versus ρ for $Q_{\mathrm{dB}} = 10$ dB, $N_t = 2$, and $N_r = 4$.

Fig. 4.7 depicts an ABER performance comparison between the ACT and MIN variations for the FPS scheme as function of ρ for $N_t = 2$ and $N_r = 4$ with both theory and simulations. This figure confirms the motivation behind proposing the MIN variation. That is, the ASE improvement offered by the ACT variation compared to the MIN variation, comes at the expense of a slight degradation in the ABER. This lower ABER performance added to the additional decoder's complexity for the ACT variation are mainly due to using different constellations by different transmit antennas. In this scenario, an antenna index detection error may come with a decision on a signal drawn from a constellation other than the actual one used for transmission. In Fig. 4.7 we also compare the performance of the FPS scheme to the exiting SM technique where a fixed constellation is used throughout the communication [32]. In the low average SNR range, the FPS scheme behaves similar to the SM scenario with

$M = 2$ since BPSK is mostly used in that range. In the high average SNR range, on the other hand, the proposed $N_t \times N_r$ FPS scheme with M-QAM starts to use higher modulations and finally converges to the performance of a $2 \times N_r$ SM system using 16-QAM. In this range only two antennas on average verify the interference (data is buffered otherwise) and the used antenna is able to reach the highest possible modulation. In the same context, we can see from this figure that the FPS scheme has the same diversity order as that of SM, which comes only with receive diversity and does not offer any transmit diversity.

4.6 Conclusion

We proposed in this chapter a number of adaptive transmission techniques for spectrum sharing systems. Using ASM in a MIMO underlay cognitive radio scenario, the FPS and APS limited CSI schemes are proposed in order to improve the performance of the secondary link while satisfying the interference constraint to the PU. These schemes were shown to take advantage of the low system complexity and high data rates achieved by ASM in order to enhance the performance of the secondary link while only requiring a limited knowledge about the interference channel to the PU. We have also proposed an ideal case, assuming full interference link's CSI at the ST, as a benchmark for the limited CSI schemes. This ideal case comes with the advantage of removing the need of data buffering but at the expense of an ABER performance degradation. In order to enhance this performance, the APS scheme is proposed a delay-ABER tradeoff scheme between the FPS and the Full CSI techniques. Indeed, the APS scheme was shown to capture the advantages of the ideal and FPS techniques, both in terms of delay and ABER.

Chapter 5

Enhanced Space-Shift Keying with Reconfigurable Antennas

5.1 Introduction

Since the turn of the century, cellular industry has been experiencing a tremendous growth in mobile data traffic. Challenged by this unprecedented data surge, researchers and network operators have proposed and implemented new protocols, transmission technologies, and network infrastructure solutions aiming to maximize both the spectral efficiency and the achievable throughput. While these solutions are optimized from the spectral efficiency perspective, they are generally not well designed to address other related complexity and power consumption issues [29]. Thus, achieving high data rates with these techniques comes at the expense of high energy consumption and increased system complexity [95]. In this context, SM, SSK, and GSSK were proposed as low-complexity and energy-efficient implementations of MIMO systems. Similar to SM, the key idea behind SSK is the use of a single RF chain during each transmission. Thus, only one antenna remains active during data transmission, which comes with the advantages of avoiding inter-antenna synchronization and removing inter-channel interference. While SSK offers this low overall system complexity, it has been shown that this modulation scheme can offer better ABER performance as compared to some popular MIMO techniques including the V-BLAST architecture, the Alamouti scheme, and APM techniques [33].

Owing to its above-mentioned advantages, SSK has received a considerable attention from the research community [79, 81, 96], and references therein. However, one of the main practical implementation challenges in SSK is the fast RF switching process. Indeed, because of its specific encoding mechanism, the active transmit antenna in SSK changes in every channel use. Consequently, the single-RF implementation in this modulation technique needs a sufficiently fast RF switch operating at the symbol rate. In this context, high-speed RF switches constitute a critical part of the transmitter design [95]. In order to address this RF switching issue, single-RF MIMO systems can be implemented using the concept of parasitic antennas. Indeed, similar to the SSK modulation, new multiple antenna designs based on parasitic antennas have been proposed in order to enable multiplexing gains with a single RF element [36]. Thanks to the use of many passive antenna elements, the parasitic array in these techniques is capable of changing its radiation pattern on each symbol period and thus offering cost and energy effective solution for the implementation of MIMO systems. These parasitic systems have been recently implemented and tested in indoor propagation environments [37, 97].

Inspired by the low implementation-complexity offered by parasitic antennas, we use new antenna designs based on the concept of RAs in order to improve the performance of SSK and address its implementation challenges. Indeed, all the previously considered SSK studies are based on conventional antenna theory in the sense that each antenna has fixed antenna characteristics. These conventional antennas typically come with a fixed radiation pattern for specific operating frequency and bandwidth. On the other hand, the concept of RAs, including parasitic antennas discussed above, represents a new emerging technology that provides antennas with the ability of dynamically modifying their characteristics, such as operating frequency, radiation pattern, and polarization [38]. Thanks to these modifications, RAs offer different interplays with the multipath propagation channel. The core idea of wireless communication systems based on RAs relies on how to exploit these interplays between the impulse response of the propagation channel and different RAs' radiation states. In this context, the reconfigurable properties of RAs can be used as additional degrees of freedom in order to improve the performance of wireless communication systems including MIMO techniques [39–41].

The impact of RAs on the radio characteristics of Rician propagation channels has been recently investigated in [86]. Based on a LOS multipath prorogation model, it was shown that the interplay between RAs and the propagation channel has an impact on important channel characteristics such as the Rician K-factor and the polarization correlation coefficients. Taking advantages of these additional degrees of freedom, the error performance of SSK can be improved by selecting antenna configurations that minimize the Rician K-factor and the correlation coefficients. Indeed, unlike conventional modulation schemes, the error performance of SSK was shown to improve for lower values of the Rician K-factor [98]. In fact, SSK modulation requires the wireless links to be sufficiently different from each other in order to achieve good performance which can be satisfied for higher amounts of fading, i.e., for lower values of K. Similarly, selecting RAs' configurations minimizing the correlation coefficients improves the performance of SSK.

In light of the above, combining SSK-MIMO with the concept of RAs looks to be very promising. Taking advantage of this combination, we propose a number of SSK-RA schemes aiming at improving the performance of SSK in terms of complexity, ASE, and ABER performance over generic Rician fading channels. The performance of these schemes is analyzed in terms of ASE and ABER then confirmed with selected numerical results. These results are compared to the performance of SSK in order to highlight the enhancements gained by the proposed SSK-RA schemes.

The advantages of SSK-RA, i.e., combining SSK with RAs, can be summarized as follows:

- RAs allow for using only one RF chain while offering many polarization states to select from. This alleviates the need to do RF switching, which is a potential problem of SSK from an implementation point of view.

- RAs can be designed to have more polarization states than needed. Consequently, there will be more degrees of freedom, which can be used to enhance the performance of SSK both in terms of bit error rate and/or spectral efficiency. That is, using more states is equivalent to using more antennas in the conventional SSK, which improves the spectral efficiency. On the other hand, when the best subset of states are used, the bit error rate performance will be improved.

- Considering Rician channels, SSK performs better when the Rician K-factor is low since it implies the channels are more random. In the context of RAs, there is an interplay between the channel characteristics and the polarization states (more on this later). Therefore, one may pick states yielding the lowest K-factor. It is true that there will be some correlation among the various states, which degrades the performance. However, this can be controlled by selecting states having the lowest correlation possible.

- Further performance enhancements may be achieved in a closed-loop setting where the receiver feeds back information about the states that yield the best performance.

The remainder of the chapter is organized as follows. Section 5.2 starts with an introduction to the concept of RAs then gives the details behind the system and radio channel models including the interplay between RAs and the multipath propagation channel and finally presents the channel correlation model. Section 5.3 defines the proposed SSK-RA schemes and their modes of operation. Section 5.4 presents the optimal detector and Section 5.5 analyses the error performance of the proposed schemes. Next, Section 5.6 illustrates and confirms the performance of the SSK-RA schemes via selected numerical results and Section 5.7 gives selected preliminary results for SSK-RA in spectrum sharing systems. Finally, Section 5.8 concludes the chapter.

5.2 System and Channel Models

5.2.1 Reconfigurable Antennas (RAs)

Multiple-antenna communication systems are based on conventional antenna theory in the sense that each antenna has fixed characteristics. In this context, conventional antennas typically have a fixed radiation pattern at a specific operating frequency and bandwidth. On the other hand, RAs is a new emerging technology that provides antennas with the capability of dynamically modifying their characteristics, such as operating frequency, radiation pattern, and polarization. This reconfiguration capability can be achieved via different approaches such as changing the physical structure of the antenna, altering the feed methods, and con-

trolling the current density. The performance level and the design requirements determine the choice of the reconfiguration methods to be employed. The core idea of RAs is based on creating different paths by changing the current distribution in an antenna. The geometry of different paths for different current distributions determines how the antenna radiates its energy into a propagation channel and/or how the antenna receives radio frequency from this channel. The path geometry control is performed as internal mechanisms via different techniques including RF switches, varactors, micro-electro-mechanical (MEM) switches, and tunable materials [38].

Reconfigurable antenna technology is different from smart antenna technology since the reconfiguration process lies inside the antenna rather than in the external network as in beam-forming techniques. The most challenging part in antenna reconfiguration is the capability of the RA to tune several antenna parameters simultaneously such as resonance frequency, radiation pattern and polarization. For instance, the pattern reconfiguring of a dipole antenna takes place via its polarization parameter α. This parameter modifies the antenna gain pattern for both vertical and horizontal polarizations. These antenna gains are respectively given as follows [85]

$$G_v(\theta, \phi, \alpha) = D \left(\cos\theta \cos\phi \sin\alpha - \sin\theta \cos\alpha \right)^2 \frac{\cos^2 (\pi\zeta/2)}{(1-\zeta^2)^2}, \tag{5.1}$$

$$G_h(\theta, \phi, \alpha) = D \sin^2\phi \, \sin^2\alpha \, \frac{\cos^2 (\pi\zeta/2)}{(1-\zeta^2)^2}, \tag{5.2}$$

where α is the angle between the antenna and the z-axis with respect to the vertical zx-plane, $\zeta = \sin\theta \cos\phi \sin\alpha + \cos\phi \cos\alpha$, and the coefficient D corresponds to the directivity of the antenna and is equal to 1.64 (2.15 dB) for a half-wavelength dipole antenna. The angles θ and ϕ are the elevation and azimuthal angles of the rays arriving from the dipole antennas dipole antenna with respect to the z-axis and the x-axis, respectively. When $\alpha = 0^o$, the vertical polarized radiation pattern has the well-known donut shape in 3D and this shape changes for different values of α as we show later.

The radiation pattern for every value of α is called antenna radiation state or, simply, antenna state. The core idea of wireless systems based on RAs relies on how to exploit

the controlled interplay between the impulse response of the propagation channel and different RAs' antenna radiation states. The term "controlled" is meant for controlled antenna states. Indeed, each antenna radiation state may have different interplay with different multipath components. Consequently, the radio channel characteristics are affected in different RF propagation domains, i.e., delay, angular and Doppler domains. These changes can be measured with their corresponding correlation parameters such as coherence spectra, spatial correlation, and coherence time, which have impact on the performance of wireless communication systems. One of the important parameters that can be affected by these interplay results is the Rician channel K-factor in LOS radio propagation channel. The interplay can increase and decrease the K-factor, and thus can be exploited in order to improve the performance of wireless communication systems.
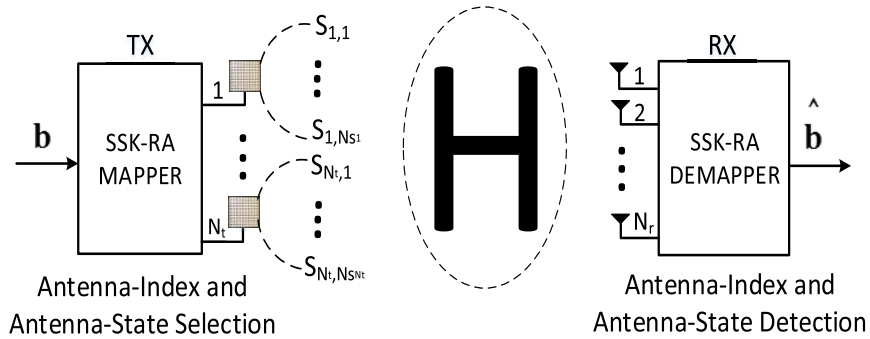

Figure 5.1: SSK-RA System model.

5.2.2   System Model

We consider the system model shown in Fig. 5.1, which consists of a MIMO wireless link with N_t transmit and N_r receive antennas. The transmit antennas, represented by squares, are reconfigurable antennas offering each different numbers of possible polarization states. Let N_{s_i} be the number of states available for antenna i and let $S_{i,1}, \ldots, S_{i,N_{s_i}}$ denote these antenna-states. Assuming that half-wavelength dipole antennas are used at the transmitter,

different states are obtained by changing the polarization of these transmit antennas. In this context, different antenna states represent different radiation patterns of an antenna. To be more specific, reconfiguring the pattern of an antenna takes place by changing the inclination angle α from the z-axis in the vertical zx-plane (selected examples of radiation patterns of a half-wavelength dipole antenna for different polarization parameters α are given later). The receive antennas, presented by triangles, are conventional antennas offering no reconfigurability. Similar to SSK, the selection of the antenna and the polarization to be used for transmission is performed based on the incoming bits. Indeed, once transmit antenna i is selected using $\log_2(N_t)$ bits, one of the N_{s_i} antenna states is selected using the subsequent $\log_2(N_{s_i})$ bits. The details behind antenna and polarization selection processes for the proposed SSK-RA schemes is explained in details in Section 5.3.

5.2.3 Impact of RAs on the Radio Channel

The impact of RAs on the radio channel characteristics has been recently investigated in [86]. Using a LOS multipath prorogation model, it was shown that changing the polarization parameter of a half-wavelength dipole antenna does not affect the type of statistical distribution of the channel but rather changes the distribution parameters. In particular, assuming a Rician fading channel, it was shown that changing the antenna state of the RA impacts one of the important parameters of the Rician distribution: the K-factor. Indeed, the interplay between the propagation channel and the RAs' patterns can increase or decrease the K-factor.[1] The variability of K for different antenna radiation states is given by

$$K = a\,k(\alpha) + b, \tag{5.3}$$

where $k(\alpha)$ is the basic variability trend as a function of the polarization factor α and is given as [86]

$$
\begin{aligned}
k(\alpha) = {}& 1.252 - 0.4597\cos{(7.503\alpha)} + 0.3736\sin{(7.503\alpha)} \\
& + 1.256\cos{(15\alpha)} - 0.3776\sin{(15\alpha)}.
\end{aligned}
\tag{5.4}
$$

---

[1]This variation can be exploited in order to improve the performance of LOS wireless communication systems as explained in Section 5.3.

The parameters a and b are scaling factors that depend on the propagation environment; indoor (e.g., office, hall, corridor, etc) and outdoor (e.g., urban, suburban, rural, etc). a and b can be derived using [99, Table I] and are given in Table 5.1 where d represents the distance between the transmitter and receiver and $K(0^o)$ represents the K-factor for $\alpha = 0^o$.

Table 5.1: Scaling parameters for different environments (5 GHz band).

	Indoor (office)	Indoor (hall)	Microcell	Rural
d (m)	5	10	50	500
$K(0^o)$ dB	$8.3 - .06d$	$33.6 + .13d$	$3 + .0142d$	$3.7 + .01d$
a	3.5	15	1.5	4
b	1	5	0.7	0.54

Based on these results, the variation of K as a function of the polarization parameter α is summarized in Fig. 5.2 considering different propagation environments in the 5 GHz band.
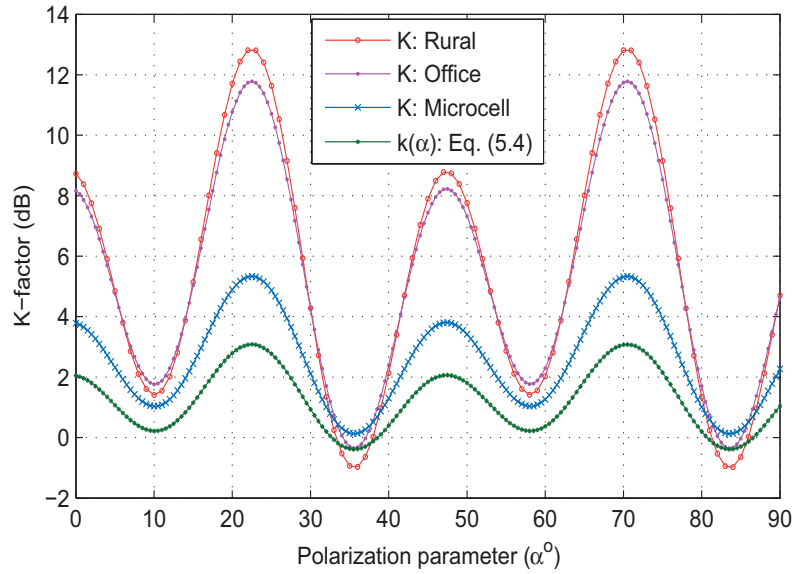

Figure 5.2: K-factor variation with different radiation patterns and propagation environments for LOS propagation in the 5 GHz band.

5.2.4 Radio Channel Model

Inspired by the LOS propagation model considered in [86], we assume that the received signal from each state experiences correlated and non-identically distributed Rician fading

over the transmit-receive wireless link. The radio channel is considered as a combination of the propagation channel (impact of the environment without antenna, i.e., assuming isotropic antenna) and the effect of antennas with the multipath components. In SSK-RA, similar to SSK, only one antenna is switched on for data transmission while all remaining antennas are kept silent. Assuming that antenna i, $i = 1, 2, \ldots, N_t$, is activated for transmission, let h_{ji_l}, $l = 1, 2, \ldots, N_{s_i}$, and $j = 1, 2, \ldots, N_r$ be the channel coefficient between antenna i and the jth receive antenna when antenna state $S_{i,l}$ is used (i.e., polarization parameter α_l is selected at antenna i). Given that the fading parameter for each of these channel coefficients is a function of the polarization angle and the propagation environment, each h_{ji_l} has a complex Gaussian distribution with mean μ_l and variance σ_l^2, i.e., $\mathcal{CN}(\mu_l, \sigma_l^2)$. Thus, the K-factor for this Rician channel when antenna i is used with antenna-state $S_{i,l}$ is given by $K_l = \mu_l^2/(2\sigma_l^2)$. Letting $\mathbf{H_i} = (\boldsymbol{h_{ji_l}})_{j,l}$ be the $N_r \times N_{s_i}$ channel matrix between different states in antenna i and different receive antennas, the extended channel matrix including all transmit antennas and states has a dimension of $N_r \times N_s$, where $N_s = \sum_{i=1}^{N_t} N_{s_i}$, and is given by $\mathbf{H} = [\mathbf{H_1\, H_2}\, \ldots\, \mathbf{H_{N_t}}]$. The transmitted signal through this channel experiences an N_r-dim normalized AWGN $\boldsymbol{\eta} = \frac{1}{\sqrt{N_0}}[\eta_1,\ \eta_2\, \ldots,\ \eta_{N_r}]^T$ having i.i.d entries following a complex Gaussian distribution with zero mean and variance N_0, i.e., $\mathcal{CN}(0, N_0)$.

5.2.5 Correlation Model

Assuming correlated Rician fading over the transmit-receive wireless link, the proposed correlation model takes into account the correlation between different states within the same and different antenna. Thus, we look into two different types of correlation: polarization correlation and spatial correlation.

Polarization Correlation

The polarization correlation, denoted by ρ_p, describes the correlation between different states within the reconfigurable antenna. Similar to the variation of the K-factor with different polarization parameters, the correlation factor between different antenna-states is a function of the used polarization angle. Using curve-fitting, we derive the expression of the polarization

correlation coefficient ρ_p as a function of α as

$$\rho_p(\alpha) = 0.277 + 0.823\cos{(0.035\alpha)} - 0.098\cos{(0.07\alpha)}. \qquad (5.5)$$

Fig. 5.3 depicts the variation of ρ_p as a function of the polarization angle in reference to the angle $\alpha = 0^o$. Thus, in order to find the polarization correlation between two states corresponding to two different polarization angles α_1 and α_2, we can use the figure or Eq. (5.5) by letting $\alpha = \alpha_1 - \alpha_2$. For example, the polarization correlation between the angles 20° and 50° is equal to 0.75 as seen in Fig. 5.3 for $\alpha = 30^o$.
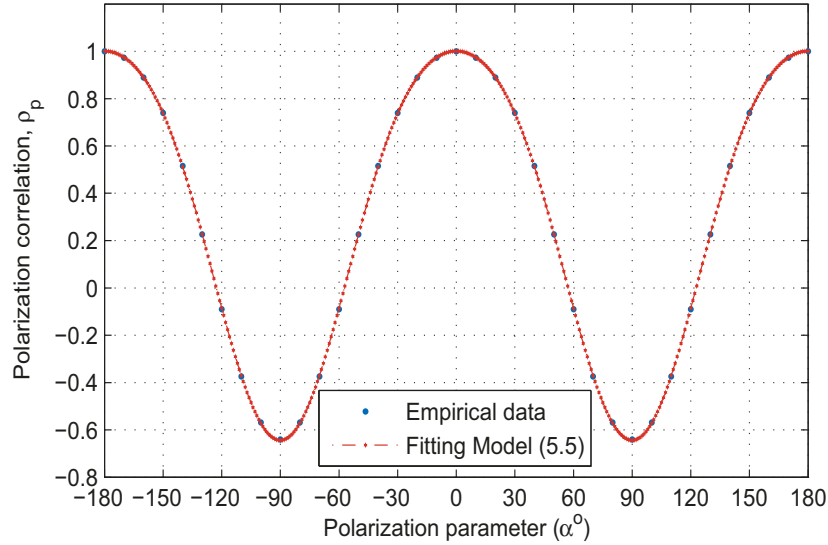

Figure 5.3: Polarization correlation as a function of α.

Spatial Correlation

While states within the same antenna experience correlation coefficients according to (5.5), states within different transmit antennas are subject to spatial correlation ρ_s in addition to the polarization correlation ρ_p. For the same antenna-state within different antenna elements, we use the exponential correlation model where the spatial correlation reduces exponentially with the distance between different antennas [100]. In this context, the correlation between two antennas i and j separated by distance $d_{i,j}$ is given by $\rho_s^{d_{i,j}/(\lambda/2)}$, where ρ_s is a constant

factor between 0 and 1 used to study the performance of different correlation coefficients, λ is the wavelength, and $d_{i,j}/(\lambda/2)$ is the normalized distance. Assuming that all transmit antennas are uniformly separated by $\lambda/2$, the spatial correlation between antenna i and antenna j is then given by $\rho_s^{|i-j|}$.

Combined Correlation Model

For simplicity of implementation, we consider the "Kronecker model" [101] as a combined channel correlation model taking both spatial and polarization correlations into consideration. It is recognized that this model does not capture all possible correlation scenarios to their full extend [102], however, it is used here since it shows similar performance trends for different correlation models. The correlated channel matrix $\mathbf{H}$ is given as a function of the uncorrelated channel matrix $\mathbf{H^u}$ as

$$\mathbf{H} = \mathbf{R_{Rx}^{1/2}} \; \mathbf{H^u} \; \mathbf{R_{Tx}^{1/2}}, \tag{5.6}$$

where $\mathbf{R_{Rx}}$ is an $N_r \times N_r$ matrix representing the correlation between different receive antennas. At the receiver side, only spatial correlation is considered and the correlation between receive antennas j_1 and j_2 is given by $\mathbf{R_{Rx}}(j_1, j_2) = \rho_s^{|j_1-j_2|}$. $\mathbf{R_{Tx}}$ is an $N_s \times N_s$ matrix representing the correlation between different antenna-states either within the same or different transmit antennas. $\mathbf{R_{Tx}}$ can be represented as

$$\mathbf{R_{Tx}} = \begin{bmatrix} \mathbf{R_{1,1}} & \cdots & \mathbf{R_{1,N_t}} \\ \vdots & \ddots & \vdots \\ \mathbf{R_{N_t,1}} & \cdots & \mathbf{R_{N_t,N_t}} \end{bmatrix}, \tag{5.7}$$

where $\mathbf{R_{i_1,i_2}}$, $(i_1 = 1, \ldots, N_t, \; i_2 = 1, \ldots, N_t)$, is a $N_{s_{i_1}} \times N_{s_{i_2}}$ matrix representing the correlation between the states in antenna i_1 and antenna i_2. Assuming that state u at antenna i_1 and state v at antenna i_2 correspond to the polarization parameters α_u and α_u, respectively, the elements in the u-th row and the v-th column of $\mathbf{R_{i_1,i_2}}$ is then given by

$$\mathbf{R_{i_1,i_2}}(u, v) = \rho_p(\alpha_u - \alpha_v) \times \rho_s^{|i_1-i_2|}, \tag{5.8}$$

where $u = 1, \ldots, N_{s_{i_1}}$ and $v = 1, \ldots, N_{s_{i_2}}$. The multiplication of the spatial and polarization correlations is chosen by intuition and does not capture the real correlation scenario. However, the choice of this model encompasses all three possible scenarios: (i) for different states within the same antenna, the correlation reduces to the polarization correlation ρ_p, (ii) for the same state within different antennas, the correlation reduces to the spatial correlation ρ_s, and (iii) for distinct states within different antennas, the correlation includes both the polarization and spatial correlations.

5.3 Proposed SSK-RA Variations

Unlike conventional modulation schemes, the ABER performance of SSK was shown to improve for lower values of the Rician K-factor [98]. Indeed, SSK modulation requires the wireless links to be sufficiently different from each other in order to achieve good performance which can be satisfied for higher amounts of fading, i.e., for lower values of K. Based on this result, the initial selection of different antenna states available at each antenna is not done arbitrarily in our schemes. To be more specific, using the variability of the K-factor and the polarization correlation ρ_p as a function of the polarization parameters given by (5.3) and (5.5), respectively, the choice of the antenna states minimizing the K-factor and the correlation coefficients is done according to different selection criteria. In what follows, we first present three different scenarios used for antenna-states. Then, we present the mode of operation of SSK-RA once a decision is made on the antenna-states that can be used at each transmit antenna.

5.3.1 State Selection Scenarios

Minimizing K

It was shown earlier that the variation of the K-factor as a function of the polarization parameters has some sort of periodicity. Thus, taking advantage of this behaviour, the states available at each antenna are chosen to minimize the channel's K-factor. In this context, the first used scenario assumes that the states with the minimum value of the K-factor achieved

by all possible polarization angles α, $\alpha \in [-180^o, 180^o]$, are selected independently of their polarization correlation ρ_p. This first selection scenario is summarised by Algorithm 4 below.

Algorithm 4 Minimizing K

For $i = 1 : N_t$

    For $j = 1 : N_{s_i}$

        Find $\alpha_j = \underset{\alpha \neq \alpha_l}{\arg \min} \, K(\alpha)$, $l = 1, \ldots, j - 1$;

    End

    Use states $\alpha_1, \alpha_2, \ldots, \alpha_{N_{s_i}}$ in antenna i;

End

Minimizing ρ_p

This second scenario aims at selecting antenna-states with the minimum polarization correlation values. In this case, minimum values of ρ_p are chosen independently of K as shown in Algorithm 5 below.

Algorithm 5 Minimizing ρ_p

Set $\alpha_0 = 0^o$

For $i = 1 : N_t$

    For $j = 1 : N_{s_i} - 1$

        Find $\alpha_j = \underset{\alpha}{\arg \min} \, \rho_p(\alpha, \alpha_l)$, $l = 1, \ldots, j - 1$

    End

  Use states $\alpha_0, \alpha_1, \ldots, \alpha_{N_{s_i} - 1}$ in antenna i

End

**Joint Minimization of K and ρ_p**

In this third scenario, the Rician K-factor and the polarization correlation are jointly minimized in order to further enhance the performance of the two previous SSK-RA scenarios. In this case, the selected states need to verify that K and ρ_p are below certain thresholds given respectively by $K_{\min}$ and $\rho_{\min}$. These minimum values are chosen while compromising between the computational complexity and performance. Indeed, lower values of these

thresholds improve the performance but increase the time and complexity to find the states that can be used. We summarize the joint selection process of the Rician K-factor and the polarization correlation ρ_p in Algorithm 6 below.

**Algorithm 6** Joint Minimization of K and ρ_p

---

Let $S = \{\alpha, \text{ such that } K(\alpha) \leq K_{\min}\}$ and $L = |S|$
For $i = 1 : N_t$
    For $u = 1 : L$
        $N = 1$, $\text{State}(1) = \alpha_u$
        For $v = u + 1 : L$
            If $\rho_p(\alpha_u, \alpha_v) \leq \rho_{\min} \Rightarrow N = N + 1$, $\text{State}(N) = \alpha_v$
                If $N = N_{s_i} \Rightarrow$ Stop, use these N_{s_i} states
                    for antenna i, and move to antenna $i + 1$
        End
    End
End

5.3.2 Mode of Operation

Once the transmitter decides on which states to be available at each transmit antenna according to the above different scenarios, the SSK-RA schemes use joint antenna and state selection based on the incoming bits without requiring any feedback from the receiver. Indeed, similar to SSK, the transmitter encodes $\log_2(N_t)$ bits into the index of a single transmit-antenna. If antenna i is selected for transmission, the next $\log_2(N_{s_i})$ bits are encoded into the index of a single antenna-state (assuming that the number of states is a power of two). Thus, antenna i is activated for transmission for the next time slot using the selected antenna state. An example of antenna-state mapping when four states are available at each antenna is given in Fig. 5.4 at the top of next page. Different antenna patterns of vertical polarization of the rotation angles are also given in the same figure.
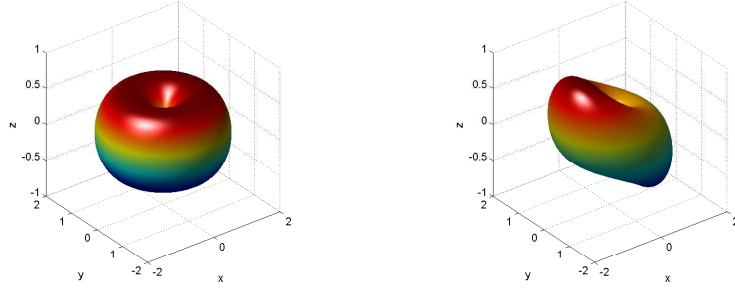
(a) 00 → Polarization angle $\alpha = 0^o$ (b) 01 → Polarization angle $\alpha = 20^o$
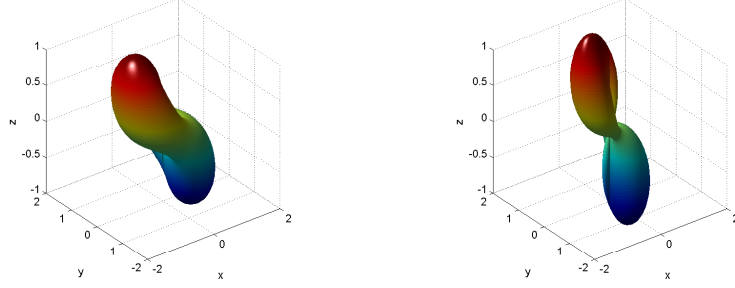
(c) 11 → Polarization angle $\alpha = 40^o$ (d) 10 → Polarization angle $\alpha = 60^o$

Figure 5.4: Antenna patterns of vertical polarization of the rotation angles. Example of antenna state selection and mapping based on the incoming bits.

5.4   Optimal Detection

Assuming that the i-th antenna is selected for transmission using state $S_{i,l}$, the output of the channel can be expressed as

$$y = \sqrt{\rho}\, h_{i_l} + \eta, \tag{5.9}$$

where h_{i_l} denotes the l-th column of $\mathbf{H_i}$ (equivalently, h_{i_l} denotes the $(\sum_{n=1}^{i-1} N_{s_n} + l)$-th column of the extended channel matrix $\mathbf{H}$) and $\rho = P_t/N_0$ where P_t is the power used at the transmitter. Please note that ρ is different from the previous two chapters where it was defined as the average receive SNR. In this chapter, we define the SNR ρ using the transmit power for fairness of comparison between SSK and SSK-RA. Indeed, when using RAs the received power is different from an antenna state to the other for the same P_t because the

change in the antenna radiation pattern.

The detector's main task is to find the antenna-index and the antenna-state used for transmission. Assuming equally likely inputs, full receive channel state information, and perfect time-synchronization at the receiver, this information can be decoded using the optimal ML detector as follows [33]

$$[\hat{i}, \hat{l}] = \arg \max_{i,l} f_{\boldsymbol{Y}}(\boldsymbol{y}|\boldsymbol{x_{i_l}}, \mathbf{H}) = \arg \max_{i,l} D_{i_l}, \tag{5.10}$$

where $\boldsymbol{x_{i_l}}$ is a $\sum_{n=1}^{Nt} N_{s_n} \times 1$ vector with all entries equal to zero except the $(\sum_{n=1}^{i-1} N_{s_n} + l)$th entry being equal to one, $f_{\boldsymbol{Y}}(\boldsymbol{y}|\boldsymbol{x_{i_l}}, \mathbf{H}) = \pi^{-N_r} \exp\left(-\|\boldsymbol{y} - \sqrt{\rho}\,\mathbf{H}\,\boldsymbol{x_{i_l}}\|_{\mathrm{F}}^2\right)$ is the PDF of the received signal conditioned on $\boldsymbol{x_{i_l}}$ and $\mathbf{H}$. D_{i_l} denotes the decision metric used in order to conclude that the i-th antenna is used with state $S_{i,l}$ and is given by

$$D_{i_l} = \mathrm{Re}\left\{\left(\boldsymbol{y} - \frac{\sqrt{\rho}}{2}\boldsymbol{h_{i_l}}\right)^H \boldsymbol{h_{i_l}}\right\}, \tag{5.11}$$

where $\|\cdot\|_{\mathrm{F}}$ and $(\cdot)^H$ respectively denote the Frobenius norm and the conjugate transpose of a vector/matrix. $\mathrm{Re}\{\cdot\}$ denotes the real part of a complex number.

5.5 Bit Error Rate Performance Analysis

5.5.1 General Scenario

Similar to SSK [33], the ABER performance of SSK-RA is derived using UB. Considering the general case of N_t RAs at the transmitter and N_{s_i} available states at the i-th transmit antenna, the UB on the ABER can be formulated as

$$\mathrm{ABER} \leq \frac{1}{N_{t,s} - 1} \sum_{n=1}^{N_t} \sum_{u=1}^{N_{s_n}} \sum_{m=n+1}^{N_t} \sum_{v=1}^{N_{s_m}} \mathrm{ABER}_{n_u, m_v}, \tag{5.12}$$

where $N_{t,s} = \sum_{i=1}^{N_t} N_{s_i}$ represents the total number of states available at all transmit antennas and ABER_{n_u, m_v} is defined as the pairwise error probability between transmit-antenna n using

state u and transmit-antenna m using state v, i.e., the probability of detecting the u-th state in antenna n when, instead, the v-th state in antenna m is actually used for transmission, and vise-versa.

Let $\boldsymbol{x}_{n_u}$ denote the signal transmitted using antenna state u in the n-th antenna. Following the same steps as in [33], the conditional error probability of deciding on $\boldsymbol{x}_{m_v}$ given that $\boldsymbol{x}_{n_u}$ is actually transmitted is given by

$$
\begin{aligned}
\mathrm{P_e} \quad (\boldsymbol{x}_{n_u} \to \boldsymbol{x}_{m_v} | \mathbf{H}) &= \mathrm{P_e}(D_{m_v} > D_{n_u} | \mathbf{H}) \\
&= Q\left(\sqrt{\rho \sum_{l=1}^{N_r} |h_{ln_u} - h_{lm_v}|^2}\right) = Q\left(\sqrt{\rho \gamma_{m_u,n_v}}\right),
\end{aligned} \tag{5.13}
$$

where $Q(x) = 1/\sqrt{2\pi} \int_x^\infty e^{-\frac{z^2}{2}} dz$ is the Q-function and $\gamma_{m_u,n_v} = \sum_{l=1}^{N_r} |h_{ln_u} - h_{lm_v}|^2$.

Letting $\boldsymbol{\psi}_l = \boldsymbol{h}_{ln_u} - \boldsymbol{h}_{lm_v} = \boldsymbol{\psi}_l^{\mathbf{R}} + j\,\boldsymbol{\psi}_l^{\mathbf{I}}$, where R and I denote the real part and the imaginary part, respectively, we define the $2\,N_r \times 1$ vector $\Psi = [\psi_1^{\mathrm{R}}, \ldots, \psi_{N_r}^{\mathrm{R}}, \psi_1^{\mathrm{I}}, \ldots, \psi_{N_r}^{\mathrm{I}}]^{\mathrm{T}}$, where $[\cdot]^{\mathrm{T}}$ denotes the transpose of a vector/matrix. Let K_u denote the of the Rician K-factor between the u-th state and any receiver antenna. Thus, this channel has mean $\mu_u = \sqrt{K_u/(K_u+1)}$ and variance $\sigma_u^2 = 1/(2\,K_u + 1)$. With these definitions, Ψ is a Gaussian distribution vector with a $2\,N_r \times 1$ mean vector $\boldsymbol{\mu_\Psi}$ having equal components given by

$$
\boldsymbol{\mu_\Psi}(l) = |\mu_u - \mu_v|, \qquad \text{for } l = 1, \ldots, 2\,N_r \tag{5.14}
$$

and a $2\,N_r \times 2\,N_r$ covariance matrix $\boldsymbol{\Sigma_\Psi}$ given by

$$
\boldsymbol{\Sigma_\Psi} = \begin{bmatrix} \boldsymbol{\Sigma_\Psi^{RR}} & \mathbf{0} \\[1em] \mathbf{0} & \boldsymbol{\Sigma_\Psi^{II}} \end{bmatrix}, \tag{5.15}
$$

where $\mathbf{0}$ is an $N_r \times N_r$ matrix with all elements equal to zero. $\boldsymbol{\Sigma_\Psi^{RR}} = \boldsymbol{\Sigma_\Psi^{II}}$ are $N_r \times N_r$

matrices with the element on the l_1-th row and l_2-th column given by

$$\boldsymbol{\Sigma}_{\boldsymbol{\Psi}}^{\mathbf{RR}}(l_1, l_2) = \left(\sigma_u^2 - 2\sigma_u\sigma_v\rho_p(\alpha_u - \alpha_v)\rho_s^{|m-n|} + \sigma_v^2\right)$$
$$\times \rho_s^{|l_1-l_2|}, \quad \text{for } l_1 = 1, \ldots, 2\,N_r \text{ and } l_2 = 1, \ldots, 2\,N_r \tag{5.16}$$

where α_u and α_v are the polarization angles for state u and state v, respectively.

Based on the results derived above, γ_{m_u,n_v} is the summation of the absolute square values of N_r complex Gaussian random variables with mean and covariance matrix given by (5.14) and (5.15) respectively. Thus, the moment generating function (MGF) of γ_{m_u,n_v} can be obtained using the result of [103, Eq. (25)] as

$$\mathcal{M}_{\gamma_{m_u,n_v}}(s) = \prod_{i=1}^{2N_r} \left[\sqrt{\frac{1}{(1+2\,\lambda_i\,s)}}\, e^{-\frac{\delta_i^2\,s}{1+2\,\lambda_i\,s}}\right] = \prod_{i=1}^{2N_r} (1+2\,\lambda_i\,s)^{-1/2}\, e^{-\sum_{j=1}^{2N_r}\frac{\delta_j^2\,s}{1+2\,\lambda_j\,s}}, \tag{5.17}$$

where δ_i is the i-th element of the vector $\boldsymbol{\delta} = \boldsymbol{U}^{\mathbf{T}}\,\boldsymbol{\mu_\Psi}$ and $\boldsymbol{U}$ is a $2N_r \times 2N_r$ orthogonal matrix containing the eigenvectors of $\boldsymbol{\Sigma_\Psi}$. λ_i is the i-th diagonal element of the diagonal matrix $\boldsymbol{D}$ of the eigenvalues of $\boldsymbol{\Sigma_\Psi}$, i.e., $\boldsymbol{\Sigma_\Psi} = \boldsymbol{U}\boldsymbol{D}\boldsymbol{U}^{\mathbf{T}}$, where $\boldsymbol{D} = \text{diag}(\lambda_1, \lambda_2, \ldots, \lambda_{2\,N_r})$.

Using the results of [103, Theorem I], the PDF of γ_{m_u,n_v} can be obtained as

$$f_{\gamma_{m_u,n_v}}(\gamma) = \xi \sum_{k=0}^{\infty} \rho_k \frac{\gamma^{N_r+k-1}e^{-\frac{\gamma}{2\lambda_1}}}{2\,\lambda_1^{N_r+k}\Gamma(N_r+k)}, \tag{5.18}$$

where

$$\xi = \prod_{i=1}^{2N_r} \left[\sqrt{\frac{2\,\lambda_1}{2\,\lambda_i}}\, e^{-\frac{\delta_i^2}{2\,\lambda_i}}\right], \tag{5.19}$$

$\Gamma(\cdot)$ is the Gamma function, $\lambda_1 = \min\{\lambda_i : 1 \leq i \leq 2N_r\}$, $\rho_0 = 1$, and ρ_k is obtained recursively by the formula

$$\rho_k = \frac{1}{2k}\sum_{i=1}^{k}\left[\sum_{j=1}^{2N_r}\left(1-\frac{\lambda_1}{\lambda_j}\right)^i + \frac{i\lambda_1\delta_j^2}{\lambda_j^2}\left(1-\frac{\lambda_1}{\lambda_j}\right)^i\right]\rho_{k-i}. \tag{5.20}$$

Following the steps of [98], the ABER for the case of the considered states is derived using

the PDF approach as

$$\text{ABER}_{n_u, m_v}(\rho) = \int_0^\infty Q\left(\sqrt{\rho z}\right) f_{\gamma_{m_u, n_v}}(z) dz$$

$$= \frac{\xi}{2\sqrt{\pi}} \sum_{k=0}^\infty \left[\frac{2\,\rho_k}{\Gamma(k+1/2)} G_{2\,2}^{2\,1}\left(\left. \begin{matrix} 1/2-k & 1 \\ 0 & 1/2 \end{matrix} \right| \lambda_1 \rho/2 \right) \right], \tag{5.21}$$

where $G_{p\,q}^{m\,n}\left(\left. \begin{matrix} a_1,...,a_p \\ b_1,...,b_q \end{matrix} \right| z \right)$ is the Meijer-G function defined in [104, Ch 8, pp. 519]. Thus, an upper bound on the ABER can be obtained using (5.12) and (5.21).

5.5.2   Special i.i.d Scenario

In this special case, the selected states are uncorrelated and they have the same value of K (i.e., same mean and variance). Let K_c denote this common value of K. Thus, $\boldsymbol{h_{ln_u}} - \boldsymbol{h_{lm_v}}$ is distributed as $\mathcal{CN}(0, 2\sigma_c^2)$, where $\sigma_c^2 = 1/(2\,K_c + 1)$. Consequently, the MGF of γ_{m_u, n_v} for this case is simplified as

$$\mathcal{M}_{\gamma_{m_u, n_v}}^{\text{i.i.d}}(s) = \frac{1}{(1 + 2\sigma_c^2\, s)^{N_r}}. \tag{5.22}$$

In this case, the ABER can be obtained using the MGF-approach as

$$\text{ABER}_{m_u, n_v} = \frac{1}{\pi} \int_0^{\frac{\pi}{2}} \mathcal{M}_{\gamma_{m_u, n_v}}\left(\frac{\rho}{2\sin^2(\theta)} \right) d\theta. \tag{5.23}$$

Using [105, Eq. (5.17)] and (5.23), we derive the closed-form expression of ABER_{m_u, n_v} as

$$\text{ABER}_{m_u, n_v}^{\text{i.i.d}} = \frac{1}{2} - \frac{1}{8}\sqrt{\frac{\sigma_c^2 \rho}{\sigma_c^2 \rho + 1}} \sum_{k=0}^{N_r-1} \binom{2k}{k}\left(\frac{1}{\sigma_c^2 \rho + 1} \right)^k. \tag{5.24}$$

This result can also be derived using the PDF approach where the PDF of γ_{m_u, n_v} in this case is given by

$$f_{\gamma_{m_u, n_v}}^{\text{i.i.d}}(\gamma) = \frac{1}{(2\sigma_c^2)^{N_r}(N_r - 1)!} \gamma^{N_r - 1} e^{-\gamma/2\sigma_c^2}. \tag{5.25}$$

In this special case, ABER_{m_u, n_v} is the same for any pair of transmit antennas and states.

Thus, the ABER for the proposed SSK-RA schemes in this case is upper-bounded as

$$\mathrm{ABER}^{\mathrm{i.i.d}} \leq \frac{N_{t,s}}{2} \mathrm{ABER}_{m_u,n_v}. \tag{5.26}$$

5.6 Numerical Examples

we illustrate the performance of the proposed SSK-RA schemes via selected numerical examples. These results are obtained by Monte-Carlo simulations and confirmed with analytical results. In order to highlight the performance improvements achieved by the SSK-RA schemes, we also compare the obtained results to the conventional SSK.

The use of RAs at the transmitter offers another degree of freedom that can be used to improve the ASE of SSK. Indeed, while SSK offers a throughput of $\log_2(N_t)$ bits per channel use, the SSK-RA schemes offer an ASE η given by

$$\eta = \log_2(N_t) + \frac{1}{N_t} \sum_{i=1}^{N_t} \log_2(N_{s_i}), \tag{5.27}$$

where N_{s_i} was previously defined as the number of states available at the ith transmit antenna. For a fair comparison, the ABER results are generated for the SSK and SSK-RA systems operating at the same ASE. In this context, we consider an $N_t \times N_r$ SSK-MIMO system with conventional antennas and we compare its performance to an SSK-RA system having the same number of receive antennas but coming with one reconfigurable transmit antenna operating with N_t states (i.e., $1_{N_t} \times N_r$). While both settings offer an ASE of $\log_2(N_t)$ and achieve spatial multiplexing with a single RF chain, SSK-RA comes with much lower complexity. Indeed, while an $1_{N_t} \times N_r$ system requires only one RF chain to be implemented, the $N_t \times N_r$ SSK scenario requires multiple chains to be available [37]. Moreover, switching between antenna states results from altering the surface current distribution and thus comes with lower complexity and lower cost when compared to switching between RF chains during each transmission period. Furthermore, the integration of a single reconfigurable antenna with multiple states in cost and size sensitive wireless devices, such as mobile terminals, is more practical than the implementation of multiple antennas in these devices [36].
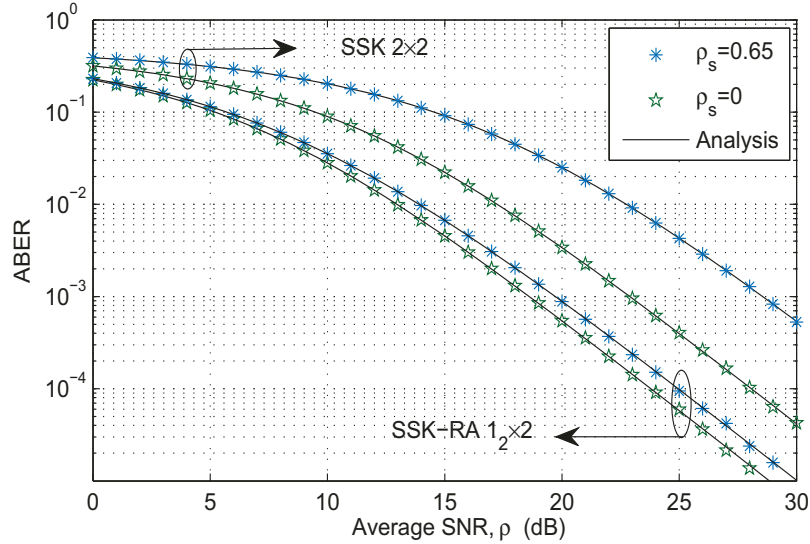
Figure 5.5: ABER comparison for SSK-RA and SSK with simulation and theory with the following setup: (i) scenario taking the minimum K-factor independently of ρ_p, (ii) indoor environment (office), (iii) equal throughput of 1 bit/s/Hz, $N_r = 2$, and $\rho_s = 0$ and 0.65.

Fig. 5.5 depicts the ABER performance of SSK and SSK-RA as a function of $\rho = P_t/N_0$ for an indoor office environment with both theory and simulations for $N_r = 2$. For the SSK-MIMO system, we consider conventional transmit antennas with a fixed polarization angle $\alpha = 0^o$. Based on the results provided in Table 5.1, the Rician fading channel for this given environment and antenna polarization has a K-factor equal to 8.16 dB. From Fig. 5.5, we can clearly see the ABER performance improvement offered by the SSK-RA schemes thanks to the use of RAs. In this presented scenario, the states minimizing the Rician K-factor are considered to be available at the transmit antenna independently of their polarization correlation ρ_p (i.e., minimum K scenario). Fig. 5.5 also shows the impact of the spatial correlation ρ_s on the ABER performance. We can see that the considered $1_2 \times N_r$ SSK-RA scheme is more robust to increasing values of ρ_s. Indeed, using a single transmit antenna alleviates this impact and only receive antennas are subject to the spatial correlation while transmit states experience polarization correlation having lower impact than ρ_s. This explains the higher ABER degradation experienced by conventional SSK for higher values of ρ_s.

Fig. 5.6 depicts the ABER performance of SSK and SSK-RA as a function of ρ for the same setup considered in Fig. 5.5 but with four receive antennas instead of two. From this
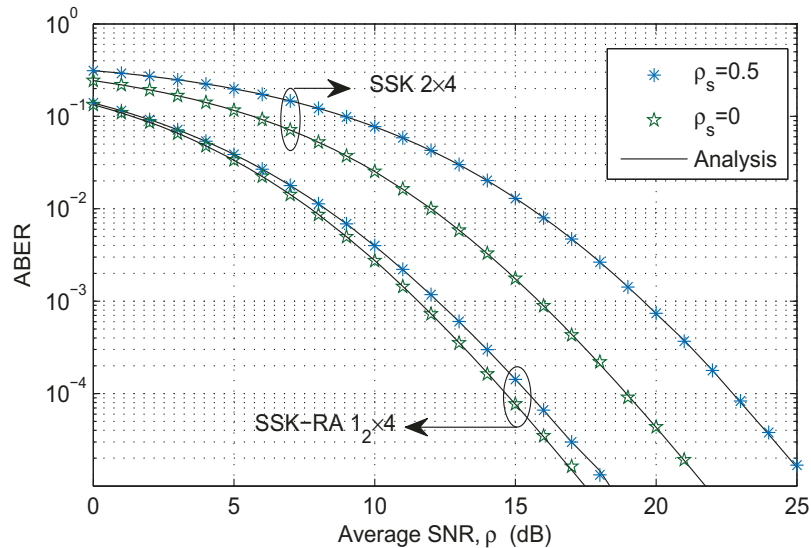
Figure 5.6: ABER comparison for SSK-RA and SSK with simulation and theory with the following setup: (i) Minimum K scenario, (ii) indoor environment (office), (iii) equal throughput of 1 bit/s/Hz, $N_r = 4$, and $\rho_s = 0$ and 0.5.

figure, we can confirm the considerable ABER performance improvement offered by SSK-RA thanks to the use of RAs. Indeed, for $\rho_s = 0$, SSK-RA requires 5 dB less than SSK in order to achieve the same ABER of 10^{-5}. This gap grows to around 8 dB for a spatial polarization equal to 0.5 and increases for higher values of ρ_s. In addition to this considerable ABER improvement, SSK-RA with a single transmit antenna and multiple states comes with much lower implementation cost and complexity when compared to SSK with multiple transmit antennas. Furthermore, Fig. 5.6 confirms that the diversity order of SSK-RA, similar to SSK, increases with N_r.

Fig. 5.7 depicts the ABER performance comparison between different SSK-RA state-selection scenarios as a function of ρ for an indoor office environment. The joint selection of K and ρ_p according to Algorithm 6 offers the best ABER performance. Indeed, while the first scenario minimizes the values of K, it has no control over the polarization correlation. Similarly, the second scenario allows for selecting states with low polarization correlation but these states may come with higher values of K than the previous scenarios. We can also conclude that the Rician K-factor has higher impact on the ABER performance than ρ_p does. In this context, the scenario selecting the minimum K can be seen as a performance-
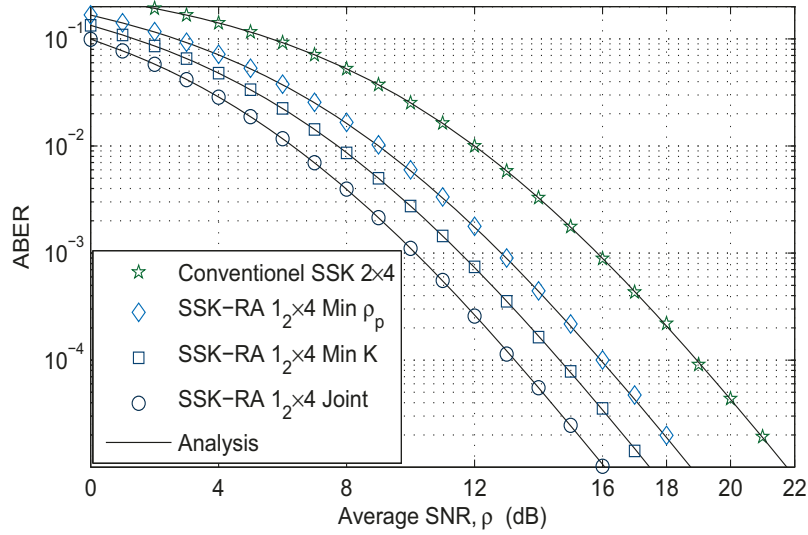
Figure 5.7: ABER comparison for different SSK-RA scenarios for $\rho_s = 0$ and $N_r = 4$. For the joint scenario, we use $K_{\min} = 1$ dB and $\rho_{p_{\min}} = 0.25$.

computation tradeoff scheme between the two other scenarios. Indeed, the joint process offer the best ABER performance but comes with higher computational complexity in order to find the antenna-states that jointly minimize the K-factor and ρ_p.

Fig. 5.8 highlights the effect of increasing the number of antenna-states at the transmitter on the ABER performance of SSK-RA. In this context, we compare the performance of SSK and SSK-RA for different throughputs of 1, 2, and 3 bits/s/Hz. The results obtained in Fig. 5.8 are generated assuming that different antennas and different states are uncorrelated for SSK and SSK-RA and selecting the antenna-states with the minimum Rician K-factors. We can see from this figure that increasing the number of states in SSK-RA, similar to increasing the number of antennas in SSK, reduces the ABER performance. Fig. 5.8 confirms the performance improvement gained by SSK-RA compared to SSK both in terms of ABER and ASE. Indeed, we can see that the $1_4 \times 4$ and $1_8 \times 4$ SSK-RA implementations not only offers higher throughput than the 2×4 SSK system but also considerably improves the error performance. This confirms the advantage of SSK-RA in terms of ASE and ABER performance in addition to the reduced implementation complexity when using only one antenna with multiple states at the transmitter.
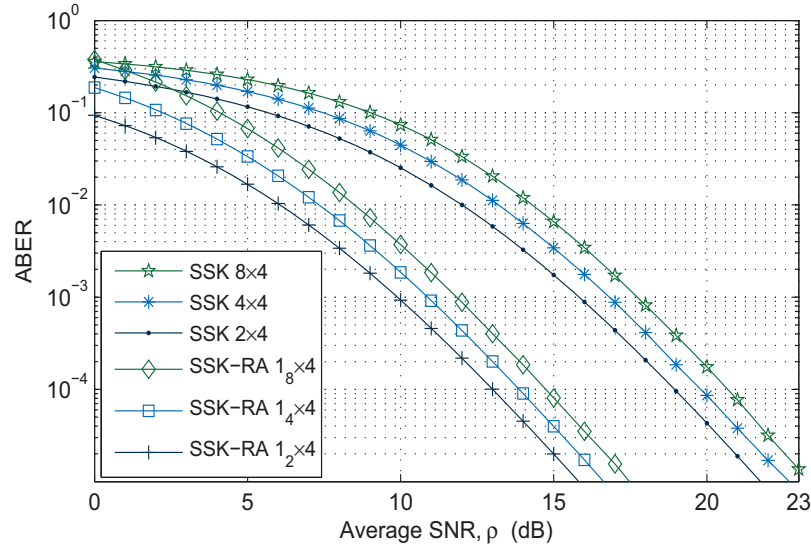
Figure 5.8: ABER comparison for SSK-RA and SSK with independent states and antennas for different number of available states and antennas at the transmitter and for $N_r = 4$.

Fig. 5.9 depicts the ABER performance comparison between the SSK and SSK-RA schemes as a function of ρ for different indoor and outdoor propagation environments in the 5 GHz band. For a given distance d between the transmitter and receiver, the performance of SSK is simulated for a Rician fading channel with $\alpha = 0^o$ given in Table 5.1 for different propagation environments. This figure shows that different environments experience comparable performance in the SSK-RA schemes. Indeed, as it can be seen from Fig. 5.2, the minimum values of the Rician K-factor reached by different environments are within the same range, which leads to comparable results. Moreover, we can see from Fig. 5.9 that SSK is inferior to SSK-RA in all scenarios. Furthermore, scenarios corresponding to high values of K for 0° (i.e., worse SSK performance) also come with the lowest values of $K_{\min}$ (i.e., better SSK-RA performance). This performance variation is mainly due to the scaling parameters a and b defined in (5.3) since the Rician K-factor scales with these parameters.
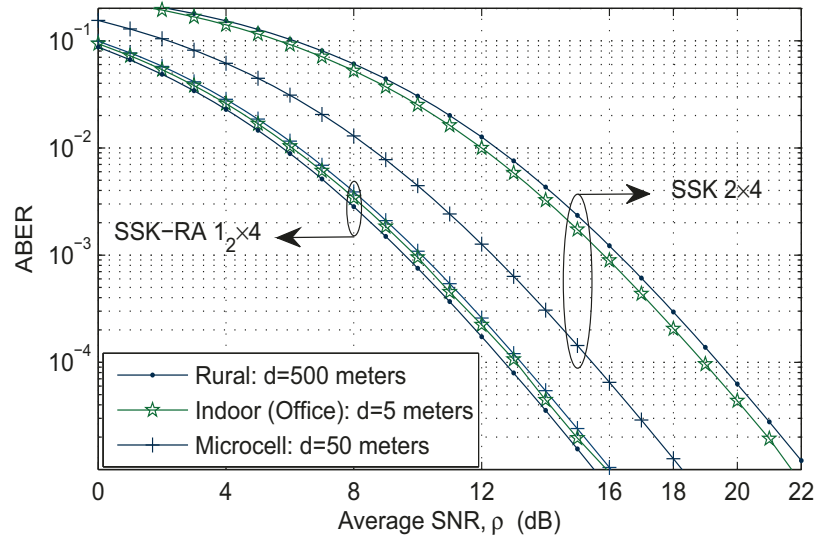
Figure 5.9: ABER comparison for SSK and SSK-RA schemes with the joint scenario for different propagation environments in the 5 GHz band when $\rho_s = 0$, $N_r = 4$, $K_{\min} = 1$dB and $\rho_{\min} = 0.25$.

5.7 SSK-RA for Spectrum Sharing Systems

5.7.1 System Model

We consider the system model shown in Fig. 5.10 extending the SSK-RA system settings to spectrum sharing systems. Under this scenario, the ST is allowed to share the spectrum with the PU as long as an interference constraint to this latter with a peak value Q is respected. The feedback link between the PU and the ST are assumed to be reliable and carry different levels of feedback information depending on the assumptions made about the interference link. Based on this feedback information, the ST determines the list of antennas-states that can be used for transmission in each antenna. Different scenarios can be considered depending on the amount of CSI available to the ST about both the interference and the secondary link. In this context, several schemes can be proposed in order to improve the performance of spectrum sharing systems. In what follows, we only consider the case where only an ACK/NACK process is used to let the ST know if a given state verifies the interference or not. We also assume that no feedback is needed from the SR to the ST. In this case, once

the states verifying the interference constraint are known, the ST selects the state to be used for transmission during the next time slot based on the incoming bits.
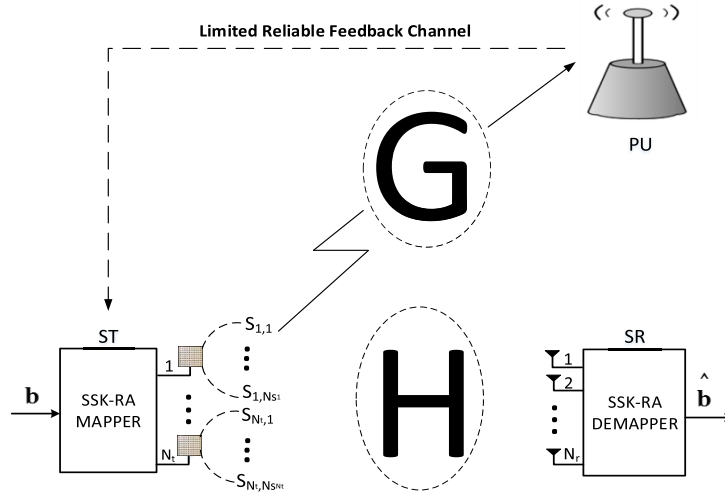

Figure 5.10: SSK-RA-CR System model.

5.7.2 Preliminary Results

All the advantages offered by RAs with SSK are also applicable when the SSK-RA schemes are extended to spectrum sharing systems. In this context, we still benefit from the high spectral efficiency and energy efficiency and from the low implementation complexity of SSK-RA. The challenge in this case is to design RAs with states minimizing the interference to the primary link and maximizing the received SNR at the secondary link.

In Fig. 5.11, we depict the ABER performance comparison between SSK and SSK-RA in spectrum sharing systems as function of ρ. We consider the simple case where only two states among the states verifying the interference constraint are eligible for transmission. In this scenario, SSK-RA-CR without feedback uses the two states that both verify the interference to the PU and minimize the K-factor of the secondary link. On the other hand, SSK-RA-CR with feedback uses the two states that both verify the interference to the PU and maximize the instantaneous SNR at the SR. Fig. 5.11 shows the considerable ABER performance improvement offered by SSK-RA-CR when compared to SSK-CR. Moreover, for this considered case, SSK-RA-CR comes with lower complexity by avoiding RF switching while offering the

same ASE as SSK-CR. Another advantage offered by SSK-RA-CR is reducing the buffering delay experienced by SSK-CR. Indeed, while SSK-CR needs to buffer data if less that two antennas verify the interference constraint, SSK-RA-CR can find two antenna states verifying this constraint thanks to the large number of antenna states that can be used by each antenna. For instance, in the case of the antenna polarization angle α reconfiguration, there are 361 available antenna states ($\alpha \in [-180^o, 180^o]$).
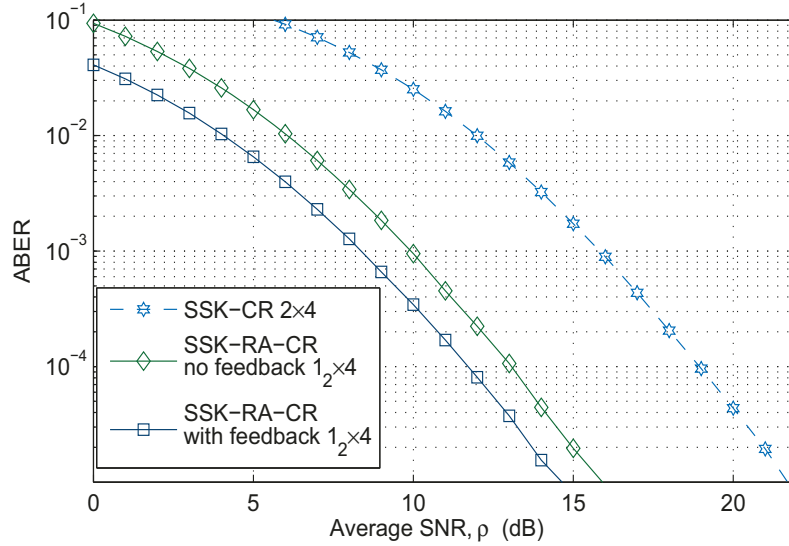

Figure 5.11: ABER comparison for SSK and SSK-RA schemes for spectrum sharing systems.

Based on these preliminary simulation, it is clear that studying all the previously proposed schemes in this thesis with RAs instead of conventional antennas can offer further performance improvements in terms spectral efficiency, energy efficiency, delay, and implementation complexity. This makes the of use of RAs a very promising solution not only for CR systems but also for future wireless communication systems in general.

5.8   Conclusion

Using the concept of reconfigurable antennas, we proposed in this chapter a number of SSK-RA schemes aiming at improving the performance of SSK in terms of complexity, throughput, and error performance. In order to achieve this goal, the proposed SSK-RA schemes jointly use SSK with antenna-state selection while taking advantage of the interplay between RAs

and the multipath propagation channel. Indeed, the reconfigurable properties of RAs together with the effect of these properties on the propagation channel offer additional degrees of freedom that we exploited to enhance SSK's performance. In this chapter, the performance of the proposed SSK-RA schemes was analysed in Rician fading channels in terms of ABER and ASE. Several simulation examples through which we corroborate these analytical results were also provided. Based on these results, the proposed schemes are shown to enhance the performance of SSK both in terms of ASE and ABER. For the same ASE as SSK, the proposed scenarios not only provide much better error performance but also considerably reduce the overall system complexity.

Chapter 6

Conclusions and Future Work

6.1   Conclusions

Cognitive radio is considered as one of the major solutions addressing the issues of spectrum scarcity and underutilization. Under the umbrella of CR, spectrum sharing systems are proposed in order to deal with this spectrum inefficiency by allowing secondary users to coexist and transmit simultaneously with primary users in the existing licensed spectrum. In this context, several protocols, transmission technologies, and network infrastructure solutions aiming at maximizing both spectral efficiency and the achievable throughput in these systems have been investigated. Taking advantage of this promising field, we have tackled in this thesis a major thrust of research in spectrum sharing systems by proposing several adaptive transmission schemes aiming at improving the overall performance of these systems.

While many of the existing techniques are optimized from the spectral efficiency perspective in order to deal with the unprecedented data surge experienced by wireless data traffic, these solutions are generally not well designed to address the related complexity and power consumption issues. Consequently, achieving high data rates with these techniques comes at the expense of high energy consumption and increased system complexity. In this context, our main focus in this thesis is to come with adaptive transmission schemes designed to improve the performance of spectrum sharing systems in terms of spectral efficiency, energy efficiency, and implementation complexity. To this end, we use a number of adaptive transmission techniques in order to achieve this performance. For instance, we use adaptive

modulation to increase the spectral efficiency, the concept of single RF-chain to improve the energy efficiency, and RAs to reduce the implementation complexity of these techniques.

In Chapter 3, we presented a number of adaptive transmission techniques offering different performance tradeoffs depending on the availability of the CSI at the ST. These techniques use a combination of multiple adaptive solutions in order to improve the improve the performance of existing techniques. These enabling solutions include adaptive modulation, power adaptation, switched transmit diversity, transmit beamforming, STBC, and antenna selection techniques. Consequently, these techniques offer different options for the implementation of spectrum sharing systems depending on the required quality of service.

In Chapter 4, we designed adaptive spatial modulation for spectrum sharing systems as an adaptive transmission scheme using AM and SM. This proposed scheme improves the spectral efficiency of SM while offering a low energy option for CR systems. The proposed ASM-CR schemes offer tradeoffs in terms in terms of ASE, average delay, and ABER.

In Chapter 5, we employed RAs in order to further improve the performance of SM and SSK through the use of RAs instead of conventional antennas. In this context, we take advantage of the reconfigurable properties of RAs as additional degrees of freedom in order to further enhance the performance of SM and SSK in terms of throughput, system complexity, and error performance. Indeed, based on the variation of the Rician K-factor and the polarization correlation coefficients with different antenna states, the proposed schemes offer considerable performance improvement and make the use of RAs in spectrum sharing systems and more generally in future wireless communication systems a very promising option.

6.2   Future Work

In light of the above, the proposed schemes offer different solutions for using adaptive transmission techniques in spectrum sharing systems. These schemes come with performance enhancements in terms of spectral efficiency energy efficiency, error performance,and complexity. Based on the obtained results, several other frameworks and scenarios can be considered for the optimization and the study of the proposed techniques. Indeed, using more practical settings, we can address several future research paths that can further improve the

performance of not only spectrum sharing systems but future wireless communication systems in general. In this context, we aim at extending the work presented in the thesis to different scenarios while considering more practical considerations.

- We first plan to further investigate the proposed SSK-RA schemes for CR systems. Indeed, it is of interest to use RAs in these systems by finding antenna-states that minimize the interference to the primary used and also maximize the received SNR at the secondary user. In this scenario, the use of radiation pattern reconfiguration allows for finding antenna-states verifying the interference constraint and enhancing the performance of the secondary link.

- Moreover, it is of interest to study the performance of SM with RAs. Indeed, this combination increases the ASE especially with the use of AM. Thus, the goal is to come with ASM-RA schemes in spectrum sharing systems offering high spectral, energy efficiencies, and low implementation complexity. These schemes are expected to offer much better performance when compared to conventional APM techniques.

- As possible extensions, the proposed schemes can be studied in several other cognitive scenarios. These scenarios include the problem of secondary users' scheduling and resource allocation, the effect of multiple primary users, the introduction of cooperation and relaying, and the study of spectrum sensing by dealing with opportunistic spectrum access. Moreover, it is interesting to analyse the performance of these scenarios for different fading channels and different considerations including outdated CSI, non-ideal feedback, and imperfect channel conditions.

- More generally, it is of interest to investigate the advantages of using RAs in future wireless communication systems. Indeed, unlike conventional antennas, RAs offer new dimensions and degrees of freedom that can be used in order to fit in smart and self-organizing future networks. In this context, we aim at developing realistic models for RA systems that accounts for different environment. Using field measurements and real data, we can confirm the obtained theoretical results and ultimately propose RAs' implementations that can improve real systems.

Bibliography

[1] FCC, "Spectrum Policy Task Force," *ET Docket 02-135*, Nov. 2002.

[2] S. Haykin, "Cognitive radio: Brain-empowered wireless communications," *IEEE JSAC*, vol. 23, no. 2, pp. 201–220, Feb. 2005.

[3] M. Gastpar, "On capacity under received-signal constraints," in *Proc. 42nd Annual Allerton Conf. Comm., Control Comp.*, Monticello, Illinois.

[4] ——, "On capacity under receive and spatial spectrum-sharing constraints," *IEEE Trans. Inform. Theory*, vol. 53, no. 2, pp. 471–487, Feb. 2007.

[5] A. Ghasemi and E. S. Sousa, "Fundamental limits of spectrum-sharing in fading environments," *IEEE Trans. Commun.*, vol. 6, no. 2, pp. 649–658, Feb. 2007.

[6] T. Clancy, "Achievable capacity under the interference temperature model," in *Proc. 26th IEEE International Conference on Computer Communications (INFOCOM'07)*, Anchorage, May 2007, pp. 794–802.

[7] X. Kang, Y.-C. Liang, A. Nallanathan, H. K. Garg, and R. Zhang, "Optimal power allocation for fading channels in cognitive radio networks: Ergodic capacity and outage capacity," *IEEE Trans. Wireless Commun.*, vol. 8, no. 2, pp. 940–950, February 2009.

[8] J. Mitola and G. Maguire, "Cognitive radio: Making software radios more personal," *IEEE Personal Communications*, vol. 6, no. 4, pp. 13–18, Aug. 1999.

[9] K. A. Qaraqe, Z. Bouida, M. Abdallah, and M.-S. Alouini, "Joint switched transmit diversity and adaptive modulation in spectrum sharing systems," in *Proc. 2011 Sixth*

International ICST Conference on Cognitive Radio Oriented Wireless Networks and Communications (CROWNCOM), Osaka, Japan, June 2011, pp. 86–90.

[10] Z. Bouida, K. Qaraqe, M. Abdallah, and M.-S. Alouini, "Performance analysis of joint multi-branch switched diversity and adaptive modulation schemes for spectrum sharing systems," *IEEE Trans. Commun.*, vol. 60, no. 12, pp. 3609–3619, Dec 2012.

[11] H. Wang, J. Lee, S. Kim, and D. Hong, "Capacity enhancement of secondary links through spatial diversity in spectrum sharing," *IEEE Trans. Wireless Commun.*, vol. 9, no. 2, pp. 494–499, Feb. 2010.

[12] F. Rashid-Farrokhi, K. Liu, and L. Tassiulas, "Transmit beamforming and power control for cellular wireless systems," *IEEE J. Select. Areas Commun.*, vol. 16, no. 8, pp. 1437–1450, Oct 1998.

[13] T. K. Y. Lo, "Maximum ratio transmission," *IEEE Trans. Commun.*, vol. 47, no. 10, pp. 1458–1461, Oct 1999.

[14] C.-H. Tse, K.-W. Yip, and T.-S. Ng, "Performance tradeoffs between maximum ratio transmission and switched-transmit diversity," in *Proc. 11th IEEE Int. Symp. on Personal, Indoor, Mobile Radio Communications (PIMRC)*, London, UK, Sep. 2000, pp. 1485–1489.

[15] R. Zhang and Y.-C. Liang, "Exploiting multi-antennas for opportunistic spectrum sharing in cognitive radio networks," *IEEE Journal of Selected Topics in Signal Processing*, vol. 2, no. 1, pp. 88–102, Feb 2008.

[16] A. Tajer, N. Prasad, and X. Wang, "Beamforming and rate allocation in MISO cognitive radio networks," *IEEE Trans. Signal Processing*, vol. 58, no. 1, pp. 362–377, Jan. 2010.

[17] V. Tarokh, N. Seshadri, and A. R. Calderbank, "Space-time codes for high data rate wireless communication: Performance criterion and code construction," *IEEE Trans. Inform. Theory*, vol. 44, no. 03, pp. 744–765, Mar 1998.

[18] S. M. Alamouti, "A simple transmit diversity technique for wireless communications," *IEEE J. Select. Areas Commun.*, vol. 16, pp. 1451–1458, Oct 1998.

[19] Z. Chen, J. Yuan, B. Vucetic, and Z. Zhou, "Performance of Alamouti scheme with transmit antenna selection," *IEEE Electron. Lett.*, vol. 39, pp. 1666–1668, Nov 2003.

[20] L. Yang and J. Qin, "Performance of Alamouti scheme with transmit antenna selection for M-ray signals," *IEEE Trans. Wireless Commun.*, vol. 5, no. 12, pp. 3365–3369, Dec 2006.

[21] A. Maaref and S. Aissa, "Adaptive modulation using orthogonal STBC in MIMO Nakagami fading channels," in *2004 IEEE Int. Symp. on Spread Spectrum Techniques and Applications*, Aug. 2004, pp. 145–149.

[22] K. J. Hole, H. Holm, and G. E. Øien, "Adaptive multidimensional coded modulation over flat fading channels," *IEEE J. Select. Areas Commun.*, vol. 18, no. 7, pp. 1153–1158, Jul. 2000.

[23] M.-S. Alouini and A. J. Goldsmith, "Adaptive modulation over Nakagami fading channels," *Kluwer J. Wireless Communications*, vol. 13, pp. 119–143, May 2000.

[24] A. J. Goldsmith and S.-G. Chua, "Variable-rate variable-power MQAM for fading channels," *IEEE Trans. Commun.*, vol. 45, no. 10, pp. 1218–1230, October 1997.

[25] V. Asghari and S. Aissa, "Adaptive rate and power transmission in spectrum-sharing systems," *IEEE Trans. Wireless Commun.*, vol. 9, no. 10, pp. 3272–3280, October 2010.

[26] Y. Chen, M. S. Alouini, L. Tang, and F. Khan, "Analytical evaluation of adaptive-modulation-based opportunistic cognitive radio in Nakagami-m fading channels," *IEEE Trans. Veh. Technol.*, vol. 61, no. 7, pp. 3294–3300, September 2012.

[27] A. Goldsmith, S. Jafar, N. Jindal, and S. Vishwanath, "Capacity limits of MIMO channels," *IEEE J. Select. Areas Commun.*, vol. 21, no. 5, pp. 2363–2371, Jun 2003.

[28] M. Chiani, M. Z. Win, and A. Zanella, "On the capacity of spatially correlated MIMO Rayleigh-fading channels," *IEEE Trans. Inform. Theory*, vol. 49, no. 10, pp. 2363–2371, Oct. 2003.

[29] F. Heliot, M. Imran, and R. Tafazolli, "On the energy efficiency-spectral efficiency trade-off over the MIMO Rayleigh fading channel," *IEEE Trans. Commun.*, vol. 60, no. 5, pp. 1345–1356, May 2012.

[30] R. Y. Mesleh, H. Haas, C. W. Ahn, and S. Yun, "Spatial modulation - A new low complexity spectral efficiency enhancing technique," in *Proc. ChinaCom 2006*, Beijing, China, Oct 2006, pp. 1–5.

[31] R. Y. Mesleh, H. Haas, S. Sinanovic, C. W. Ahn, and S. Yun, "Spatial modulation," *IEEE Trans. Veh. Technol.*, vol. 57, no. 4, pp. 2228–2241, Jan 2008.

[32] J. Jeganathan, A. Ghrayeb, and L. Szczecinski, "Spatial modulation: optimal detection and performance analysis," *IEEE Commun. Lett.*, vol. 12, no. 8, pp. 545–547, August 2008.

[33] J. Jeganathan, A. Ghrayeb, L. Szczecinski, and A. Ceron, "Space shift keying modulation for MIMO channels," *IEEE Trans. Wireless Commun.*, vol. 8, no. 7, pp. 3692–3703, July 2009.

[34] J. Jeganathan, "Space shift keying modulation for MIMO channels," Master's thesis, Concordia University, Montreal, QC, August 2008.

[35] K. Ishibashi and S. Sugiura, "Effects of antenna switching on band-limited spatial modulation," *IEEE Wireless Commun. Lett.*, vol. 3, no. 4, pp. 345–348, August 2014.

[36] A. Kalis, A. G. Kanatas, and C. B. Papadias, "A novel approach to MIMO transmission using a single RF front end," *IEEE J. Select. Areas Commun.*, vol. 26, no. 6, pp. 972–980, August 2008.

[37] O. N. Alrabadi, C. Divarathne, P. Tragas, A. Kalis, N. Marchetti, C. B. Papadias, and R. Prasad, "Spatial multiplexing with a single radio: Proof-of-concept experiments in an indoor environment with a 2.6-GHz prototype," *IEEE Commun. Lett.*, vol. 15, no. 2, pp. 178–180, Feb. 2011.

[38] J. T. Bernhard, *Reconfigurable Antennas.* Synthesis Lectures on Antennas, Morgan & Claypool Publisherse, 2007.

[39] J. Boerman and J. Bernhard, "Performance study of pattern reconfigurable antennas in MIMO communication systems," *IEEE Trans. Antennas Propagat.*, vol. 56, no. 1, pp. 231–236, January 2008.

[40] D. Piazza *et. al.*, "Design and evaluation of a reconfigurable antenna array for MIMO systems," *IEEE Trans. Antennas Propagat.*, vol. 56, no. 3, pp. 869–881, March 2008.

[41] A. Grau, H. Jafarkhani, and F. D. Flaviis, "A reconfigurable multiple-input multiple-output communication system," *IEEE Trans. Wireless Commun.*, vol. 5, no. 5, pp. 1719–1733, May 2008.

[42] B. Wang and K. Liu, "Advances in cognitive radio networks: A survey," *IEEE Journal of Selected Topics in Signal Processing*, vol. 5, no. 1, pp. 5–23, February 2011.

[43] Z. Bouida, K. Tourki, A. Ghrayeb, M.-S. Alouini, and K. Qaraqe, "Power adaptation for joint switched diversity and adaptive modulation schemes in spectrum sharing systems," *IEEE Commun. Lett.*, vol. 16, no. 9, pp. 1482–1485, September 2012.

[44] Z. Bouida, A. Ghrayeb, K. Qaraqe, and M.-S. Alouini, "Adaptive transmission schemes for MISO spectrum sharing systems," in *Proc. SPAWC 2013*, Darmstadt, Germany, June 2013, pp. 460–464.

[45] ——, "Adaptive transmission schemes for MISO spectrum sharing systems: Tradeoffs and performance analysis," *IEEE Trans. Wireless Commun.*, vol. 13, no. 10, pp. 5352–5365, Oct 2014.

[46] Z. Bouida, A. Ghrayeb, and K. Qaraqe, "Adaptive spatial modulation for spectrally-efficient MIMO systems," in *Proc. IEEE Wireless Communications and Networking Conference (WCNC'14)*, Istanbul, Turkey, April 2014.

[47] ——, "Adaptive spatial modulation for spectrally-efficient MIMO spectrum sharing systems," in *Proc. IEEE International Symposium on Personal, Indoor, and Mobile Radio Communications (PIMRC'14)*, Washington DC, USA, September 2014.

[48] ——, "Joint adaptive spatial modulation and power adaptation for spectrum sharing systems with limited feedback," in *Proc. IEEE Wireless Communications and Networking Conference (WCNC'15)*, New Orleans, USA, March 2015.

[49] ——, "Adaptive spatial modulation for spectrum sharing systems with limited feedback," *IEEE Trans. Commun.*, Submitted, August 2014.

[50] ——, "Enhanced space-shift keying (SSK) with reconfigurable antennas," in *2015 IEEE International Conference on Communications (ICC'15)*, London, England, June 2015.

[51] ——, "Enhancing the performance of space-shift keying (SSK) through reconfigurable antennas," *IEEE Trans. Wireless Commun.*, Submitted, December 2014.

[52] J. M. Peha, "Approaches to spectrum sharing," *IEEE Commun. Mag.*, vol. 43, no. 2, pp. 10–12, Feb. 2005.

[53] A. Jovicic and P. Viswanath, "Cognitive radio: An information-theoretic perspective," *IEEE Trans. Inform. Theory*, vol. 55, no. 9, pp. 3945–3958, Sep. 2009.

[54] H. Suraweera, P. Smith, and M. Shafi, "Capacity limits and performance analysis of cognitive radio with imperfect channel knowledge," *IEEE Trans. Veh. Technol.*, vol. 59, no. 4, pp. 1811–1822, May 2010.

[55] J. Xiang, Y. Zhang, T. Skeie, and L. Xie, "Downlink spectrum sharing for cognitive radio femtocell networks," *IEEE Sys. Jour.*, vol. 4, no. 4, pp. 524–534, December 2010.

[56] S. Al-Rubaye, A. Al-Dulaimi, and J. Cosmas, "Cognitive femtocell," vol. 6, no. 1, pp. 44–51, March 2011.

[57] A. Gjendemsjø, G. E. Øien, and H. Holm, "Optimal power control for discrete-rate link adaptation schemes with capacity-approaching coding," in *Proc. IEEE Global Telecommunications Conference (GLOBECOM'05)*, St. Louis, MO, USA, December 2005, pp. 3498–3502.

[58] A. Gjendemsjø, G. E. Øien, and P. Orten, "Optimal discrete-level power control for adaptive coded modulation schemes with capacity approaching component codes," in

Proc. IEEE International Conference on Communications (ICC'06), Istanbul, Turkey, March 2007.

[59] K. A. Qaraqe, Z. Bouida, M. Abdallah, and M.-S. Alouini, "Joint switched transmit diversity and adaptive modulation in spectrum sharing systems," in *Proc. 2011 Sixth International ICST Conference on Cognitive Radio Oriented Wireless Networks and Communications (CROWNCOM)*, Osaka, Japan, June 2011.

[60] Z. Bouida, M. Abdallah, K. Qaraqe, and M.-S. Alouini, "Spectrally efficient switched transmit diversity for spectrum sharing systems," in *Proc. IEEE Vehicular Tech. Conf. (VTC'11-Fall)*, San Francisco, CA, USA, September 2011.

[61] W. C. Jakes, *Microwave Mobile Communications*, 2nd ed. IEEE Press, 1994.

[62] M. A. Blanco and K. J. Zdunek, "Performance and optimization of switched diversity systems for the detection of signals with Rayleigh fading," *IEEE Trans. Commun.*, vol. COM-27, no. 12, pp. 1887–1895, Dec. 1979.

[63] A. A. Abu-Dayya and N. C. Beaulieu, "Analysis of switched diversity systems on generalized-fading channels," *IEEE Trans. Commun.*, vol. 42, no. 11, pp. 2959–2966, Nov. 1994.

[64] Y.-C. Ko, M.-S. Alouini, and M. K. Simon, "Analysis and optimization of switched diversity systems," *IEEE Trans. Veh. Technol.*, vol. 49, no. 5, pp. 1813–1831, Sep. 2000.

[65] C. Tellambura, A. Annamalai, and V. K. Bhargava, "Unified analysis of switched diversity systems in independent and correlated fading channels," *IEEE Trans. Commun.*, vol. 49, no. 11, pp. 1955–1965, Nov. 2001.

[66] H.-C. Yang and M.-S. Alouini, "Performance analysis of multibranch switched diversity systems," *IEEE Trans. Commun.*, vol. 51, no. 5, pp. 782–794, May 2003.

[67] H.-C. Yang, M. K. Simon, and M.-S. Alouini, "Scan and wait combining (SWC): A switch and examine strategy with a performance-delay tradeoff," *IEEE Trans. Wireless Commun.*, vol. 5, no. 9, pp. 2477–2483, Sep. 2006.

[68] Y. Mietzner, R. Schober, L. Lampe, W. Gerstacker, and P. Hoeher, "Multiple-antenna techniques for wireless communications - a comprehensive literature survey," *IEEE Communications Surveys Tutorials*, vol. 11, no. 2, pp. 87–105, Second Quarter 2009.

[69] F. Heliot, M. Imran, and R. Tafazolli, "On the energy efficiency-spectral efficiency trade-off over the MIMO Rayleigh fading channel," *IEEE Trans. Commun.*, vol. 60, no. 5, pp. 1345–1356, May 2012.

[70] A. Mohammadi and F. Ghannouchi, "Single RF front-end MIMO transceivers," *IEEE Commun. Mag.*, vol. 49, no. 12, pp. 104–109, Dec. 2011.

[71] Y. Chau and S.-H. Yu, "Space modulation on wireless fading channels," in *2001 Veh. Technol. Conf. - Fall*, Atlantic City, NJ, Oct 2001, pp. 1668–1671.

[72] H. Haas, E. Costa, and E. Schulz, "Increasing spectral efficiency by data multiplexing using antenna arrays," in *13th IEEE International Symposium on Personal, Indoor and Mobile Radio Communications*, Lisboa, Portugal, Sep 2002, pp. 610–613.

[73] S. Song, Y. Yang, Q. Xionq, K. Xie, B.-J. Jeong, and B. Jiao, "A channel hopping technique I: Theoretical studies on band efficiency and capacity," in *2004 International Conference on Communications, Circuits and Systems*, Chengdu, China, Jun 2004, pp. 229–233.

[74] M. D. Renzo, H. Haas, and P. M. Grant, "Spatial modulation for multiple-antenna wireless systems: a survey," *IEEE Commun. Mag.*, vol. 49, no. 12, pp. 182–191, Dec. 2011.

[75] A. Alshamali and B. Quza, "Performance of spatial modulation in correlated and uncorrelated Nakagami fading channel," *J. Commun.*, vol. 4, no. 3, pp. 170–174, Apr. 2009.

[76] S. U. Hwang, S. Jeon, S. Lee, and J. Seo, "Soft-output ML detector for spatial modulation OFDM systems," *IEICE Electronics Express*, vol. 6, no. 19, pp. 1426–1431, Oct. 2009.

[77] R. Mesleh, M. D. Renzo, H. Haas, and P. M. Grant, "Trellis coded spatial modulation," *IEEE Trans. Wireless Commun.*, vol. 9, no. 7, pp. 2349–2361, July 2010.

[78] N. Serafimovski, M. D. Renzo, S. Sinanovic, R. Mesleh, and H. Haas, "Fractional bit encoded spatial modulation (FBE-SM)," *IEEE Commun. Lett.*, vol. 14, no. 5, pp. 429–431, May 2010.

[79] M. D. Renzo and H. Haas, "A general framework for performance analysis of space shift keying (SSK) modulation for MISO correlated Nakagami-m fading channels," *IEEE Trans. Commun.*, vol. 58, no. 9, pp. 2590–2603, September 2010.

[80] M. Di Renzo and H. Haas, "On the performance of space shift keying MIMO systems over correlated rician fading channels," in *2010 International ITG Workshop on Smart Antennas (WSA)*, Bremen, Germany, Feb 2010, pp. 72–79.

[81] S. Ikki and R. Mesleh, "A general framework for performance analysis of space shift keying (SSK) modulation in the presence of gaussian imperfect estimations," *IEEE Commun. Lett.*, vol. 16, no. 2, pp. 228–230, February 2012.

[82] R. Mesleh, S. Ikki, and M. Alwakeel, "Performance analysis of space shift keying with amplify and forward relaying," *IEEE Commun. Lett.*, vol. 15, no. 12, pp. 1350–1352, August 2011.

[83] R. Mesleh, S. Ikki, E.-H. Aggoune, and A. Mansour, "Performance analysis of space shift keying (SSK) modulation with multiple cooperative relays," *EURASIP Journal on Advances in Signal Processing*, vol. 2012, no. 1, pp. 201–211, August 2012.

[84] J. Jeganathan, A. Ghrayeb, and L. Szczecinski, "Generalized space shift keying modulation for MIMO channels," in *IEEE 19th International Symposium on Personal, Indoor, and Mobile Radio Communications (PIMRC'08)*, Cannes, France, Sep 2008, pp. 1–5.

[85] T. Taga, "Analysis for mean effective gain of mobile antennas in land mobile radio environments," *IEEE Trans. Veh. Technol.*, vol. 39, no. 2, pp. 117–131, May 1990.

[86] H. El-Sallabi, M. Abdallah, and K. Qaraqe, "Modelling of parameters of Rician fading distribution as a function of polarization parameter in reconfigurable antenna," in *IEEE/CIC ICCC 2014 Symposium on Wireless Communications Systems*, Shanghai, China, Oct 2014, pp. 1–5.

[87] S. W. Kim, D. S. Ha, and J. H. Reed, "Minimum selection GSC and adaptive low-power RAKE combining scheme," in *Proc. IEEE Int. Symp. on Circuit and Systems (ISCAS'03)*, Bangkok, Thailand, May 2003.

[88] J. R. Carson, "A generalization of the reciprocal theorem," *Bell Syst. Tech. J.*, vol. 3, pp. 393–399, 1924.

[89] M. Daghfous, R. Radaydeh, and M.-S. Alouini, "Performance of adaptive MS-GSC in the presence of cochannel interference," *IEEE Trans. Veh. Technol.*, vol. 60, no. 6, pp. 2829–2837, Jul. 2011.

[90] H.-C. Yang, "New results on ordered statitics and analysis of minimum selection generalized selection combining (GSC)," *IEEE Trans. Wireless Commun.*, vol. 5, no. 7, pp. 1876–1885, July 2006.

[91] *Physical Layer Procedures (TDD)*, Third Generation Partnership Project, Technical Specification Group Radio Access Network Std. Rev. TS25.224 (Rel. 7), March 2006.

[92] H.-C. Yang and M.-S. Alouini, *Ordered Statistics Wireless Communications*, 1st ed. Cambridge University Press, 2011.

[93] J. Proakis, *Digital Communications*, 4th ed. McGraw-Hill, 2001.

[94] N. R. Naidoo, H. Xu, and T. A.-M. Quazi, "Spatial modulation: optimal detector asymptotic performance and multiple-stage detection," *IET Commun.*, vol. 5, no. 10, pp. 1368–1376, July 2011.

[95] M. D. Renzo, H. Haas, A. Ghrayeb, S. Sugiura, and L. Hanzo, "Spatial modulation for generalized MIMO: Challenges, opportunities, and implementation," *Proc. of the IEEE*, vol. 102, pp. 56–103, Jan 2014.

[96] D. Yang, C. Xu, L.-L. Yang, and L. Hanzo, "Transmit-diversity-assisted SSK for colocated and distributed/cooperative MIMO elements," *IEEE Trans. Veh. Technol.*, vol. 60, no. 6, pp. 2864–2869, July 2011.

[97] O. Alrabadi, J. Perruisseau-Carrier, and A. Kalis, "MIMO transmission using a single RF source: Theory and antenna design," *IEEE Trans. Antennas Propagat.*, vol. 60, no. 2, pp. 654–664, February 2012.

[98] M. D. Renzo and H. Haas, "Space shift keying (SSK-) MIMO over correlated Rician fading channels: Performance analysis and a new method for transmit-diversity," *IEEE Trans. Commun.*, vol. 59, no. 1, pp. 116–129, January 2011.

[99] H. El-Sallabi, D. Baum, P. Zetterberg, P. Kyosti, T. Rautiainen, and C. Schneider, "Wideband spatial channel model for MIMO systems at 5 Ghz in indoor and outdoor environments," in *IEEE 63rd VTC'Spring*, Melbourne, May 2006, pp. 2916–2921.

[100] M. Chiani, M. Win, and A. Zanella, "On the capacity of spatially correlated MIMO Rayleigh-fading channels," *IEEE Trans. Inform. Theory*, vol. 49, no. 10, pp. 2363–2371, Oct. 2003.

[101] W. Weichselberger, M. Herdin, H. Ozcelik, and E. Bonek, "A stochastic MIMO channel model with joint correlation of both link ends," *IEEE Trans. Commun.*, vol. 5, no. 1, pp. 90–100, Jan. 2006.

[102] H. Ozcelik *et. al.*, "Deficiencies of 'Kronecker' MIMO radio channel model," *Electron. Lett*, vol. 39, no. 16, pp. 1209–1210, Aug. 2003.

[103] J. Cheng and T. Berger, "Capacity of a class of fading channels with channel state information (CSI) feedback," in *Proc. Allerton Conf. Comm., Control Comp.*, Urbana, Illinois, Oct 2001, pp. 1152–1160.

[104] A. P. Prudnikov, Y. A. Brychkov, and O. I. Marichev, *Integrals and Series: More Special Functions, Vol. 3*, 2003.

[105] M. K. Simon and M.-S. Alouini, *Digital Communication over Fading Channels*, 2nd ed. New York, NY: John Wiley & Sons, 2005.